

12-2011

ROLE OF THE GCN5 HISTONE ACETYLTRANSFERASE IN SPINOCEREBELLAR ATAXIA TYPE 7 AND IN IMMATURE NEURONS

Yi Chun Chen

Follow this and additional works at: https://digitalcommons.library.tmc.edu/utgsbs_dissertations



Part of the [Disease Modeling Commons](#), [Molecular Genetics Commons](#), and the [Nervous System Diseases Commons](#)

Recommended Citation

Chen, Yi Chun, "ROLE OF THE GCN5 HISTONE ACETYLTRANSFERASE IN SPINOCEREBELLAR ATAXIA TYPE 7 AND IN IMMATURE NEURONS" (2011). *The University of Texas MD Anderson Cancer Center UTHealth Graduate School of Biomedical Sciences Dissertations and Theses (Open Access)*. 208.
https://digitalcommons.library.tmc.edu/utgsbs_dissertations/208

This Dissertation (PhD) is brought to you for free and open access by the The University of Texas MD Anderson Cancer Center UTHealth Graduate School of Biomedical Sciences at DigitalCommons@TMC. It has been accepted for inclusion in The University of Texas MD Anderson Cancer Center UTHealth Graduate School of Biomedical Sciences Dissertations and Theses (Open Access) by an authorized administrator of DigitalCommons@TMC. For more information, please contact digitalcommons@library.tmc.edu.

**ROLE OF THE GCN5 HISTONE ACETYLTRANSFERASE IN
SPINOCEREBELLAR ATAXIA TYPE 7 AND IMMATURE NEURONS**

by

Yi Chun Chen, M.S.

APPROVED:

Supervisory Professor: Sharon Y. R. Dent, Ph.D.

Richard R. Behringer, Ph.D.

Xiaobing Shi, Ph.D.

Stephanie S. Watowich, Ph.D.

John H. Wilson, Ph.D.

APPROVED:

Dean, The University of Texas
Graduate School of Biomedical Sciences at Houston

ROLE OF THE GCN5 HISTONE ACETYLTRANSFERASE IN
SPINOCEREBELLAR ATAXIA TYPE 7 AND IMMATURE NEURONS

A
DISSERTATION

Presented to the Faculty of
The University of Texas
Health Science Center at Houston and
The University of Texas M. D. Anderson Cancer Center
Graduate School of Biomedical Sciences
in Partial Fulfillment of the Requirements
for the Degree of
DOCTOR OF PHILOSOPHY

By

Yi Chun Chen, M.S.

Houston, Texas

December, 2011

Acknowledgements

I could not express enough of my gratitude to my mentor, Dr. Sharon Dent, for her guidance and warm thoughts through out this work. I am also very thankful to my committee members, Drs. Richard Behringer, John Wilson, Howard Gutstein, Stephanie Watowich, and Xiaobing Shih, as well as my examine committee members Drs. Pierre McCrea and Suyun Huang for their advice on experimental design and discussion.

This work would not be complete without the wonderful discussion and experimental support from Drs. Huda Zoghbi, Jennifer Getchal, and Cai-An Mao.

As well I thank the assistance from the Animal Facility of MDAnderson.

My thanks must go also to the members of Dent lab for all the fun times, intellectual stimulations and warm friendship. Especially, I am grateful to Rebecca Lewis for assistance on mouse works; Wenchu Lin for created *Gcn5* mouse lines; Marendra Wilson-Pham, Jill Butler, Renee Chosed, Andria Schibler and John Latham for their help on writing; Marek Napierala, Eunah Kim, Calley Hirsh, Boyko Atanassov and Evangelia Koutelou for intensive discussion and inspiration; Madelene Coombes, Andrew Salinger, Ping Bu and Urszula Polak for kind help. All of them had made the time when I am part of the Dent lab a wonderful and unforgettable journey. I am also grateful to Dr. Michelle Barton and lab members of Barton, Behringer, and Halder lab for scientific discussion on wide variety of subjects and generously sharing reagents.

I must also acknowledge my family and the many friends for their encouragement and support that made everything easier when it is hard.

ROLE OF THE GCN5 HISTONE ACETYLTRANSFERASE IN SPINOCEREBELLAR ATAXIA TYPE 7 AND IMMATURE NEURONS

Publication No. _____

Yi Chun Chen, M.S.

Supervisory Professor: Sharon Y. R. Dent, Ph.D.

Spinocerebellar Ataxia type 7 (SCA7) is a neurodegenerative disease caused by expansion of a CAG repeat encoding a polyglutamine tract in ATXN7, a component of the SAGA histone acetyltransferase (HAT) complex. Previous studies provided conflicting evidence regarding the effects of polyQ-ATXN7 on the activity of Gcn5, the HAT catalytic subunit of SAGA. Here I showed that reducing Gcn5 expression accelerates both cerebellar and retinal degeneration in a mouse model of SCA7. Deletion of Gcn5 in Purkinje cells in mice expressing wild type Atxn7, however, causes only mild ataxia and does not lead to the early lethality observed in SCA7 mice. Reduced Gcn5 expression strongly enhances retinopathy in SCA7 mice, but does not affect the transcriptional targets of Atxn7, as expression of these genes is not further altered by Gcn5 depletion. These findings demonstrate that loss of Gcn5 functions can contribute to the time of onset and severity of SCA7 phenotypes, but suggest that non-transcriptional functions of SAGA may play a role in neurodegeneration in this disease.

Table of Contents

Chapter I. Background and Significance	1
Potential role of Gcn5 in Spinocerebellar Ataxia type 7 (SCA7)	2
General information about Gcn5.....	5
Histone acetyltransferase activity of Gcn5 and protein acetylation.....	7
Gcn5 HAT-independent functions.....	12
Gcn5 is a component of multicomponent complexes	14
Physiological roles of Gcn5	16
Gcn5 functions during development	16
Potential neuronal functions of Gcn5 in adult mammals.....	17
Transcriptional downregulation is associated with altered Gcn5 functions in SCA7 retina	18
Goal and Significance.....	19
 Chapter II. Materials and Methods	 21
Generation of Gcn5;Atxn7 and Purkinje cell-specific Gcn5 mutant mouse models	 22

Generation of <i>Gcn5^{fn/fn}</i> mice	22
Survival analysis.....	23
Histological analyses	23
Electron microscopy	24
Footprint analyses	24
Wirehang test	25
Dowel test.....	25
Rotarod test.....	26
Northern blot analysis.....	26
Quantitative RT-PCR and primers	26
 Chapter III. Results	 29
Short lifespan of polyQ-Atxn7 mice	30
Reducing Gcn5 shortens lifespan of polyQ-Atxn7 mice.....	39
Reducing Gcn5 worsens ataxia of polyQ-Atxn7 mice.....	40
Reducing Gcn5 worsens cerebellar degeneration of polyQ-Atxn7 mice.....	53
Depletion of Gcn5 in the postnatal Purkinje neurons affects motor coordination	67
Reducing Gcn5 worsens retinal degeneration in SCA7 mice	76
Reducing Gcn5 does not affect retinal degeneration in SCA7 mice	81

Potential role of Gcn5 in the late neural development (preliminary)	84
Chapter IV. Discussion and future directions	93
Loss of Gcn5 function contributes to neurodegeneration in SCA7 mouse.....	96
Potential role of ubiquitin and Usp22 DUB activity in SCA7	97
Implication of non-transcriptional functions of Gcn5/SAGA involved in the early degenerating retina of SCA7	100
Future direction- determine the functions of Gcn5 in photoreceptors and Bergmann glia in SCA7 neuropathogenesis.....	102
Future direction- role of Usp22 in SCA7	105
Potential role of Gcn5 in immature neurons	107
Future direction- role of Gcn5 in early postmitotic neurons in the hindbrain	107
Bibliography	110
Vita	131

List of Figures

<u>Figure 1:</u> Structure of mouse <i>Gcn5</i> gene and polypeptide product.....	8
<u>Figure 2:</u> <i>Gcn5</i> mutation reduces lifespan of <i>Atxn7</i> ^{100Q/5Q} mice	33
<u>Figure 3:</u> Lifespan of <i>Atxn7</i> ^{100Q/100Q} and <i>Atxn7</i> ^{100Q/100Q} ; <i>Gcn5</i> ^{Δ/+} mice.....	35
<u>Figure 4:</u> PolyQ-Atxn7 forms nuclear inclusion in Purkinje cells of <i>Atxn7</i> ^{100Q} mice	37
<u>Figure 5:</u> Reduced level of Gcn5 in cells of Gcn5 mutants	42
<u>Figure 6:</u> Reduced level of Gcn5 in mice with <i>Gcn5</i> ^{Δ/+} mutation.....	44
<u>Figure 7:</u> Gcn5 RNA levels remain constant during disease progression in <i>Atxn7</i> ^{100Q/100Q} and <i>Atxn7</i> ^{100Q/100Q} ; <i>Gcn5</i> ^{Δ/+} mice	46
<u>Figure 8:</u> Reducing the level of Gcn5 enhances clasping phenotypes of <i>Atxn7</i> ^{100Q/100Q} mice	49
<u>Figure 9:</u> Reducing the level of Gcn5 enhances gait ataxia of <i>Atxn7</i> ^{100Q/100Q} mice	51
<u>Figure 10:</u> <i>Gcn5</i> hypomorphic alleles enhance ataxia phenotypes of <i>Atxn7</i> ^{100Q/5Q} mice	54
<u>Figure 11:</u> Analysis of other motor skills of <i>Atxn7</i> ^{100Q/100Q} mice with <i>Gcn5</i> mutations.....	56

<u>Figure 12:</u> No dramatic atrophy in the cerebellum of <i>Atxn7</i> ^{100Q/100Q} mice with or without a background of <i>Gcn5</i> ^{Δ/+} at age of 5 months.....	58
<u>Figure 13:</u> Cerebellar atrophy is more severe in <i>Atxn7</i> ^{100Q/100Q} mice in a background of <i>Gcn5</i> ^{Δ/+} at age of 9 months.....	60
<u>Figure 14:</u> Purkinje cell morphological change is more severe in <i>Atxn7</i> ^{100Q/100Q} mice in a background of <i>Gcn5</i> ^{Δ/+}	63
<u>Figure 15:</u> Purkinje cell degeneration is more severe in <i>Atxn7</i> ^{100Q/100Q} mice in a background of <i>Gcn5</i> ^{Δ/+}	65
<u>Figure 16:</u> Purkinje cell-specific depletion of <i>Gcn5</i>	68
<u>Figure 17:</u> Depleting <i>Gcn5</i> in Purkinje cells causes no dramatic effect in the cerebellum at P7.....	70
<u>Figure 18:</u> Purkinje cell-specific loss of <i>Gcn5</i> causes mild ataxia.....	72
<u>Figure 19:</u> Purkinje cell-specific loss of <i>Gcn5</i> causes mild cerebellar atrophy...	74
<u>Figure 20:</u> Level of Purkinje cell-specific transcripts in <i>Gcn5</i> conditional null mice	77
<u>Figure 21:</u> Reducing <i>Gcn5</i> worsens retinal degeneration in <i>Atxn7</i> ^{100Q/100Q} mice	79
<u>Figure 22:</u> <i>Atxn7</i> ^{100Q/100Q} ; <i>Gcn5</i> ^{Δ/+} mice have shorter outer segment at 1.5 month of age	82
<u>Figure 23:</u> Gradual decrease of SCA7 target transcripts in both <i>Atxn7</i> ^{100Q/100Q} and <i>Atxn7</i> ^{100Q/100Q} ; <i>Gcn5</i> ^{Δ/+} mice	85

<u>Figure 24:</u> Cerebellar morphology of <i>Gcn5</i> hypomorphic mice at E18.5	88
<u>Figure 25:</u> Differential appearance of <i>Gcn5</i> ^{fn/fn} mice at E18.5.....	91

List of Tables

<u>Table 1:</u> Expression pattern of components of SAGA and ATAC in the hindbrain	6
<u>Table 2:</u> Transcriptional targets of Gcn5.....	11
<u>Table 3:</u> Substrates of Gcn5.....	13
<u>Table 4:</u> Progeny of crosses between <i>Gcn5</i> ^{flox(neo)/+} and <i>Atxn7</i> ^{100Q/5Q} ; <i>Gcn5</i> ^{flox(neo)/+} mice	41

Chapter I

Background and Significance

Gcn5 is a histone acetyltransferase (HAT) that catalyzes protein acetylation and is important for gene regulation in many cells in the body. However its functions in neurons were unknown at the beginning of my studies. Evidence that I provide here regarding the role of Gcn5 in a neurodegenerative disease, Spinocerebellar Ataxia type 7 (SCA7), and in neurons strongly suggests that Gcn5 not only functions in the neurons but is also central to neurotoxicity observed in SCA7.

Potential role of Gcn5 in Spinocerebellar Ataxia type 7 (SCA7)

SCA7 is one of 9 inherited polyGlutamine (polyQ) expansion neurodegenerative diseases. Most SCA7 patients develop adult onset of progressive neurological symptoms that are linked to cerebellar, brainstem, and retinal neurodegeneration. The symptoms include ataxia, dysarthria, dysphagia, slow eye movement associated with brainstem dysfunctions, and decreased visual acuity (David et al., 1997; David et al., 1998; Giunti et al., 1999).

All SCA7 patients develop progressive ataxia. Cerebellar degeneration is responsible for the uncoordinated movement, since the cerebellum controls motor coordination for limb movement and posture maintenance (David et al., 1998). Gross cerebellar atrophy is generally observed in SCA7. Among all cell types, Purkinje cell degeneration was most profound in the cerebellum of SCA7 patients (Carpenter and Schumacher, 1966; Gouw et al., 1994; Jobsis et al., 1997; Martin et al., 1994; Rub et al., 2005). Purkinje cells align into one cell layer (Purkinje cell layer, PCL) between the molecular layer (ML) and granule cell layer

(GCL) in the cerebellum. The dendrites of Purkinje cells stretch and form synaptic connections in the molecular layer, while their axons pass through the granule cell layer and the white matter to connect to cerebellar and vestibular nuclei as the sole output of the information processed in the cerebellum. Therefore degeneration of Purkinje cells disturbs cerebellar functions.

As a result of retinal dysfunction and degeneration, SCA7 patients develop progressive loss of color vision and visual acuity in addition to cerebellar ataxia (David et al., 1997; Gouw et al., 1994). Retinal degeneration is a unique feature of SCA7 among all spinocerebellar ataxias (Enevoldson et al., 1994; Neetens et al., 1990). Retinography and pathological analysis indicate that the photoreceptors, the cell types responsible for receiving light, are the most affected cell types in the retinas of SCA7 patients (Aleman et al., 2002; Martin et al., 1994; Michalik et al., 2004; Neetens et al., 1990; Rub et al., 2005).

The cause of SCA7 is an expansion mutation of CAG repeats in the 2nd exon of one allele of *ATXN7* (Krols, 1997; David, 1997). Repeats longer than 35 CAGs in *ATXN7* lead to neurodegenerative symptoms (David et al., 1998; Giunti et al., 1999). The length of polyCAG correlates to the onset and progression of the neurological symptoms and degeneration of SCA7 (Giunti et al., 1999). This correlation suggests that the longer the polyCAG repeat in *ATXN7*, the stronger the neurotoxicity it bears. In very rare cases, repeats longer than 100 CAGs cause infantile forms of SCA7, in which patients develop neurodegeneration and

lethality within two years of age (Grattan-Smith et al., 2001; Tsivgoulis et al., 2008; van de Warrenburg et al., 2001).

As an in-frame mutation, the expanded CAG repeat is translated into an expanded polyGlutamine (polyQ) tract that tends to fold into beta-sheets in the N-terminal region of polyQ-Atxn7 protein. This beta-sheet folding of the polyQ stretch causes polyQ-Atxn7 to aggregate into nuclear inclusions (NIs). The aggregative feature of polyQ-protein was thought to link to an aberrant gain-of-function that leads to neurodegeneration. However, since Atxn7 is ubiquitously expressed in most cell types, and polyQ-ATXN7 nuclear inclusions were observed in many non-degenerative cell types in clinical studies, NIs were later proposed to be a cellular protective response to the mis-folded protein (Holmberg et al., 1998; Jonasson et al., 2002).

To date, how ubiquitously expressed polyQ-Atxn7 specifically causes neurotoxicity is unclear. SCA7 patients still await effective therapeutics. Although clinical case reports and pathological findings thoroughly described the change in degenerative sites, most of this information was obtained at terminal stages of the disease. As a result, clinical studies have provided very limited information to the molecular mechanisms of how polyQ-Atxn7 causes neurotoxicity and disease progression. Therefore, using animal models to define the cause of neurotoxicity is crucial for uncovering the mechanisms of SCA7 neuropathogenesis at early stages.

Since Atxn7 does not carry enzymatic activities, the mechanism underlying SCA7 has been pointed to its interactors. Atxn7 is known to be part of a multi-component complex, SAGA, which carries protein-modifying activities (Helmlinger et al., 2004b). This suggests the neurotoxicity could be linked to abnormal SAGA functions. Most SAGA components are highly expressed in the cell types that are most affected in the cerebellum (Table 1), suggesting function of SAGA is conserved in these cells. Here I provide evidence on the role of Gcn5, one of the enzymatic components of SAGA, in the cerebellum in the central nervous system (CNS) and the retina in the peripheral nervous system (PNS) since these two sites are specifically affected in the SCA7.

General information about Gcn5

To further understand the neuronal functions of Gcn5, next I will introduce known functions of Gcn5.

The highly conserved sequence among eukaryotes suggests Gcn5 carries important roles. In mice, *Gcn5* is located on chromosome 11. Alternative splicing of this gene results in two different Gcn5 transcripts, a long and a short Gcn5 form (Gcn5L and Gcn5S; (Xu et al., 1998). Both forms are translated into polypeptides. Gcn5L is composed of three conserved domains: a PCAF N-

Table 1: Expression pattern of components of SAGA and ATAC in the mouse hindbrain

Family	Protein	Expression	ATAC	SAGA
HATs	Gcn5L	PCL, BS, other cells	+	+
	PCAF	PCL, other cells	-	-
	ATAC2- CSRP2BP	PCL, BS	+	-
ATM-like	TRRAP	PCL	+	+
Ada	Tada3	PCL	+	+
	Tada2a- CG10411	all cells	+	-
	Tada2b	NA	-	+
	Tada1	No expression	-	+
Spt	Supt3h	PCL, BS	-	+
	Supt7l	NA	-	+
Sap	Sap130	PCL, GCL	-	+
	Sgf29-ccdc101	PCL, GCL, BS	-	+
Taf_{II}	Taf5l	PCL, BS	-	+
	Taf6l	No expression	-	+
	Taf9	GCL	-	+
	Taf15	PCL	-	+
	Taf20	NA	-	+
	Taf30	NA	-	+
	Taf31	NA	-	+
	PAF65a	NA	-	+
	PAF65b	NA	-	+
ATAC unique factors	WDR5	PCL, BS	+	-
	DR1	All cells	+	-
	MBIP	PCL	+	-
	YEATS2	BS	+	-
	Mocs2	BS, PCL	+	-
DUB module	Atxn7	PCL, GCL, BS	-	+
	Usp22	PCL, GCL, BS	-	+
	Atxn7L3	PCL	-	+
	Eny2	PCL, BS	-	+

PCL: Purkinje cell layer; BS: brainstem; GCL: granule cell layer

RNA in situ data: Allen Brain Institutes.

Mammalian ATAC: Guelman, 2009

mPCAF: Ogryzko, 1998

hSAGA: Gamper, 2009

terminal-like domain, a NAT_SF, and a bromo domain (Figure 1), while Gcn5S contains only NAT_SF and a bromo domain (Xu, 1998 et al.; Conserved Domain Database, NCBI). The PCAF N-terminal domain has no known functions and is only conserved in metazoans. The NAT_SF super family domain carries HAT activity, and the bromo domain binds to acetylated lysines, and also facilitates acetylation of nucleosomes in yeast (Li and Shogren-Knaak, 2009).

Histone acetyltransferase activity of Gcn5 and protein acetylation.

With the NAT_SF domain, Gcn5 carries HAT activity. Among five families of HATs, Gcn5 belongs to the Gcn5-related N-acetyltransferase (GNAT) family that also includes Pcaf, Hat1, Elp3, and Hpa2. All the HATs of GNAT family are localized to and functions within the nucleus (reviewed by Roth et al., 2001).

Although originally found to acetylate histones, HATs also acetylate non-histone proteins. HATs transfer the acetyl group from acetyl-CoA to the ϵ -amine on lysine residues on proteins and therefore are also known as lysine (K) acetyltransferases (KATs) (Hodawadekar and Marmorstein, 2007; Roth et al., 2001). Adding an acetyl group abrogates the positive charge of lysine.

Lysine acetylation occurs on histones, transcription factors, nuclear receptors, high mobility group proteins, and α -tubulin. The most abundant cellular acetylated proteins are histones and tubulin. Histone acetylation has been studied more intensively because of its important functions in packing the genetic material, DNA. To utilize the limited space in the nucleus, the positive-charged

Figure 1. Structure of mouse *Gcn5* gene and polypeptide product

Diagram shows structure of mouse *Gcn5* gene and expressed polypeptide product. Open and dark blue boxes represent untranslated region and exons of *Gcn5*. *Gcn5* gene product is a polypeptide of 830 amino acids. Blue, orange, and red boxes represent PCAF_N, NAF_SF, and bromo domains.

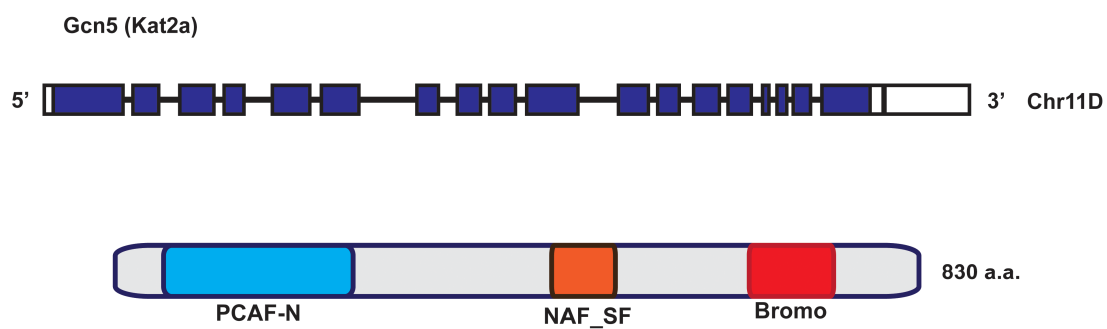


Figure 1

histones H2A, H2B, H3, and H4 are assembled into octamers for negative-charged DNA to wrap around and form the core nucleosomes. Nucleosomes can then pack into higher order chromatin structures. Upon transcription, genomic DNA needs to be “opened up” at the level of chromatin, evicting or increasing accessibility of nucleosomes to the transcriptional machinery. Acetylation on various lysines in the histone tails of H2A, H2B, H3 and H4 decreases the positive charge, freeing the histone tails from holding DNA (reviewed by Kouzarides, 2007). In addition to changing chromatin architecture, the acetyl-lysines on histone tails also create docking sites for proteins containing bromo domains that bind specifically to acetyl-lysine (Dhalluin et al., 1999; Kanno et al., 2004). As a result, acetylated histones H3 and H4 at the promoter regions of genes are associated with transcriptional activation.

As a HAT, Gcn5 acetylates both histones and non-histone substrates. Gcn5 acetylate histones on its N-terminal tails. In metazoans, histone H3 lysine 9 (H3K9), 14 (H3K14), 56 (H3K56), histone H4 lysine 8 (H4K8), 16 (H4K16), and H2A/B are acetylated by Gcn5 (Kuo et al., 1996). During transcription, transcription activators such as c-Myc and TNF β , recruit Gcn5 to nucleosomes to catalyze histone acetylation on the chromatin and facilitate transcription (transcription targets of Gcn5 are summarized in Table 2). By participating in the transcriptional coactivation of various genes, Gcn5 regulates a wide range of cellular processes. In addition to histone substrates, as a nuclear HAT, Gcn5 also acetylates nuclear proteins such as transcription factors and cell cycle

Table 2: Transcriptional targets of Gcn5

Role	Transcriptional targets	Organism	SAGA/ATAC	References
Coactivator	pho8, his3, gal1, arg1	Yeast	NA	Gregory, 1999; Filetici, 1998; Kuo, 1998; Natarajan, 1999; Govind CK, 2007
Myc coactivation	pho5	Yeast	SAGA	Flinn, 2002; Barbaric, 2003; Brown, 2001
ER coactivation	Cathepsin, c-fos	Human	SAGA	Yanagisawa, 2002
Retinoic acid (RAR) coactivation	NA	Human	SAGA	Brown, 2003
Myc coactivation	MYC-r element	Human	SAGA	Liu, 2003
P53 coactivator	P21, GADD45	Human	SAGA	An, 2004; Gamper, 2008, 2009
TGF-β/smad coactivator	PAI-1	Human	NA	Kahata, 2004
Crx coactivation	Sop, Mop,	Mouse	NA	Peng, 2007
Pol III/c-Myc coactivator	tRNA, 5S rRNA	Human	TRRAP-containing	Kenneth, 2007
Wnt/β-catenin signaling	SIAMOUS reporter	Human	NA	Sustmann, 2008
Stress response: Sty1- and Atf1-coactivator	gpd1, ctt1, hsp9, srx1	Yeast	NA	Sanso, 2011

NA: not applicable

regulators. The acetylation catalyzed by Gcn5 changes the stability or activity of the substrate proteins (summarized in table 3). In mammalian cells, Gcn5-mediated acetylation of Myc, c/EBPbeta, and GATA-2 increases the activity of these transcription factors (Faiola et al., 2005; Hayakawa et al., 2004; Patel et al., 2004; Wiper-Bergeron et al., 2007). On the other hand, PGC1a, PGC1b and CDK9 transcriptional activity is decreased after being acetylated by Gcn5 (Kelly et al., 2009; Lerin et al., 2006; Sabo et al., 2008). Gcn5 acetylation on CDC6 and CyclinA decreases stability of these proteins (Orpinell et al., 2010; Paolinelli et al., 2009). By altering the functions of these transcription factors and cell cycle regulators, Gcn5 is also involved in controlling various pathways.

Although Gcn5 was found as a nuclear HAT, a few recent papers suggest the possibility that GCN5 acetylates α -Tubulin that is located mainly in the cytosol (Conacci-Sorrell et al.; Orpinell et al., 2010). However how this nuclear HAT acetylates α -Tubulin remains unclear.

Gcn5 HAT-independent functions

Although well studied as a HAT, previous genetic findings from the Dent Lab suggests Gcn5 also functions in a HAT-independent manner. The Gcn5 HAT catalytic mutant shows later lethality than Gcn5 null mice, suggesting that Gcn5 also has functions independent of its HAT activity (Bu et al., 2007; Xu et al., 2000). Recently, Gcn5 was found to regulate NF κ B-mediated transcription independent of its HAT function by associating with COMMD1, an ubiquitin

Table 3: Substrates of Gcn5

Role	Protein targets	Organism	SAGA/ATAC	Reference
Myc:Max activity	MYC	Human	SAGA	Faiola, 2005; Patel, 2004
Haemotopetic stem cell differentiation	GATA-2	Human	NA	Hayakawa, 2004
Glucose metabolism	PGC1a	Human	NA	Lerin, 2006
Glucocorticoid-stimulated preadipocyte differentiation	C/EBPbeta	Human	NA	Wiper-Bergeron, 2007
Disrupt activity of P-TEFb	CDK9	Human	NA	Sabo, 2008
Glucose metabolism	PGC1b	Human	NA	Kelley, 2009
Regulates S phase	CDC6	Human	NA	Paolinelli, 2009
Degradation-Mitotic progression	CyclinA	Human	ATAC	Orpinell, 2010
Tubulin dynamics	α -Tubulin	Human	NA	Conacci-Sorrell, 2010

ligase, and facilitating its activity (Mao et al., 2009). However clear mechanisms of how HAT-independent functions of Gcn5 regulate cellular pathways still remains unclear. In addition, Gcn5 is also required for the full activity of another enzymatic component of the SAGA complex, the Usp22 deubiquitinase (Atanassov et al., 2010).

Gcn5 is a component of multicomponent complexes

Gcn5 is known to function as part of two distinct multicomponent complexes, ATAC and SAGA (Grant, 1997; Eberharter, 1999; Martinez, 1998; Ogryzko, 1998; Matrinez, 2001; Guelman, 2009; Gamper, 2009). ATAC and SAGA share many components such as Trrap and Ada3. However these two complexes also have distinct components that define substrates and cellular functions. Most components of SAGA are expressed in the cerebellum. The components of ATAC and SAGA and their expression pattern in the cerebellum are summarized in Table 1.

The ATAC complex uniquely contains Ada2a, Wdr5, Dr1, Mbip, Yeats2, and Mocs2, making it distinct from SAGA. Gcn5 in the ATAC complex preferentially acetylates histone H4, although it also acetylates histone H3 (Guelman et al., 2009). The ATAC complex is also known to be involved in cell cycle progression via acetylation of non-histone substrates including CyclinA (Orpinell et al., 2010).

The SAGA (Spt-Ada-Gcn5-acetyl-transferase, also as known as TFTC) complex contains Ada, Spt, Taf II proteins, and a deubiquitinase (DUB) submodule. Gcn5 within SAGA preferentially acetylates histone H3 and H2B, and has stronger activity towards chromatin than free histones as part of the SAGA complex (Gamper et al., 2009; Grant et al., 1999).

The SAGA DUB submodule includes Usp22, Eny2, Atxn7I3, and Atxn7. Usp22 is the deubiquitinase catalytic subunit but is only active as part of the DUB module (Zhao et al., 2008). The deubiquitination of histone H2B catalyzed by the DUB module is required for nuclear receptor coactivation (Zhang et al., 2008; Zhao et al., 2008). The DUB activity of USP22 also regulates protein stability of telomeric shelterin protein, TRF1 (Atanassov et al., 2009). Eny2 is also part of a nuclear pore complex and may connect the function of SAGA to RNA export in yeast (Cabal, 2006; Krushavika, 2007). Both Atxn7 and Atxn7I3 contain a SCA7 domain and one C2H2 zinc-finger domain that connects the DUB module to SAGA. The diverse amino acid sequences in the SCA7 domains of Atxn7 and Atxn7I3, however, form distinct conformations. As a result, only the SCA7 domain in Atxn7 facilitates binding to nucleosomes (Bonnet et al., 2010). Although their structures have been solved, the molecular functions of Atxn7 and Atxn7I3 are still unknown. However, SCA7, a human inherited disease caused by mutation in *ATXN7*, gives a hint to its biological role. Since SCA7 is caused by polyCAG expansion mutations in *ATXN7*, the neuronal defects in SCA7 suggests the

important role of Atxn7 in maintaining neuronal functions and survival, likely through affecting functions of SAGA.

Physiological roles of Gcn5

Although yeast model system provided nice evidence for Gcn5 functions, in mammalian systems, most of the cellular functions of Gcn5 were defined using transformed cell lines. Since lacking evidence from mammalian tissue, the physiological roles of Gcn5 have not yet been defined clearly.

The ubiquitous expression of Gcn5 through out mouse development suggests its functions are widely utilized in most cell types. Among all tissues, Gcn5 is most abundant in embryos and in brains of adult mice (Xu et al., 1998). In the central nervous system (CNS) and peripheral nervous system (PNS), the expression level of Gcn5 is most strong in three sites, hippocampus of the forebrain, Purkinje cell layer in the hindbrain, and the dorsal root ganglia of the spinal cord in mice (RNA *in situ* database from Allen Brain Institutes). Interestingly, most of the SAGA components exhibit a similar expression pattern (Table 1; RNA *in situ* database from Allen Brain Institutes), suggesting conserved functions of SAGA in CNS cells.

Gcn5 functions during development

Corresponding to its high expression levels in embryos, Gcn5 is essential for early embryonic development. Mice lacking Gcn5 die by embryonic day 10.5

(E10.5) (Xu et al., 2000). Gcn5 HAT activity also plays an essential role in neural tube closure (Bu et al., 2007). In addition to functions in neural development, proper levels of Gcn5 are also essential for correct rib and skeletal patterning in the mouse (Lin et al., 2008).

The deleterious phenotypes of *Gcn5* mutants not only suggest the importance of functions of Gcn5 during development, but also suggest the reason why no human inherited disease is directly associated with *Gcn5* mutation.

Potential neuronal functions of Gcn5 in adult mammals

Little is known about Gcn5 functions in adult tissues. The only previous evidence provided comes from *Gcn5* hypomorphic (*Gcn5^{fn/fn}*) mice that express ~20% normal cellular levels of Gcn5. Only 10% of the *Gcn5^{fn/fn}* mice survive till adulthood (Lin et al., 2008). These surviving *Gcn5^{fn/fn}* mice developed defects including ptosis (droopy eyes) and kyphosis (hunched posture) as they aged (Lin, unpublished data). Interestingly, this abnormal appearance resembles that in a mouse model of SCA7, which is caused by polyQ-Atxn7 (Yoo et al., 2003). In SCA7, adult onset ptosis and kyphosis are associated with retinal and cerebellar degeneration, respectively. As previously mentioned, both Atxn7 and polyQ-Atxn7 can incorporate into SAGA. Therefore the phenotypes in *Gcn5* hypomorphic mice urge the question whether Gcn5 plays an important role in maintaining healthy retina and cerebellum in adult mammals.

Transcriptional down regulation is associated with altered Gcn5 functions in SCA7 retina

Overexpression of polyQ-Atxn7 in yeast and in cultured human cell lines suggested that both Atxn7 and polyQ-Atxn7 incorporate into the SAGA complex. Some reports indicate that the incorporation of polyQ-Atxn7 reduces histone acetyltransferase (HAT) activity of SAGA complex (Helmlinger et al., 2006b; Helmlinger et al., 2004b; McMahon et al., 2005b). Since Gcn5 is the only component that carries HAT activity in SAGA, these data first suggested that polyQ-Atxn7 could hinder functions of Gcn5/SAGA, leading to cell toxicity.

Multiple SCA7 animal models show that polyQ-Atxn7 causes neurotoxicity (Garden et al., 2002; La Spada et al., 2001; Latouche et al., 2006; Yoo et al., 2003; Yvert et al., 2000; Yvert et al., 2001). Mice bearing one allele of 266 repeats of polyCAG in *Atxn7* recapitulate neurodegenerative phenotypes of the infantile form of SCA7, providing further evidence for polyQ-Atxn7 neurotoxicity. In these *Atxn7*^{266Q/5Q} mice, transcriptional down-regulation of photoreceptor-specific genes was associated with the early dysfunction and degeneration of photoreceptors (Yoo, 2003). Since Gcn5, as part of SAGA, functions as a transcription coactivator and interacts with polyQ-Atxn7, the transcriptional down-regulation in the polyQ-Atxn7 neurons may result from dysfunction of Gcn5. (Helmlinger et al., 2006a; La Spada et al., 2001; Palhan et al., 2005; Yoo et al., 2003). Consistent with this idea, previous work from two different groups indicates that altered function of Gcn5 strongly associates with this transcriptional

down regulation in early degenerating retina of two transgenic SCA7 models. Palhan *et al* showed that along with the transcriptional downregulation, hypo acetylated histones are enriched at gene promoters, and that Gcn5 has reduced HAT activity when polyQ-Atxn7 incorporates into SAGA. However another study provided contradictory evidence of change in function of Gcn5 (Helmlinger *et al.*, 2006a; Palhan *et al.*, 2005). In their polyQ-Atxn7 transgenic mice, Helmlinger *et al* found that polyQ-Atxn7-containing SAGA has no less HAT activity of Gcn5. Surprisingly, they also observed higher levels of SAGA enrichment along with hyperacetylated histones at the promoters of affected genes. An aberrant hyperacetylated genome was proposed to alter the structure of heterochromatin and change the distribution of RNA polymerase II. Although still inconclusive, this evidence suggests that altered Gcn5 functions play a key role in primary neurotoxicity of SCA7. However more evidence is needed to address how altered function of Gcn5 contributes to neurodegeneration in SCA7.

Goal and Significance

Current knowledge for physiological roles of Gcn5 in the mammalian nervous system is only to the stage of neurulation (Lin, 2007; Bu, 2008). Although suggested by observations in SCA7 models, whether Gcn5 is important for biological functions in postmitotic neurons still remains unclear. Since Gcn5 is expressed highly in adult neurons, **I hypothesized that Gcn5 supports normal functions of mature cerebellar and retinal neurons and that Gcn5**

dysfunction impairs cerebellar and retinal functions, which contributes to ataxia and neurodegeneration in Spinocerebellar Ataxia type-7.

To this end, I asked whether Gcn5 loss-of-function contributes to SCA7 neurodegeneration by genetically testing if reducing Gcn5 expression leads to more severe degeneration in a SCA7 mouse model. I also tested whether Gcn5 is essential in maintaining mature neuron functions by reducing Gcn5 specifically in neurons using mouse genetics. Together this study provides the first view of Gcn5 functions in mature neurons and provides new insights into possible therapeutic options for SCA7.

Chapter II

Materials and Methods

Generation of *Gcn5;Atxn7* and Purkinje cell-specific *Gcn5* mutant mouse models

Atxn7 230Q and *Atxn7* 100Q alleles were naturally occurring, contracted mutations of the 266Q tract in *Atxn7* obtained during maintenance of the *Atxn7*^{266Q/5Q} mouse line (Yoo et al., 2003). *Atxn7*^{100Q/5Q};*Gcn5*^{fn/+} or *Atxn7*^{100Q/5Q};*Gcn5*^{Δ/+} mice were generated by crossing *Gcn5*^{flox(neo)/+} or *Gcn5*^{Δ3-18/+} mice (Lin et al., 2007) with *Atxn7*^{100Q/5Q} mice. *Atxn7*^{100Q/5Q};*Gcn5*^{fn/fn} mice were generated by crossing *Gcn5*^{fn/+} and *Atxn7*^{100Q/5Q};*Gcn5*^{fn/+} mice. *Atxn7*^{100Q/100Q};*Gcn5*^{Δ/+} mice were generated by crossing *Atxn7*^{100Q/5Q};*Gcn5*^{Δ/+} and *Atxn7*^{100Q/5Q} mice.

Purkinje cell-specific *Gcn5* conditional nulls were obtained from crossing *Gcn5*^{Δ/+} mice that carry *Pcp2-cre*^{tg} (Barski et al., 2000; Barski et al., 2002) with *Gcn5*^{flox/flox} mice. Genotyping for *Gcn5* alleles and *Atxn7* alleles was performed using PCR primers as previously described (Lin et al., 2007; Yoo et al., 2003). *Pcp2-cre* genotype was assessed following the protocol for generic Cre by JAX lab website (http://jaxmice.jax.org/protocolsdb/f?p=116:2:3402763281359342:NO2:P2_MAS TER_PROTOCOL_ID,P2_JRS_CODE:288,004146). All procedures were performed in accordance with the approved IACUC protocols at MDACC.

Generation of *Gcn5*^{fn/fn} mice

Gcn5^{fn/fn} mice were generated by intercrossing *Gcn5*^{fn/+} males and females.

Survival analysis

PolyQ-Atxn7 mutant mice were housed with control littermates and given ad libitum supply of moist food upon ataxia as diagnosed. Moribund was defined by losing body weight of more than 20%, or loss of mobility. Statistical significant differences of lifespans were determined by Kaplan-Meier test.

Histological analyses

Mice were first anesthetized by intra peritoneal injection of Avertin. Deeply anesthetized animals were transcardially perfused with PBS followed by 4% paraformaldehyde. Isolated organs were fixed in 4% paraformaldehyde overnight. Fixed tissues were then preserved in paraffin or cryo- blocks. For *hematoxylin and eosin Y staining* (H&E), 6 μ m sections of paraffin-embedded mid-sagittal brain or eye were stained with H&E staining protocol (Fisher). Pictures were taken using Olympus SZX12 or Leica DM4000 microscope. For Immunofluorescent staining, 20 μ m sections of cryo-preserved tissues were used. Briefly, sections were boiled in 10 mM sodium citrate to retrieve antigen. 0.2% PBST was used for permeablizing and washing prior to incubation in anti-Gcn5 (Cell Signaling, 1:150), anti-Ataxin7 (Fisher, 1:250), anti-Calbindin (1:1000, Sigma) and anti-GFAP antibody (1:600, Dako). Signals were visualized using Alexa 555 -conjugated donkey anti-mouse or Alexa 488-conjugated donkey-anti rabbit antibody (all 1:750, Invitrogen). DAPI (Roche) counterstains the nucleus. All pictures were obtained using FV1000 Olympus confocal microscope.

Purkinje cell counts were done by counting nuclei of Purkinje cells in pictures of H&E-stained 6 μ m mid-sagittal cerebellar sections (three sections per mouse) from 3-4 mice each genotype using Image J software (National Institutes of Health). Samples were renumbered to avoid bias. Statistical significance was determined using Student's t tests.

Quantification Purkinje cell soma size. Purkinje cell perikaryons were manually outlined from 12 μ m z-stacked images of Calbindin1-labeled mid-sagittal cerebellums (3-4 images each mouse) using Image J software (National Institutes of Health). A total of 135 cells in lobule VI from 2-3 animals were analyzed for each genotype.

Electron Microscopy

Mice were intracardially perfused with 1.5% glutaldehyde plus 2 % paraformaldehyde after being deeply anesthetized by Avertin. Tissues were collected and sent to the High Resolution Electron Microscopy Facility, UTMDACC for further processing.

Footprint analyses

Behavioral tests were performed between 2-6 p.m. with animals maintained on a C57BL/6J:129/SvEv mixed background at F3 or F4 backcrossing to C57BL/6J.

Footprint analysis was done as previously described (Carter et al., 1999). Briefly, fore- and hind- paws of mouse were painted with nontoxic red and blue paints. Then the mouse was allowed to walk through a tunnel (17-inch-long, 3-inch-wide, 3-inch height) lined with a fresh paper at the bottom for each test. Statistical difference was first tested using one-way ANOVA between males and females. Data were only pooled together when there is no difference between genders. Statistical significant difference was determined by Kruskal-Wallis test.

Wirehang test

Wirehang test was performed following Shahbazian et al, 2002. Briefly, mice were habituated 2 minutes on a darkened platform (3 inch²) to establish a safety area before test. Each mouse was then allowed both fore paws to grab a 2.5 mm plastic wire attached to the platform. The time takes for the animal to reach the safety area, and the latency to fall were recorded. Three animals were tested for each genotype. The difference of time to fall among genotypes was calculated using non-parametric Kruskal-Wallis test.

Dowel test

Dowel test was performed following Shahbazian et al, 2002. Briefly, mice were habituated 2 minutes on a darkened platform (3 inch²) to establish a safety area before test. Each mouse was then allowed to land on the center of a horizontal 0.7 mm wooden dowel attached to the platform. The time takes for the animal to reach the safety area, and the latency to fall was recorded. Three

animals were tested for each genotype. The difference of time to fall among genotypes was calculated using non-parametric Kruskal-Wallis test.

Rotarod test

All mice were habituated for 7 consecutive days on the rotarod apparatus (IITC Life Science) before experimental trials. 4 tests were run each day for 4 consecutive days. Latency to fall was recorded by embedded timer triggered upon animal fell onto the floor plate. Three animals were included for each genotype. The difference of latency to fall among genotypes was calculated using non-parametric Kruskal-Wallis test.

Northern blot analysis

Total RNA was extracted using TRIZOL Reagent (Invitrogen) according to the instructions of manufacturer. 20 µg of total RNA was run on denaturing agarose then transferred to Hybond-N membrane for each sample. The membrane was then incubated with pre-hybridization buffer at 68 °C for 2 hrs before hybridization at 68°C overnight with denatured probes. All oligonucleotide probes were generated with Rediprime II random prime labeling with [32P]dCTP and linearized plasmid containing T7/T3 promoter and probe sequence. Gcn5 probe was generated following Xu et al, was used. Actin probe was used as internal control.

Quantitative RT-PCR and primers

All tissues were dissected and snap frozen in liquid nitrogen at 5-8 p.m. after overdose anesthesia with Avertin. Total RNA was prepared using TRIZOL Reagent (Invitrogen) according to the instructions of manufacturer followed by on column DNase I (Qiagen) treatment. cDNAs were generated using 200 ng of total RNA by SuperScript III reverse transcriptase (Invitrogen) with poly dT primers following the instructions of manufacturer. cDNA were quantified using specific primers and SYBR Green PCR Master Mix (Applied Biosystems). Triplicates were performed. β Actin was quantified as normalizing control. The mean value for three animals was used for the level of each genotype. Statistical difference was calculated using Student's t test. Primers used:

Gcn5-f: 5'- CAGTGGTGG AGGGGTCTCTA -3';

Gcn5-r: 5'- AAACATTGTCTGGCGCTCTC-3';

Actb-f: 5'- GGCTGTATTCCCCTCCATCG -3';

Actb-r: 5'- CCAGTTGGTAACAATGCCATGT-3';

S-opsin-f: 5'- CAGCCTTCATG GGATTTGTCT -3';

S-opsin-r: 5'- CAAAGA GGAAGTATCCGTGACAG -3';

M-opsin-f: 5'- ATGGCCCAAAGGCTTACAGG -3';

M-opsin-r: 5'- CCACAAGAATC ATCCAGGTGC -3';

rhodopsin-f: 5'- CCCTTCTCCAACGTCACAGG -3';

rhodopsin-r: 5'- TGAGGAAGTTGATGGG GAAGC -3';

Grk-f: 5'- CGGGGCAGTTTTGACGGAA -3';

Grk-r: 5'- AGCTGA GGTTGTCACGGAGA -3';

Rom1-f: 5'- CTCCAACCCCGT ATCCGTTTG -3';

Rom1-r: 5'- GAGCAGGGAATGAACAAGAGG -3';
Cnga3-f: 5' –TCGACCAC GTAGAGAACGG -3';
Cnga3-r: 5' – TGGAGGGGTCCACCACAAT -3';
Rbp3-f: 5'- ATGAGAGAATGGGTCCTGGTT -3';
Rbp3-r: 5'- GCCCAGAATCTCGTGA CTC TTC -3';
Gnat1-f: 5'– GATGCCCCGCACTGTGAAAC -3';
Gnat1-r: 5'– CCAG CGAATACCCGTCCTG -3';
Crx-f: 5'– GTTCAAGAATCGTAGGGCGAA -3';
Crx-r: 5'– TGAGATGCCCAAAGGATCTGT -3'.

Chapter III

Results

Some parts of this chapter were published in this article:

Chen YC, Gatchel JR, Lewis RW, Mao CA, Grant PA, Zoghbi HY, and Dent SYR. *Gcn5* loss-of-function accelerates cerebellar and retinal degeneration in a SCA7 mouse model.

Short lifespan of polyQ-Atxn7 mice

To assess the role of Gcn5 in the neurodegeneration observed in a mouse model of SCA7, I introduced different mutant alleles of *Gcn5* into polyQ-Atxn7 knock-in mice that express polyQ-Atxn7 from the endogenous *Atxn7* locus. I predicted that if reduced Gcn5 function contributes to SCA7 pathogenesis, reducing Gcn5 expression would enhance disease progression. Although the previously reported polyQ-Atxn7 knock-in line, *Atxn7*^{266Q/5Q}, nicely recapitulates the infantile form of SCA7 (Yoo et al., 2003), disease progression in these mice occurs rapidly, making it difficult to observe an enhancement of the already severe SCA7 phenotypes. Therefore, to better characterize the role of Gcn5 loss-of-function, I utilized SCA7 mouse lines that have a more moderate disease progression generated by Dr. Huda Zoghbi's lab.

The length of the CAG repeat in the *Atxn7* gene correlates inversely with the timing of disease onset, and directly with severity, so we characterized the disease progression and the age of lethality in *Atxn7* mutant mice bearing shorter polyQ tracts (David et al., 1998; Giunti et al., 1999; Johansson et al., 1998; Martin et al., 1999). Specifically, I compared the life span of mice bearing no expansion in *Atxn7* (*Atxn7*^{5Q/5Q}) to those bearing 100 CAG repeats (*Atxn7*^{100Q/5Q}) or 230 CAG repeats (*Atxn7*^{230Q/5Q}) in one allele of *Atxn7*. Both *Atxn7*^{100Q/5Q} and *Atxn7*^{230Q/5Q} mice develop previously described symptoms of SCA7 mouse models including weight loss, kyphosis, ataxia, ptosis, tremors, gradual loss of mobility (Yoo et al., 2003 and this study, data not shown). We recorded the age at

which these animals died or became moribund up to 24 months. Wild type *Atxn7*^{5Q/5Q} mice (wt) (Figure 2A) had a lifespan of greater than 24 months, whereas *Atxn7*^{100Q/5Q} mice had a significantly shorter lifespan ($p < 0.001$), averaging 18.7 months. *Atxn7*^{230Q/5Q} mice died at a very early age, with a lifespan averaging only 3.5 months (Figure 2A). The shorter lifespan of the animals bearing longer repeats confirms the correlation between repeat length and lethality in these mouse models of SCA7. Disease progression was accelerated by the presence of a second polyQ-expanded allele of *Atxn7*, as *Atxn7*^{100Q/100Q} mice died at an earlier age than did the *Atxn7*^{100Q/5Q} mice ($p < 0.001$), with a lifespan averaging 12.1 months (Figures 2A & 3).

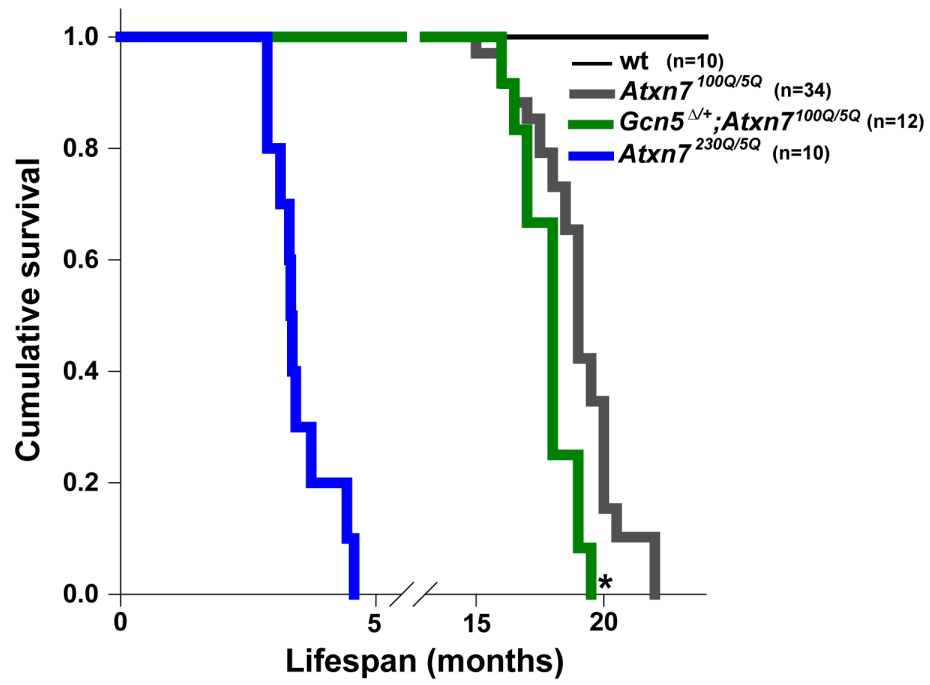
Since polyQ-Atxn7 forms nuclear inclusions, I also examined whether polyQ-Atxn7 inclusions were formed in mice that carry 100Q-Atxn7. By immunofluorescent labeling Atxn7 in the cerebellum, signals of Atxn7 are diffuse in the nuclei of the Purkinje cells of *Atxn7*^{100Q/5Q} mice at 3 months. More condensed Atxn7 nuclear signals appear in Purkinje cells at 6 months, while signals of strong nuclear inclusions appeared at 1 year in *Atxn7*^{100Q/5Q} mice (Figure 4). These findings suggest that polyQ-Atxn7 progressively forms nuclear inclusions between 6 months and 1 year of age in *Atxn7*^{100Q/5Q} mice.

Figure 2. *Gcn5* mutation reduces lifespan of *Atxn7*^{100Q/5Q} mice

(A) Survival rate of wild type (thin black line), *Atxn7*^{230Q/5Q} (blue line), *Atxn7*^{100Q/5Q} (grey line), and *Atxn7*^{100Q/5Q};*Gcn5*^{Δ/+} (green line), until 24 months of age (wt, n=10; *Atxn7*^{230Q/5Q}, n=10; *Atxn7*^{100Q/5Q}, n=34; *Atxn7*^{100Q/5Q};*Gcn5*^{Δ/+}, n=12; * p<0.05 between *Atxn7*^{100Q/5Q} and *Atxn7*^{100Q/5Q};*Gcn5*^{Δ/+}, Kaplan-Meier analysis).

(B) Survival rate of wild type (thin black line), *Atxn7*^{100Q/5Q} (grey line), and *Atxn7*^{100Q/5Q};*Gcn5*^{fn/+} (dark red line), until 24 months of age (wt, n=10; *Atxn7*^{100Q/5Q}, n=34; *Atxn7*^{100Q/5Q};*Gcn5*^{fn/+}, n=22; * p<0.05 between *Atxn7*^{100Q/5Q} and *Atxn7*^{100Q/5Q};*Gcn5*^{fn/+}, Kaplan-Meier analysis).

A



B

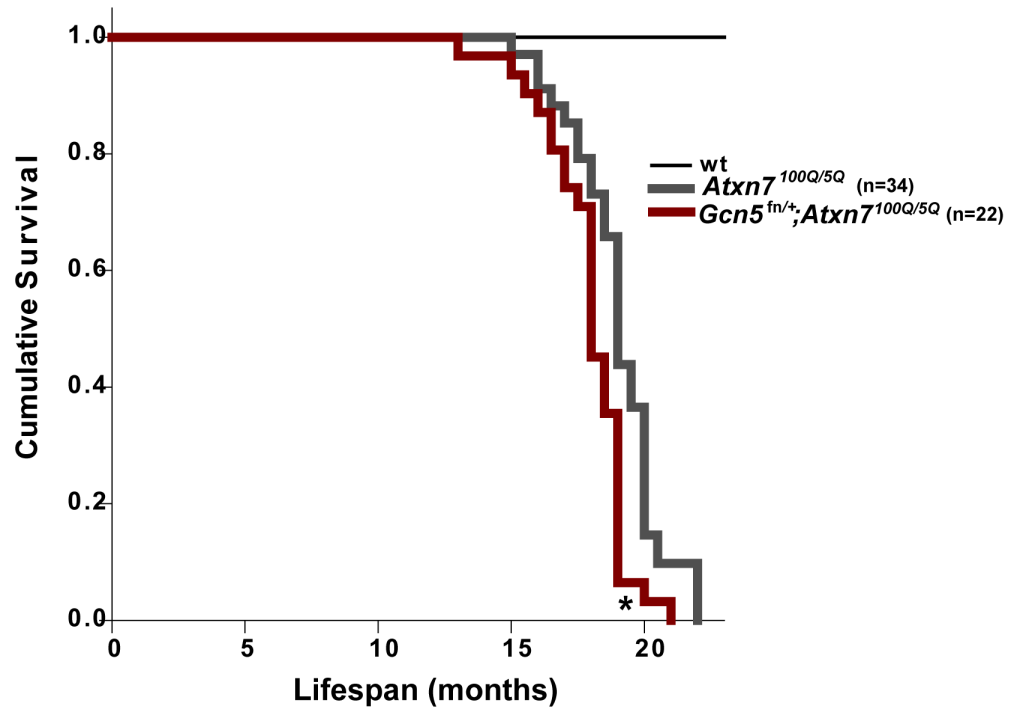


Figure 2

Figure 3. Lifespan of *Atxn7*^{100Q/100Q} and *Atxn7*^{100Q/100Q};*Gcn5*^{Δ/+} mice

Survival rate of wild type (thin black line), *Atxn7*^{100Q/100Q} (thick black line), and *Atxn7*^{100Q/100Q};*Gcn5*^{Δ/+} (red line), until 24 months of age (wt, n=10; *Atxn7*^{100Q/100Q}, n=18; *Atxn7*^{100Q/5Q};*Gcn5*^{Δ/+}, n=12; Kaplan-Meier analysis).

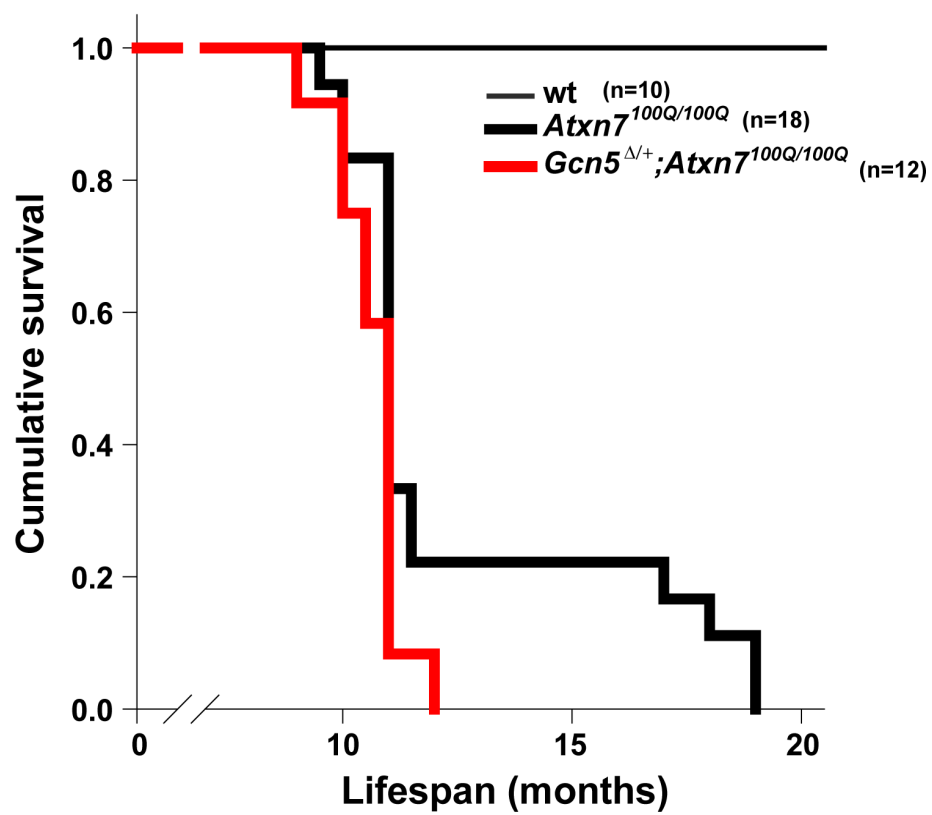


Figure 3

Figure 4. PolyQ-Atxn7 forms nuclear inclusion in Purkinje cells of *Atxn7*^{100Q} mice

Atxn7 was labeled using immunofluorescent staining on sagittal sections of cerebellum of *Atxn7*^{100Q/5Q} mice at 3, 6 month, or 1 year of age. Purkinje cells were labeled using anti-Calbindin. Nuclei were labeled with Topro-3. Arrowhead pointed to the strong signal of Atxn7 nuclear inclusion. Boxed area in picture of 1 year old cerebellum was enlarged for detailed structure.

Atxn7^{100Q/5Q}

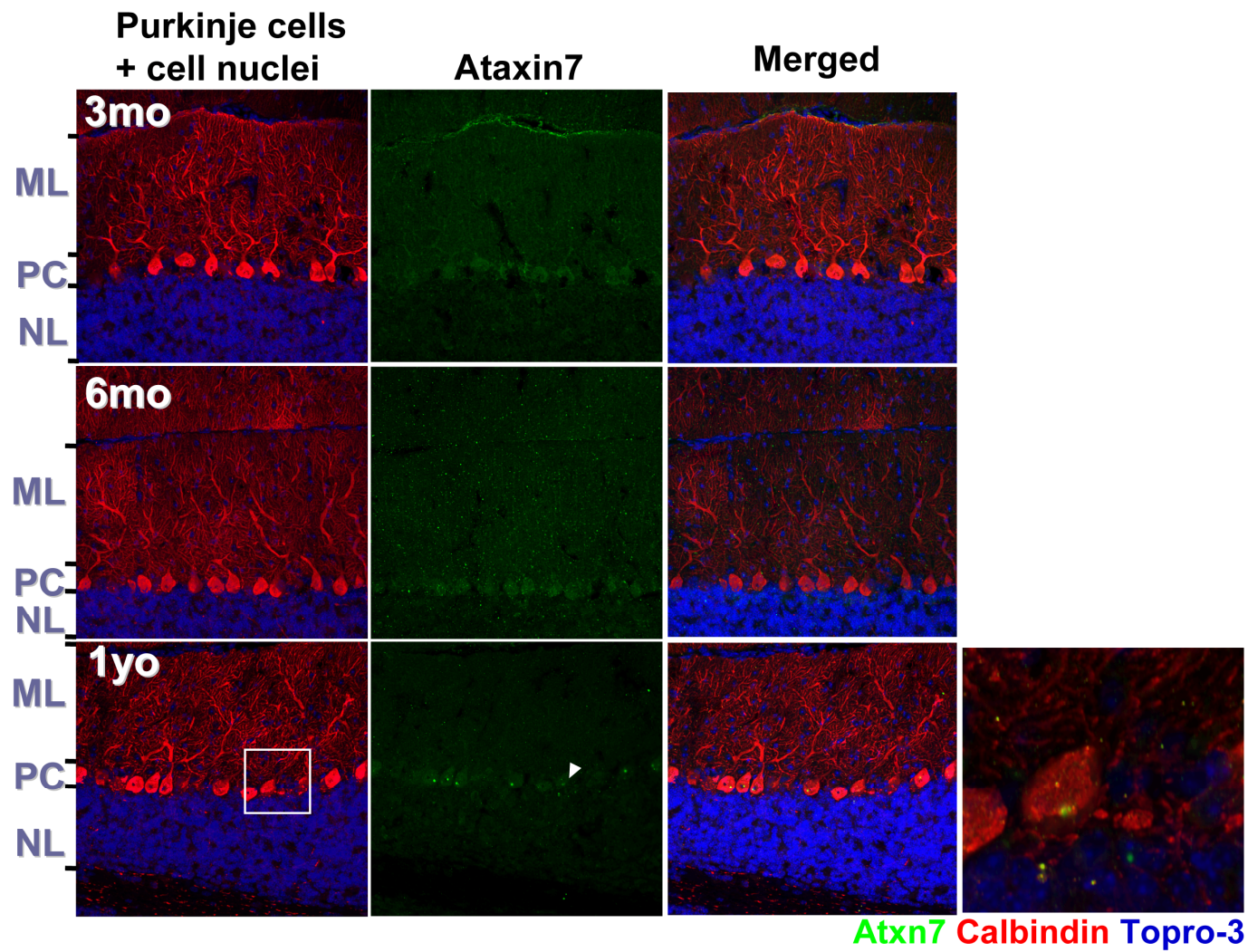


Figure 4

Altogether, these data suggest that 100Q-Atxn7 mice recapitulate human SCA7 features and provide a suitable model to test how function of Gcn5 is involved in neurotoxicity of SCA7.

Reducing Gcn5 shortens lifespan of polyQ-Atxn7 mice

Gcn5 null mice are embryonic lethal (Xu et al., 2000). Therefore, to assess the role of partial loss-of-function of *Gcn5* in SCA7 pathogenesis, I introduced a hypomorphic allele of *Gcn5*, which reduces the level of Gcn5 expression and activity, into *Atxn7*^{100Q/5Q} mice. The hypomorphic *Gcn5*^{fn} allele contains an intronic neomycin cassette insertion that lowers Gcn5 expression to ~ 20% of wild type levels in the homozygous state (Figure 5A & Lin et al., 2008a). Mice homozygous for this allele can survive to adulthood, albeit at a reduced frequency (Lin et al., 2008a). I created *Atxn7*^{100Q/5Q};*Gcn5*^{fn/fn} mice and found that the combination of these alleles resulted in lethality at postnatal day 1 (P1) (Table 4). This early lethality indicated that concomitant diminishment of both Gcn5 and Atxn7 functions is deleterious, but it also prohibited us from determining the effects of altered Gcn5 functions in mature neurons.

I therefore introduced single copies of either *Gcn5* hypomorphic allele (*Gcn5*^{fn/+}), or a deletion allele (*Gcn5*^{Δ/+}), resulting in a 50 % reduction of Gcn5 expression, into *Atxn7*^{100Q/5Q} or *Atxn7*^{100Q/100Q} mice (Figure 6 and Lin et al., 2008b). In contrast to the P1 lethality of *Atxn7*^{100Q/5Q};*Gcn5*^{fn/fn} animals, *Atxn7*^{100Q/5Q};*Gcn5*^{Δ/+} and *Atxn7*^{100Q/5Q};*Gcn5*^{fn/+} mice were born alive at expected

Mendelian frequencies and had indistinguishable cage behaviors from those of wild type littermates until the time of weaning, at 3 weeks of age. As expected, the retina, cerebellum, and the liver of *Atxn7*^{100Q/100Q};*Gcn5*^{Δ/+} mice express ~50% level of Gcn5 in *Atxn7*^{100Q/100Q} mice (Figure 6). The level of Gcn5 remains mostly unchanged along with age in various tissues (Figure 7).

The survival of *Gcn5* mutant heterozygotes was no different from that of wild type mice (Figure 2 and data not shown), but the life span of *Atxn7*^{100Q/5Q};*Gcn5*^{Δ/+} and *Atxn7*^{100Q/5Q};*Gcn5*^{fn/+} mice was significantly reduced relative to *Atxn7*^{100Q/5Q} mice ($P < 0.01$, Figure 2). Partial loss of Gcn5 function also reduced the survival of *Atxn7*^{100Q/100Q} mice (average life span of 10.7 ± 7.5 months in *Atxn7*^{100Q/100Q};*Gcn5*^{Δ/+} mice compared to 12.1 ± 2.9 months in *Atxn7*^{100Q/100Q} mice). Interestingly, while 22 % of the *Atxn7*^{100Q/100Q} mice lived over 1.5 years, none of the *Atxn7*^{100Q/100Q};*Gcn5*^{Δ/+} mice survived more than 1 year (Figure 3). These data strongly suggest that decreased Gcn5 levels accelerate the early adult lethality of mice bearing *Atxn7*^{100Q} alleles, supporting the hypothesis that Gcn5 loss-of-function may contribute to SCA7 pathogenesis.

Reducing Gcn5 worsens ataxia of polyQ-Atxn7 mice

Since ataxia (uncoordinated locomotion) is one of the major neurological symptoms of SCA7 patients and mouse models (Custer et al., 2006; David et al., 1997; David et al., 1998; Giunti et al., 1999; Yoo et al., 2003), I next asked if reducing Gcn5 function contributes to the progression of ataxia in our SCA7 mouse model. We first examined mouse hindlimb activity using a tail suspension

Table 4: Progeny of crosses between *Gcn5*^{flox(neo)/+} and

***Atxn7*^{100Q/5Q}; *Gcn5*^{flox(neo)/+} mice**

P21

Genotype	Number	Percent observed (expected)
<i>Gcn5</i> ^{+/+} ; <i>Atxn7</i> ^{5Q/5Q}	36	25 (12.5)
<i>Gcn5</i> ^{+/+} ; <i>Atxn7</i> ^{100Q/5Q}	31	19 (12.5)
<i>Gcn5</i> ^{1n/+} ; <i>Atxn7</i> ^{5Q/5Q}	50	31 (25)
<i>Gcn5</i> ^{1n/+} ; <i>Atxn7</i> ^{100Q/5Q}	39	22 (25)
<i>Gcn5</i> ^{1n/1n} ; <i>Atxn7</i> ^{5Q/5Q}	2	1 (1.25)
<i>Gcn5</i> ^{1n/1n} ; <i>Atxn7</i> ^{100Q/5Q}	0	0 (1.25)

P1

Genotype	Number	Percent observed (expected)
<i>Gcn5</i> ^{+/+} ; <i>Atxn7</i> ^{5Q/5Q}	2	10 (12.5)
<i>Gcn5</i> ^{+/+} ; <i>Atxn7</i> ^{100Q/5Q}	1	5 (12.5)
<i>Gcn5</i> ^{1n/+} ; <i>Atxn7</i> ^{5Q/5Q}	4	20 (25)
<i>Gcn5</i> ^{1n/+} ; <i>Atxn7</i> ^{100Q/5Q}	3	15 (25)
<i>Gcn5</i> ^{1n/1n} ; <i>Atxn7</i> ^{5Q/5Q}	5*	25 (12.5)
<i>Gcn5</i> ^{1n/1n} ; <i>Atxn7</i> ^{100Q/5Q}	5*	25 (12.5)

*Die soon after birth

E18.5

Genotype	Number	Percent observed (expected)
<i>Gcn5</i> ^{+/+} ; <i>Atxn7</i> ^{5Q/5Q}	3	4 (12.5)
<i>Gcn5</i> ^{+/+} ; <i>Atxn7</i> ^{100Q/5Q}	3	4 (12.5)
<i>Gcn5</i> ^{1n/+} ; <i>Atxn7</i> ^{5Q/5Q}	27	38 (25)
<i>Gcn5</i> ^{1n/+} ; <i>Atxn7</i> ^{100Q/5Q}	19	27 (25)
<i>Gcn5</i> ^{1n/1n} ; <i>Atxn7</i> ^{5Q/5Q}	9	13 (12.5)
<i>Gcn5</i> ^{1n/1n} ; <i>Atxn7</i> ^{100Q/5Q}	7	10 (12.5)

Figure 5. Reduced level of Gcn5 in cells of Gcn5 mutants.

Level of *Gcn5* transcript normalized with β -Actin in mouse embryonic fibroblasts from wildtype, *Gcn5*^{fn/+}, *Gcn5*^{fn/fn}, or *Gcn5*^{fn/ Δ} mice determined by Northern blot.

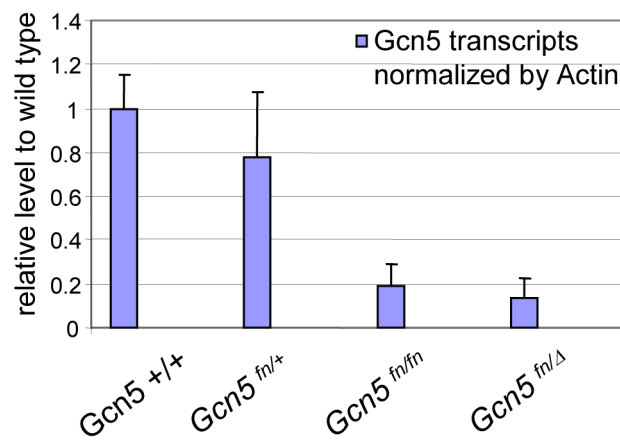
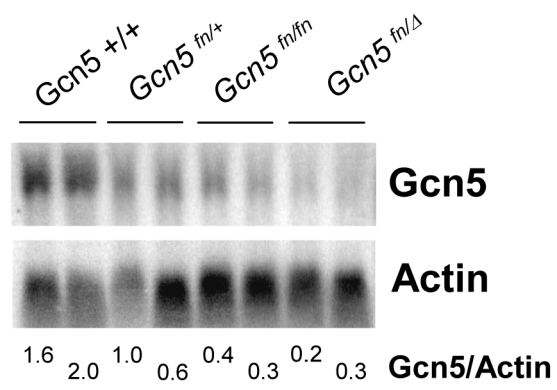


Figure 5

Figure 6. Reduced level of Gcn5 in mice with *Gcn5*^{Δ/+} mutation.

Relative transcript level of Gcn5 in the retina, cerebellum and liver of wt, *Gcn5*^{Δ/+}, *Atxn7*^{100Q/100Q} and *Atxn7*^{100Q/100Q};*Gcn5*^{Δ/+} mice determined by realtime RT PCR (n=3 mice, *p<0.05, between wt and *Gcn5*^{Δ/+}, *Atxn7*^{100Q/100Q} and *Atxn7*^{100Q/100Q};*Gcn5*^{Δ/+}, or wt and *Atxn7*^{100Q/100Q};*Gcn5*^{Δ/+}). Data are presented as mean± SD.

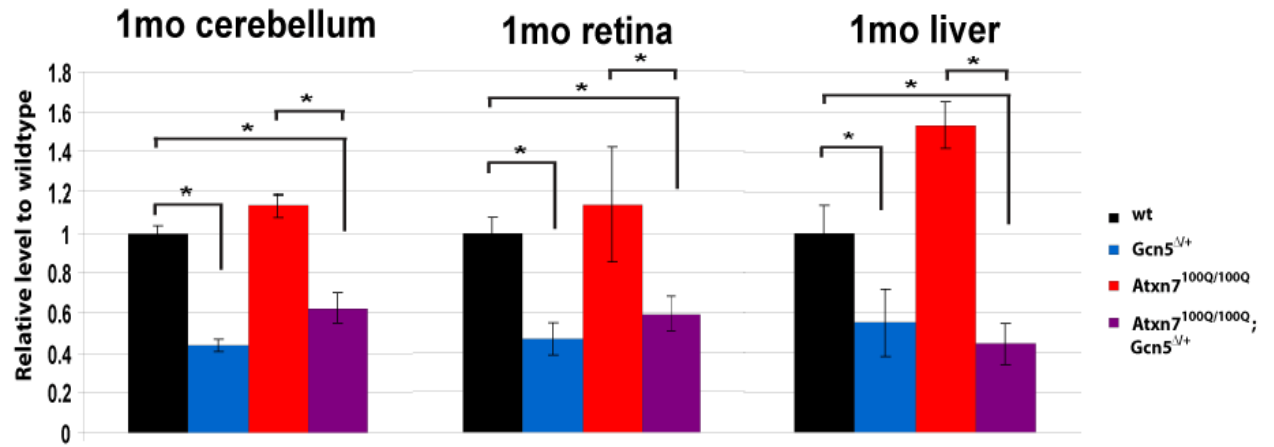


Figure 6

Figure 7. Gcn5 RNA levels remain constant during disease progression in *Atxn7^{100Q/100Q}* and *Atxn7^{100Q/100Q};Gcn5^{Δ/+}* mice.

Relative transcript levels to wt in the retina of wt, *Gcn5^{Δ/+}*, *Atxn7^{100Q/100Q}*, and *Atxn7^{100Q/100Q};Gcn5^{Δ/+}* mice at p14, 1 month, 1.5 month and 4 month of age (n=3 mice, *p<0.05, between wt and *Gcn5^{Δ/+}*, or wt and *Atxn7^{100Q/100Q};Gcn5^{Δ/+}* of same age, Student's t test). Data are presented as mean± SD.

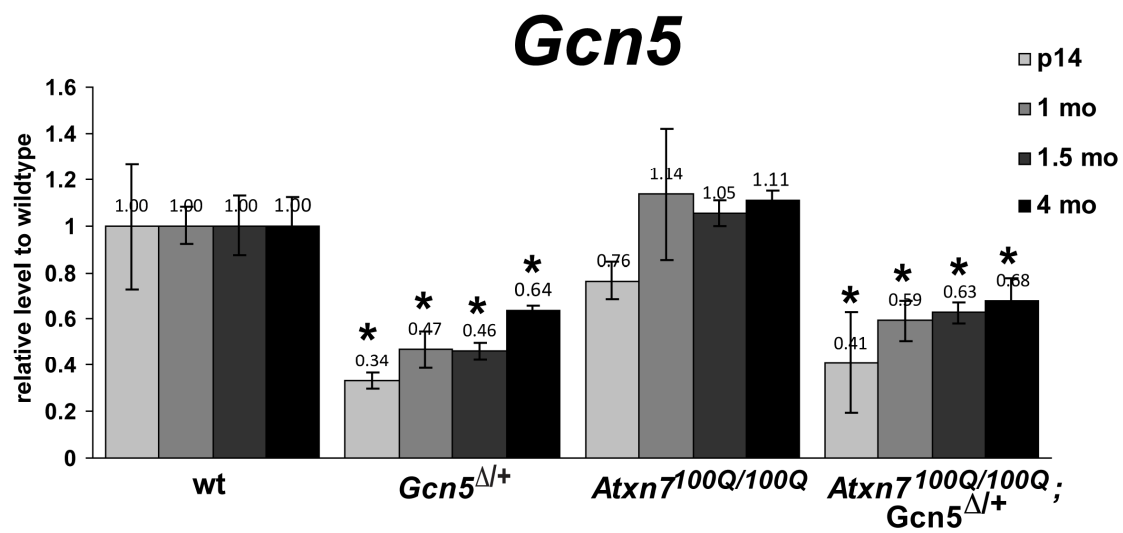


Figure 7

test (Lalonde, 1987). Wild type and *Gcn5*^{Δ/+} mice were able to coordinate stretching of their hind limbs when suspended by their tails (to prepare for landing if dropped). By 7-8 months of age, 100 % (12 out of 12) of *Atxn7*^{100Q/100Q} mice also stretched their hind limbs normally upon tail suspension, while only 33.3 % (2 out of 6) of *Atxn7*^{100Q/100Q};*Gcn5*^{Δ/+} mice were able to perform normally. Interestingly, one of the four uncoordinated *Atxn7*^{100Q/100Q};*Gcn5*^{Δ/+} mice developed a severe clasping phenotype (Figure 8), and the gait of this mouse deteriorated over time into a severe stagger, causing the mouse to frequently fall to one side up until its death at 8 months of age. Conversely, 92 % (11 out of 12) of *Atxn7*^{100Q/100Q} mice were able to normally coordinate stretching of their hind limbs, and no clasping phenotype was observed in these twelve *Atxn7*^{100Q/100Q} mice throughout their life.

To further evaluate the progression of ataxic gaits, I used a footprint test to quantify changes in the gait of *Atxn7*^{100Q/100Q}, *Atxn7*^{100Q/100Q};*Gcn5*^{Δ/+}, and wildtype mice at 4 months and 8-9 months of age. At 4 months, I found no significant differences between the gaits of *Atxn7*^{100Q/100Q}, *Atxn7*^{100Q/100Q};*Gcn5*^{Δ/+} and control mice (data not shown). However at 8-9 months of age, both *Atxn7*^{100Q/100Q} and *Atxn7*^{100Q/100Q};*Gcn5*^{Δ/+} mice walked with a significantly wider hind stance (wt, n=5, *Atxn7*^{100Q/100Q}, n=5, *Atxn7*^{100Q/100Q};*Gcn5*^{Δ/+}, n=3, p< 0.05, for hindbase width) and dispersed fore- and hind-steps (p< 0.05, for paired distance) relative to wild type mice (Figure 9). Moreover, this uncoordinated walking gait was significantly worse in *Atxn7*^{100Q/100Q};*Gcn5*^{Δ/+} and *Atxn7*^{100Q/5Q};*Gcn5*^{Δ/+} mice than in

Figure 8. Reducing the level of Gcn5 enhances clasping phenotypes of *Atxn7*^{100Q/100Q} mice.

Clasping phenotype of *Atxn7*^{100Q/100Q}; *Gcn5*^{Δ/+} but not *Atxn7*^{100Q/100Q} or wild type mice at 8 month of age during tail suspension test.

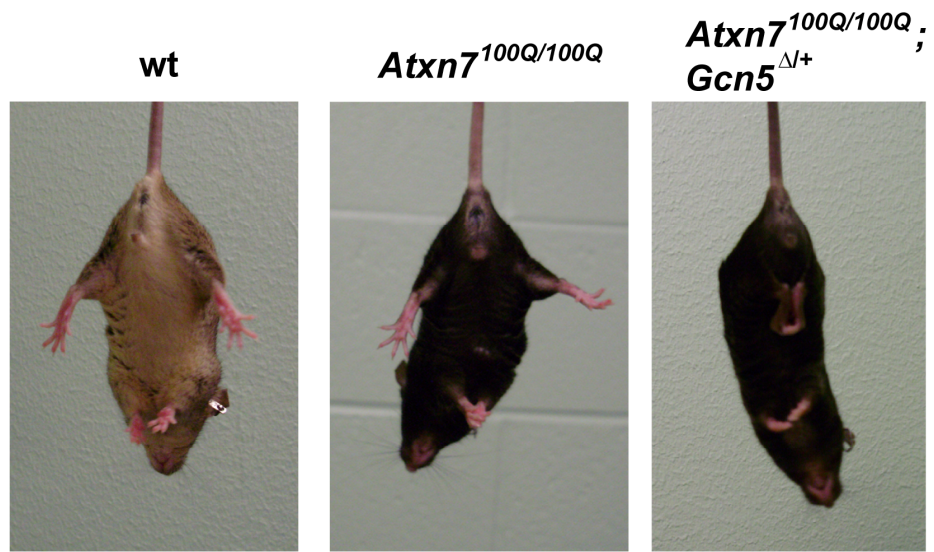
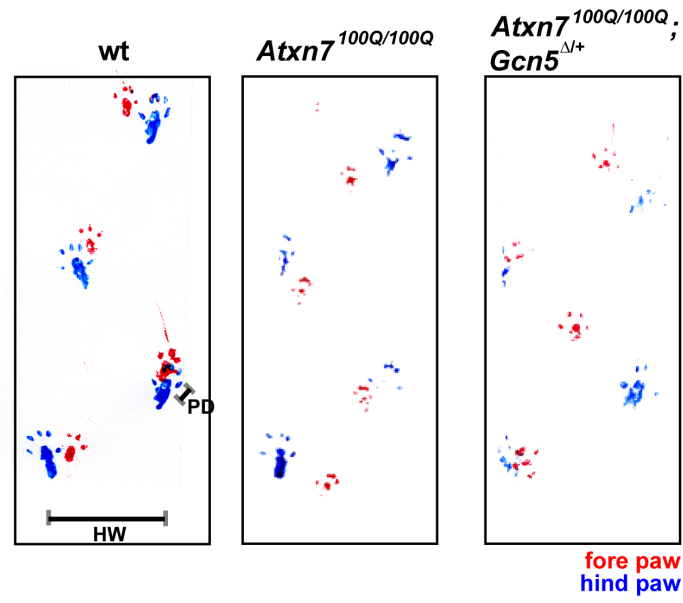
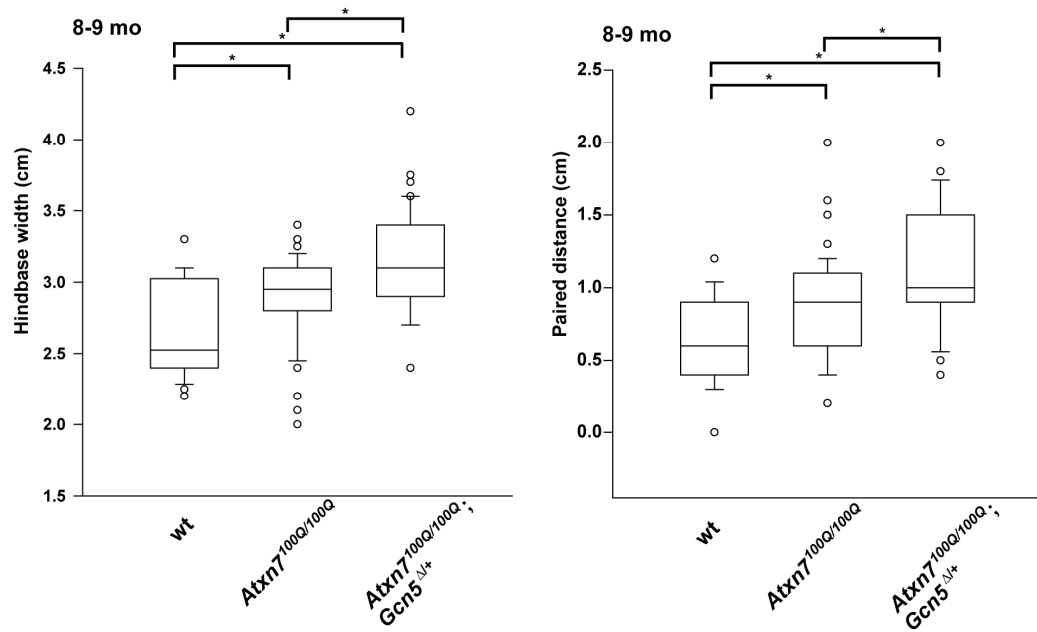


Figure 8

Figure 9. Reducing the level of Gcn5 enhances gait ataxia of *Atxn7*^{100Q/100Q} mice.

Representative traces of the gait of wild type, *Atxn7*^{100Q/100Q}, and *Atxn7*^{100Q/100Q};*Gcn5*^{Δ/+} mice recorded by footprint analysis, with red and blue footprints representing fore- and hind-paws, respectively. Uncoordinated gait of *Atxn7*^{100Q/100Q} or *Atxn7*^{100Q/100Q};*Gcn5*^{Δ/+} mice at 8-9 months of age. Paired distance (PD) measures the distance between the prints of fore- and hind-paw on the same side. Hind-base width (HW) measures the distance between the prints of the two hind-paws. (C) Quantified hind-base width or paired distance indicates *Atxn7*^{100Q/100Q};*Gcn5*^{Δ/+} mice have more uncoordinated walking gaits than *Atxn7*^{100Q/100Q} mice at 9 months of age (wt, n= 3; *Atxn7*^{100Q/100Q}, n= 4; *Atxn7*^{100Q/100Q};*Gcn5*^{Δ/+}, n= 3; *p<0.05 between wt and *Atxn7*^{100Q/100Q}, wt and *Atxn7*^{100Q/100Q};*Gcn5*^{Δ/+}, or *Atxn7*^{100Q/100Q} and *Atxn7*^{100Q/100Q};*Gcn5*^{Δ/+}, Kruskal-Wallis test). Data expressed as boxes plots (boxes, 25–75%; circles, <10 or >90%; lines, median).

A**B****Figure 9**

Atxn7^{100Q/100Q} and *Atxn7*^{100Q/5Q} mice, respectively (p<0.05) (Figures 9 & 10). To assess motor balance, *Atxn7*^{100Q/100Q}, *Atxn7*^{100Q/100Q};*Gcn5*^{Δ/+} and control wild type mice were subjected to rotating rod, dowel, and wire hang tests. Although *Atxn7*^{100Q/100Q} and *Atxn7*^{100Q/100Q};*Gcn5*^{Δ/+} mice showed a trend of dysfunction, the differences observed were not statistically significant (Figure 11). These results indicate that *Atxn7*^{100Q/5Q} and *Atxn7*^{100Q/100Q} mice progressively develop mild ataxia, and that Gcn5 partial loss-of-function accelerates the onset and progression of this ataxia in these SCA7 mouse models.

Reducing Gcn5 worsens cerebellar degeneration of polyQ-Atxn7 mice

Since cerebellar degeneration occurs in human SCA7 patients at moderate/late stages of the disease and strongly correlates with uncoordinated movement, I next asked whether more severe cerebellar atrophy occurred in *Atxn7*^{100Q/100Q} mice haplo-insufficient for Gcn5. The cerebellar vermis showed mild cortical atrophy specifically in the molecular layer of lobules VI, VII and X in both *Atxn7*^{100Q/100Q} and *Atxn7*^{100Q/100Q};*Gcn5*^{Δ/+} mice at 8-9 months of age, however the atrophy was noticeably more severe in the double mutants (Figure 12). Since the molecular layer spans the dendrites or processes of Purkinje cells and Bergmann glia, and both of these cell types are affected in SCA7 patients and mouse models (Custer et al., 2006; Yvert et al., 2000), we performed a more detailed analysis of these cells in the mutant mice. In particular, I focused on lobule VI of the cerebellar vermis, in which Purkinje and glial cell activities are

Figure 10. *Gcn5* hypomorphic alleles enhance ataxia phenotypes of *Atxn7*^{100Q/5Q} mice.

(A) Clasping phenotype of *Atxn7*^{100Q/5Q};*Gcn5*^{Δ/+} but not *Atxn7*^{100Q/5Q} or wildtype mice at 16 month old during tail suspension. (B) Earlier onset of uncoordinated gait in *Atxn7*^{100Q/5Q};*Gcn5*^{fn/+}, and *Atxn7*^{100Q/5Q};*Gcn5*^{Δ/+} mice. Representative walking gait of wildtype, *Atxn7*^{100Q/5Q}, *Atxn7*^{100Q/5Q};*Gcn5*^{fn/+}, and *Atxn7*^{100Q/5Q};*Gcn5*^{Δ/+} mice at age of 16 months recorded by footprint analysis with red and blue footprints represent fore- and hindpaws, respectively. At 15 months of age, both *Atxn7*^{100Q/5Q};*Gcn5*^{fn/+}, and *Atxn7*^{100Q/5Q};*Gcn5*^{Δ/+} mice have uncoordinated walking gait while *Atxn7*^{100Q/5Q} mice have impaired walking at 16 months of age as shown by quantified hindbase width or paired distance (wt, n= 3 ; *Atxn7*^{100Q/5Q}, n= 5; *Atxn7*^{100Q/5Q};*Gcn5*^{fn/+}, n= 3; *Atxn7*^{100Q/5Q};*Gcn5*^{Δ/+}, n= 3; *p<0.05, Kruskal-Wallis test). Data expressed as boxes plots (boxes, 25–75%; circles, <10 or >90%; lines, median).

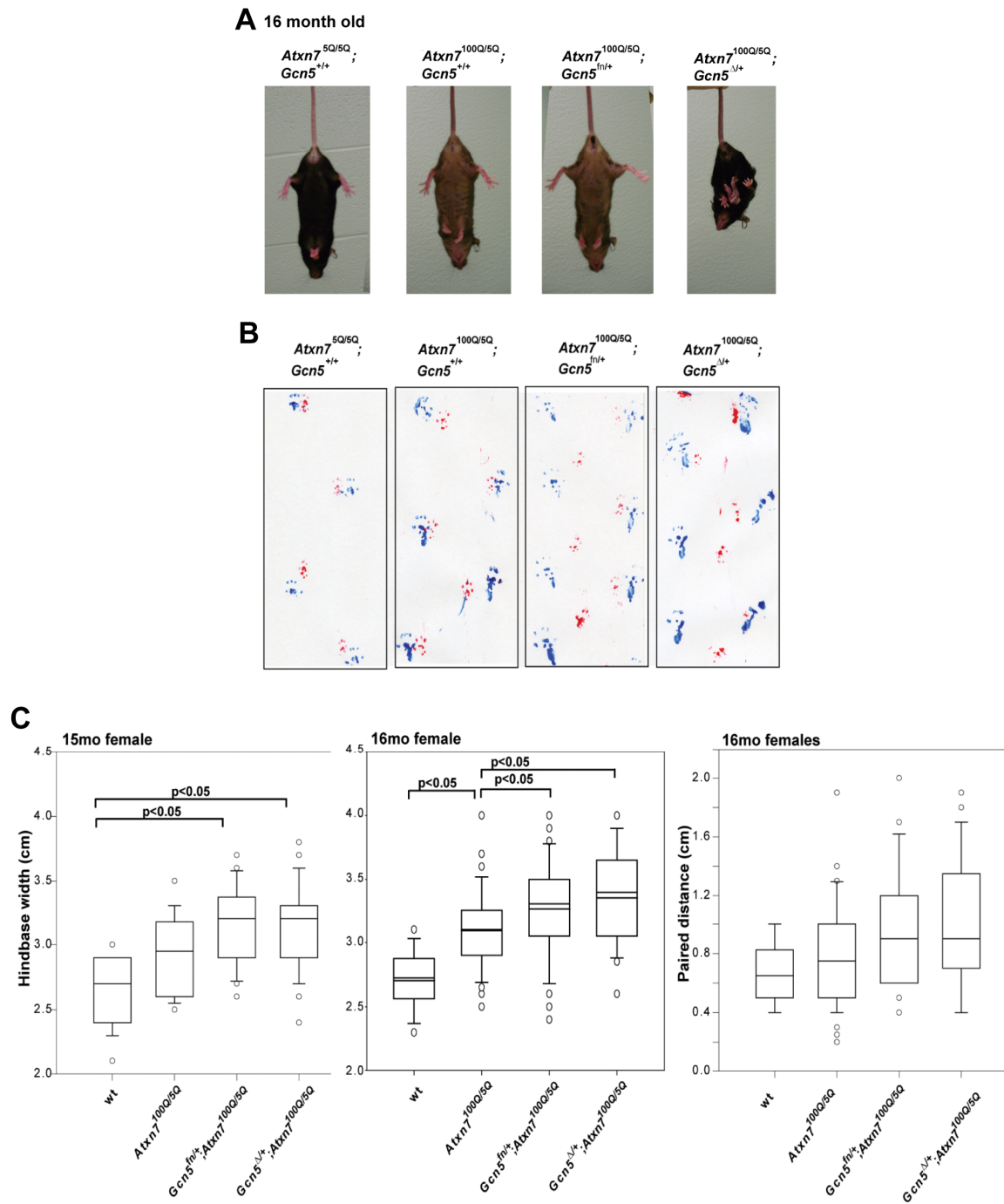
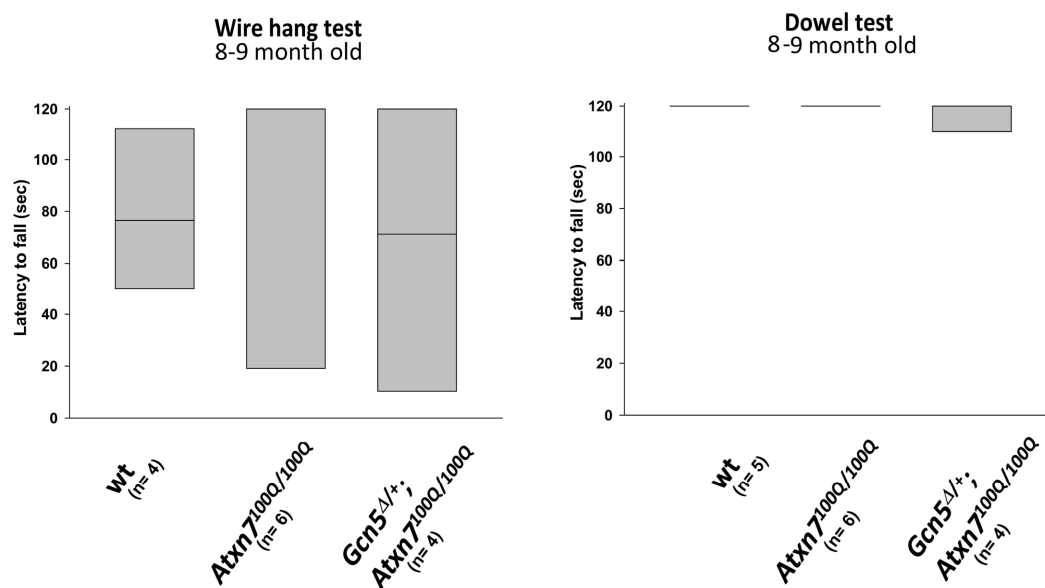


Figure 10

Figure 11. Analysis of other motor skills of *Atxn7*^{100Q/100Q} mice with *Gcn5* mutations.

(A) In wire hang or dowel tests, no statistical difference was observed between the performance of wildtype and *Atxn7*^{100Q/100Q}, or *Atxn7*^{100Q/100Q};*Gcn5*^{Δ/+} mice at age of 8-9 months. N=4-6 for each genotype. Data expressed as boxes plots (boxes, 25–75%; circles, <10 or >90%; lines, median). (B) Similar performance on rotorod for mice all genotypes at age of 8-9 months. Wildtype, black diamond; *Gcn5*^{fn/+}, open square; *Atxn7*^{100Q/100Q}, orange circle; *Atxn7*^{100Q/100Q};*Gcn5*^{fn/+}, purple circle. n=3 for each genotype. Data are presented as mean± SD.

A



B

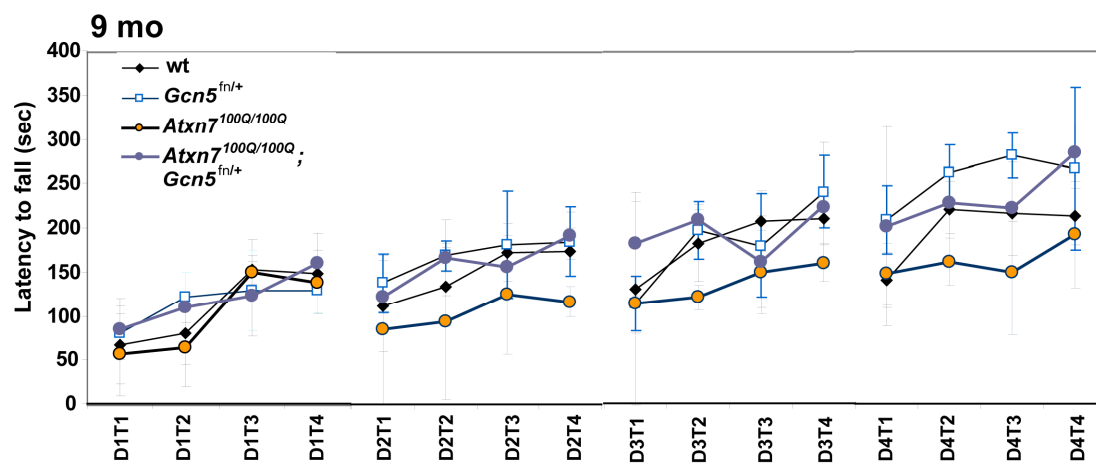


Figure 11

Figure 12. No dramatic atrophy in the cerebellum of *Atxn7*^{100Q/100Q} mice with or without a background of *Gcn5*^{Δ/+} at age of 5 months.

(A) Representative images showing morphology of midsagittal cerebellar vermis of 5 month-old wildtype, *Gcn5*^{Δ/+}, *Atxn7*^{100Q/100Q} and *Atxn7*^{100Q/100Q};*Gcn5*^{Δ/+} mice.

(B) Enlarged pictures of boxes of areas in lobule VI and X in (A) for detailed comparison. Thickness of molecular layer (ML) was marked.

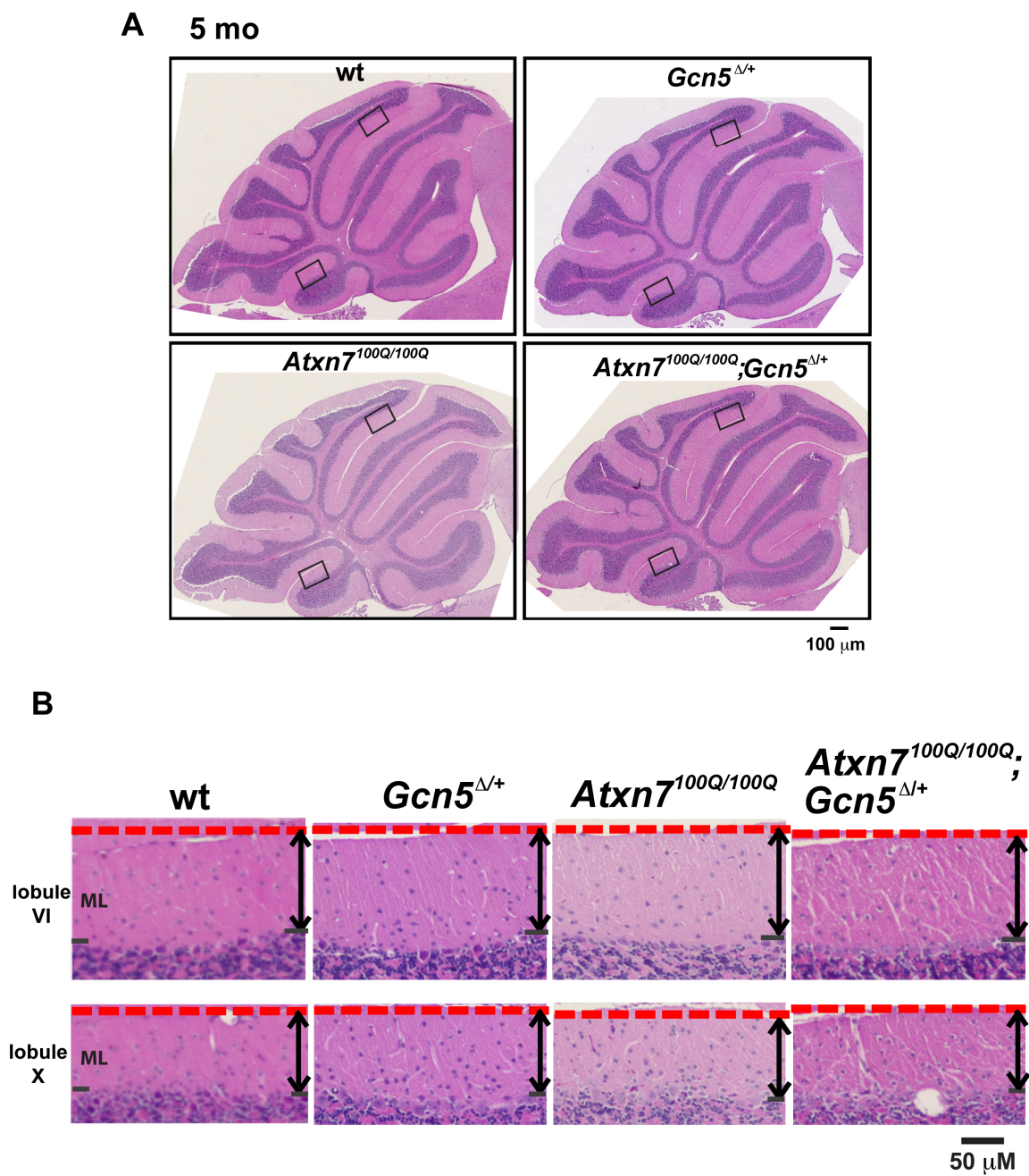


Figure 12

Figure 13. Cerebellar atrophy is more severe in *Atxn7*^{100Q/100Q} mice in a background of *Gcn5*^{Δ/+} at age of 9 months.

(A) Severe atrophy of molecular layer in lobule VI and X of mid saggital cerebellar vermis of *Atxn7*^{100Q/100Q}; *Gcn5*^{Δ/+}. Representative images showing morphology of midsagittal cerebellar vermis of 9 month-old wildtype, *Gcn5*^{Δ/+}, *Atxn7*^{100Q/100Q} and *Atxn7*^{100Q/100Q}; *Gcn5*^{Δ/+} mice. (B) Enlarged pictures of boxes of areas in lobule VI and X in (A) for detailed comparison. Thickness of molecular layer (ML) was marked.

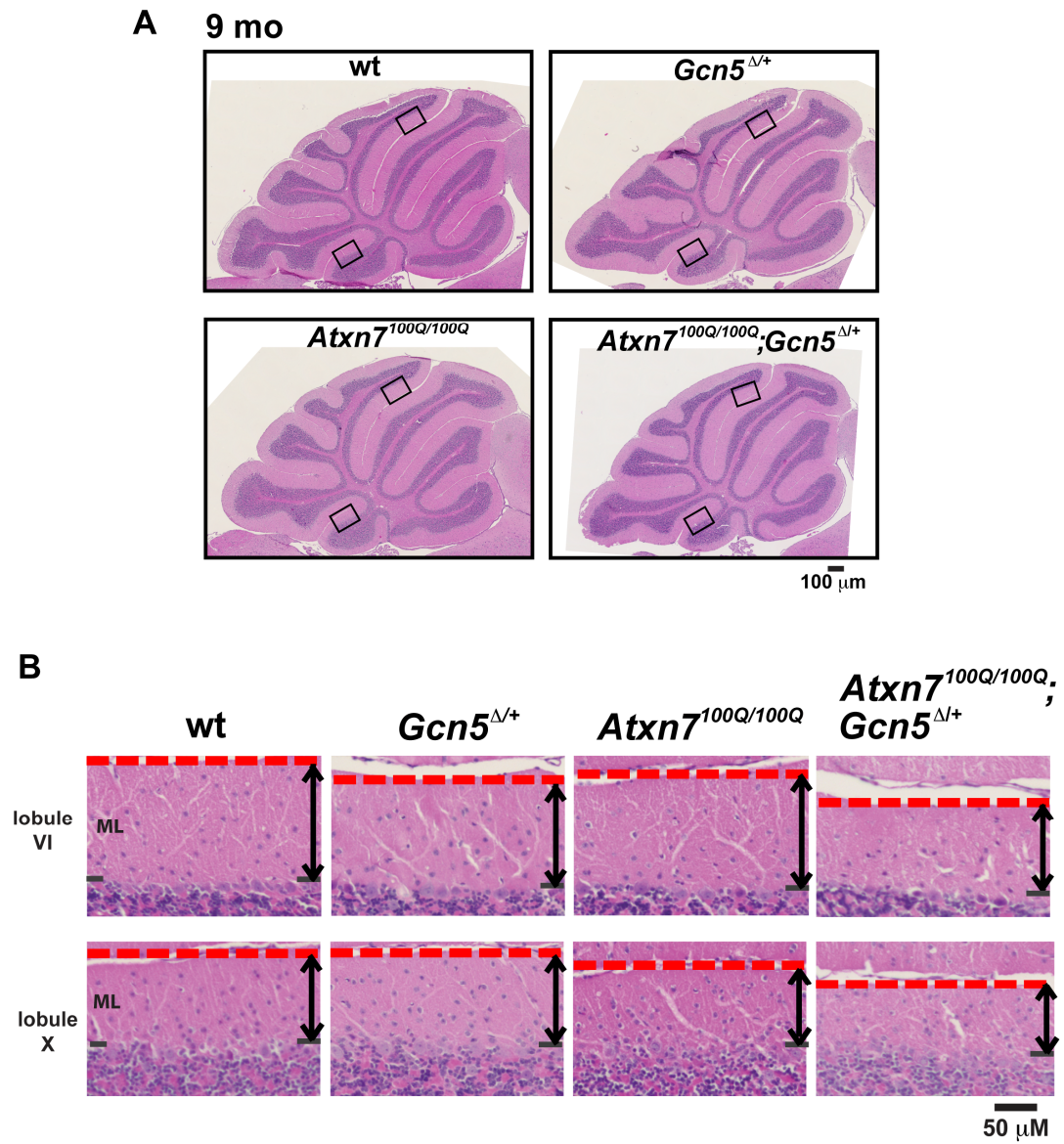


Figure 13

implicated in motor coordination of the limb (de Solages et al., 2008; Harvey et al., 1977; Nimmerjahn et al., 2009). Immunofluorescence staining revealed that Purkinje cells have weaker Calbindin 1 expression and significantly smaller soma size in both *Atxn7*^{100Q/100Q} and *Atxn7*^{100Q/100Q};*Gcn5*^{Δ/+} relative to wild type control mice (wt, 263±42 μm², n=3; *Atxn7*^{100Q/100Q}, 228±34 μm², n= 3; *Atxn7*^{100Q/100Q};*Gcn5*^{Δ/+}, 226±50 μm², n=2; p<0.01) (Figure 14 & 15). However, although no statistical difference was found for overall average soma size of the Purkinje cells between *Atxn7*^{100Q/100Q};*Gcn5*^{Δ/+} and *Atxn7*^{100Q/100Q} mice, 9 % of the Purkinje cells had uncommonly small soma in *Atxn7*^{100Q/100Q};*Gcn5*^{Δ/+} mice (Figure 15A). I next asked whether there is a loss of Purkinje cells in these cerebella. The development of Purkinje cells has no significant defects in *Atxn7*^{100Q/100Q} or *Atxn7*^{100Q/100Q};*Gcn5*^{Δ/+} cerebellum, since mice of all genotypes have similar number of Purkinje cells at 5 month old (Figure 15B). At 9 months, no significant loss of Purkinje cells occurred in *Atxn7*^{100Q/100Q} (Purkinje cell count per 6 mm sections in wt, 540± 34, n= 5; in *Atxn7*^{100Q/100Q}, 514± 36, n= 4; p= 0.15). However, *Atxn7*^{100Q/100Q};*Gcn5*^{Δ/+} mice had significantly fewer Purkinje cells (489±23, n=3) when compared to wt mice (p<0.05) at 9 months. Purkinje cell loss was significantly worse in lobule X of *Atxn7*^{100Q/100Q};*Gcn5*^{Δ/+} mice compared to *Atxn7*^{100Q/100Q} mice (*Atxn7*^{100Q/100Q};*Gcn5*^{Δ/+}, 22± 2, n= 3; *Atxn7*^{100Q/100Q}, 27± 2, n= 4; p<0.05) (Figure 15B). In contrast, Bergmann glia exhibited similar elevated levels of GFAP in both *Atxn7*^{100Q/100Q} and *Atxn7*^{100Q/100Q};*Gcn5*^{Δ/+} mice compared to control mice (Figure 14). Together these data suggest that partial loss of Gcn5

Figure 14. Purkinje cell morphological change is more severe in

***Atn7*^{100Q/100Q} mice in a background of *Gcn5*^{Δ/+}.**

Anti-Calbindin 28K and GFAP antibody immunofluorescent -labeled Purkinje cells and Bergmann glia, respectively, in cerebellar lobule VI of mice of indicated genotype at age of 8 months.

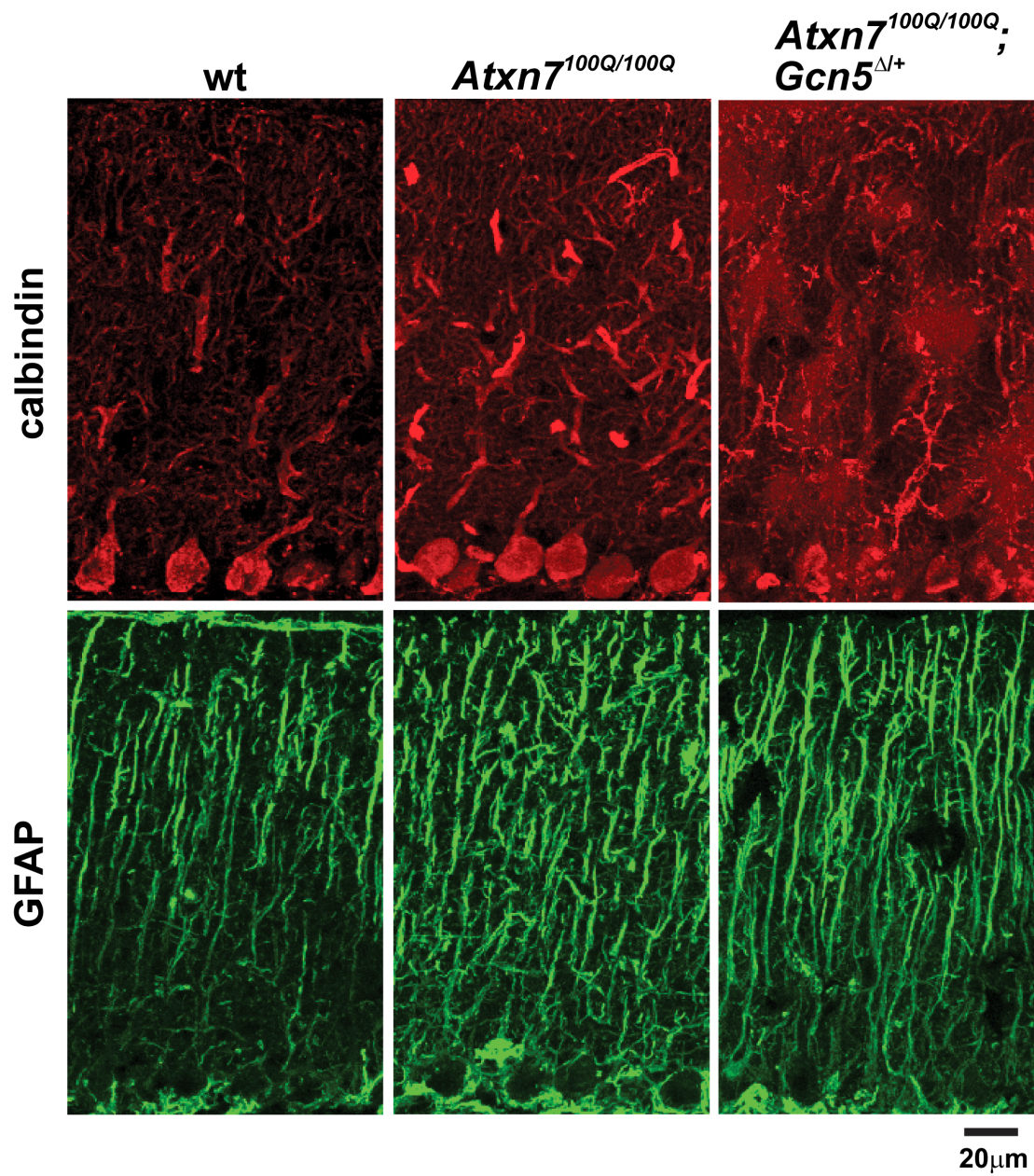


Figure 14

Figure 15. Purkinje cell degeneration is more severe in *Atxn7*^{100Q/100Q} mice in a background of *Gcn5*^{Δ/+}.

(A) Area size frequency of Purkinje cell soma shows *Atxn7*^{100Q/100Q} and *Atxn7*^{100Q/100Q};*Gcn5*^{Δ/+} mice have smaller soma at age of 8 months (wt, n=3 mice; *Atxn7*^{100Q/100Q}, n=3; *Atxn7*^{100Q/100Q};*Gcn5*^{Δ/+}, n=2; *p<0.05 between wt and *Atxn7*^{100Q/100Q}, or wt and *Atxn7*^{100Q/100Q};*Gcn5*^{Δ/+}, Student's t test). (B) Purkinje cell number is similar among all genotypes at age of 5 months, while significantly less in lobule X of *Atxn7*^{100Q/100Q} and *Atxn7*^{100Q/100Q};*Gcn5*^{Δ/+} mice at age of 8 months (wt, n=3 mice; *Atxn7*^{100Q/100Q}, n=3; *Atxn7*^{100Q/100Q};*Gcn5*^{Δ/+}, n=2; *p<0.05 between wt and *Atxn7*^{100Q/100Q}, or wt and *Atxn7*^{100Q/100Q};*Gcn5*^{Δ/+}, or *Atxn7*^{100Q/100Q} and *Atxn7*^{100Q/100Q};*Gcn5*^{Δ/+}, Student's t test). Data are presented as mean ± SEM.

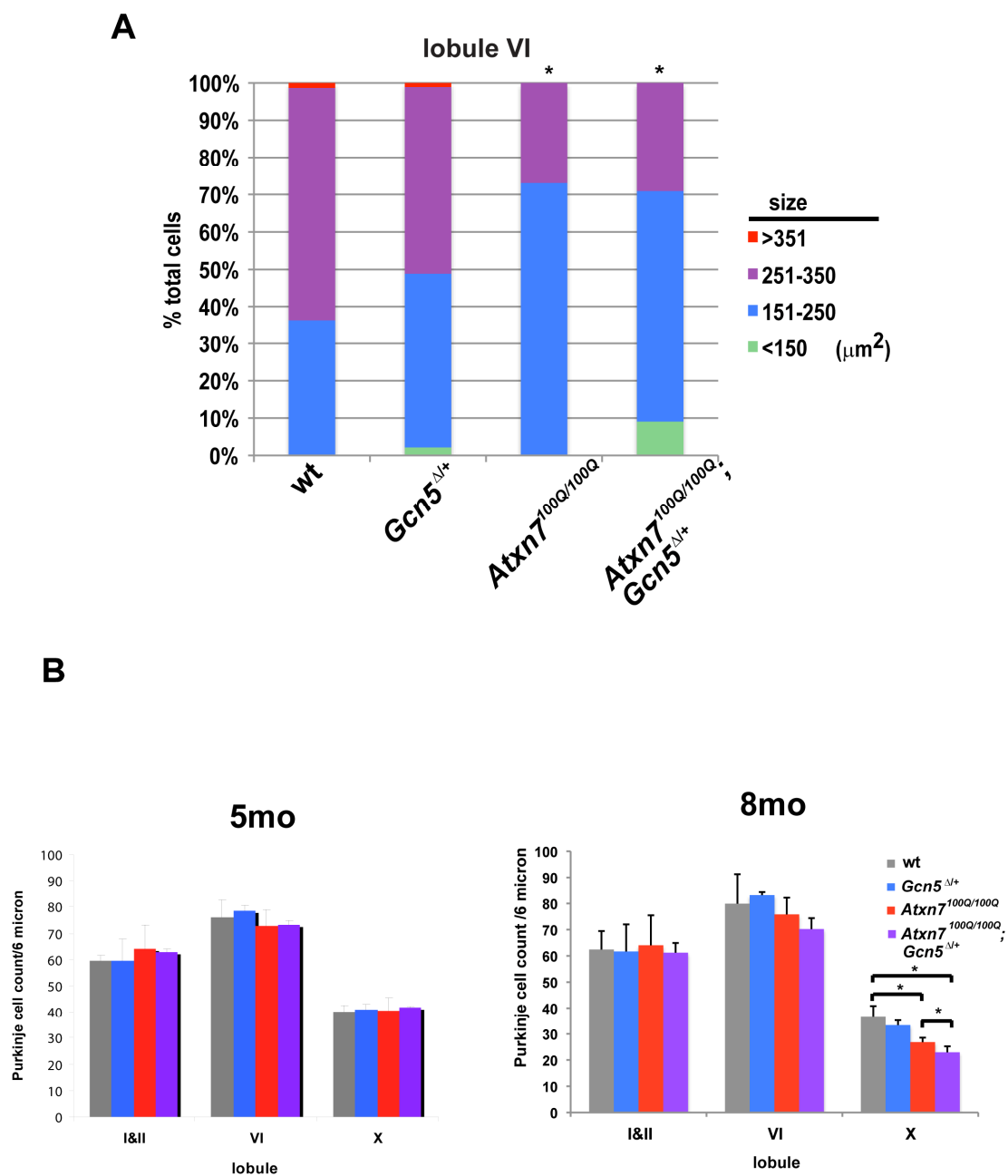


Figure 15

function accelerates cerebellar and Purkinje cell degeneration, but does not further distort Bergmann glia, in SCA7 mice.

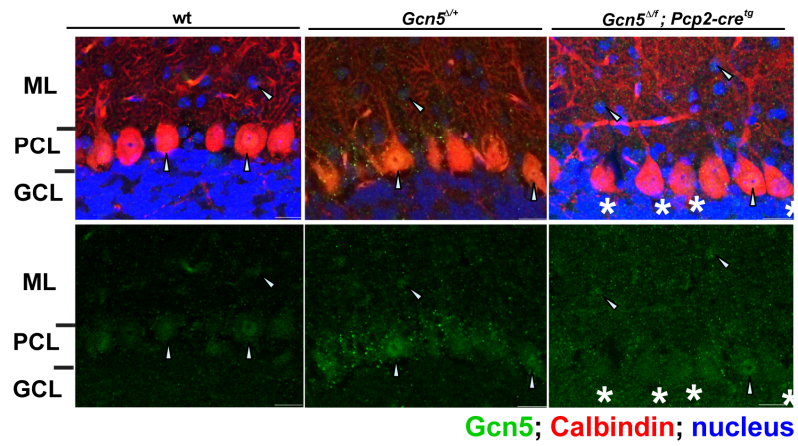
Depletion of Gcn5 in the postnatal Purkinje neurons affects motor coordination

In the above experiments, Gcn5 expression was decreased uniformly in all cell types. However, in SCA7 patients the most affected neurons in the cerebellum are Purkinje cells (Carpenter and Schumacher, 1966; Gouw et al., 1994; Martin et al., 1994; Rub et al., 2005). Therefore to determine whether Gcn5 loss in Purkinje cells is sufficient to cause an SCA7 phenotype, I generated *Gcn5* conditional knockout mice using a transgenic Cre allele expressed specifically in Purkinje cells, *Pcp2-cre^{tg}* (Barski et al., 2002), and a ‘floxed’ allele of *Gcn5* together with our deletion allele (*Gcn5^{Δf}*). Cre mediated recombination removes exons 3-18 in *Gcn5*, resulting in a null allele (Lin et al., 2007). The resulting Purkinje cell-specific *Gcn5* conditional knock-out mice were present at Mendelian ratios at the time of weaning. At age of P7, around the time Cre recombinase started to express, the morphology of the cerebelli are similar among wt, *Gcn5^{+f};Pcp2-cre^{tg}*, and *Gcn5^{Δf};Pcp2-cre^{tg}* (Figure 17), suggesting that there is no developmental effect from any of these transgenic background. Using RNA in situ hybridization or immunofluorescent staining labeling *Gcn5* transcript or protein, only minimal levels of *Gcn5* transcripts were detected in Purkinje cells in these *Gcn5* conditional mice (Figure 16). These mice exhibited normal hind limb extension in tail suspension assays, but by 11 months of age developed a mildly

Figure 16. Purkinje cell-specific depletion of *Gcn5*.

(A) Immunofluorescent labeling for Gcn5 protein on section of cerebellum of *Gcn5* conditional nulls and control mice at 4 month of age. Arrowheads indicate nuclear signals of Gcn5. Asterisks indicate Purkinje cells with weaker Gcn5 signals. Purkinje cells and nuclei were marked with Calbindin and Topro-3 staining, respectively. (B) *In situ* hybridization for *Gcn5* transcript on cerebellar section from 2 month old wt, *Gcn5*^{Δ/+}, *Gcn5*^{Δ/flox}; *Pcp2-cre*^{tg} mice. Boxes of areas were enlarged for detailed structure.

A



B

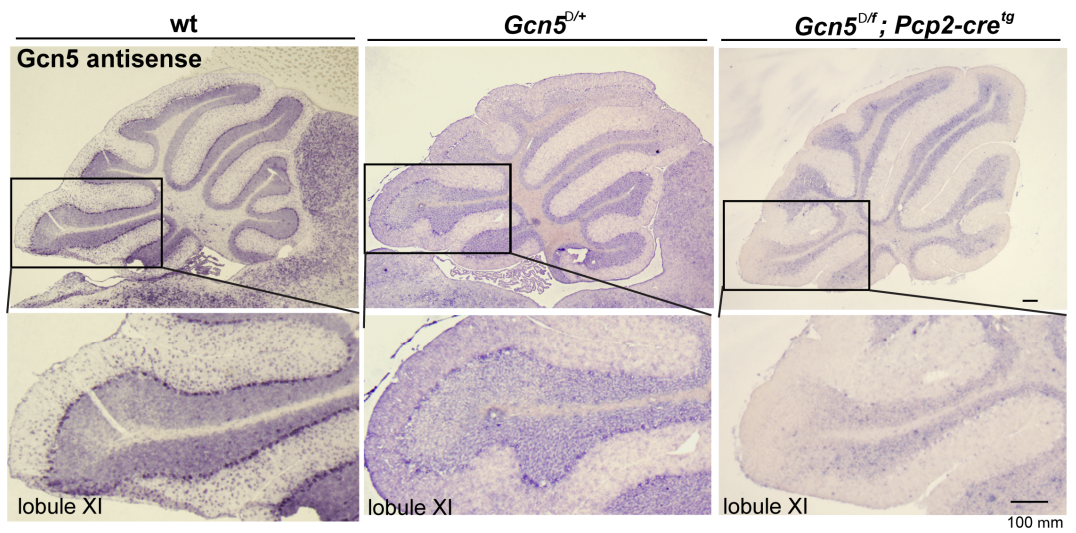


Figure 16

Figure 17. Depleting *Gcn5* in Purkinje cells causes no dramatic effect in the cerebellum at P7.

Representative pictures of mid-sagittal section of the brain or cerebellum of wt, *Gcn5*^{+/*flox*};*Pcp2-cre*^{tg}, and *Gcn5*^{Δ/*flox*};*Pcp2-cre*^{tg} mice at P7.

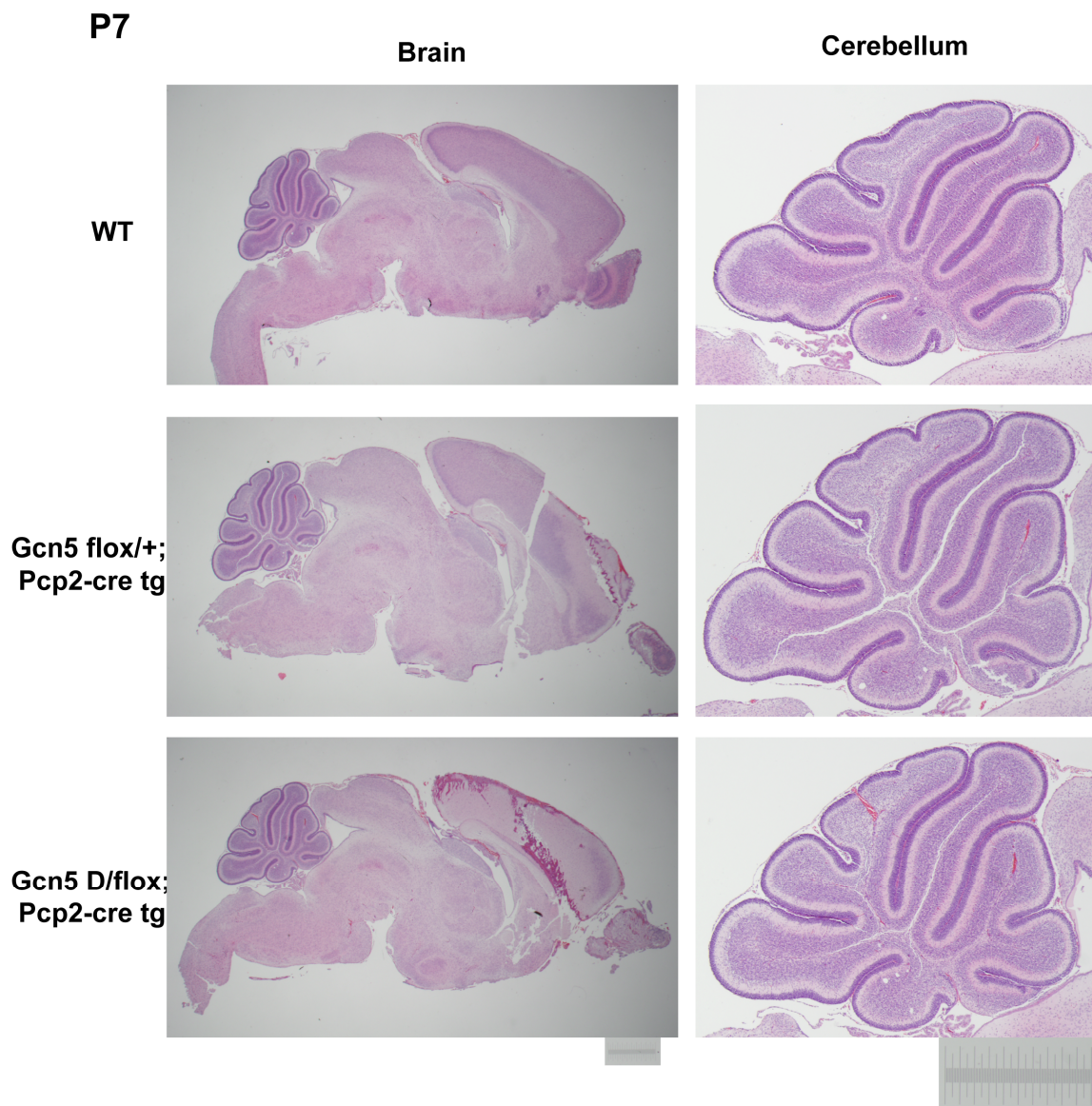


Figure 17

uncoordinated gait with wider paired distance (Figures 18). The cerebellar vermis in the conditional nulls appeared to be smaller than in wild type mice (Figure 19). Since Gcn5 functions as a transcriptional coactivator, we also determined whether loss of Gcn5 affects Purkinje cell-specific transcripts. We found that Calbindin 1 expression was mildly decreased in Purkinje cell-specific *Gcn5* null cerebella, to $74.7 \pm 5\%$ of that in wild type animals ($n=3$, $p<0.05$) (Figure 20). These data suggest that loss of *Gcn5* in Purkinje cells mildly affects Purkinje cell and cerebellar morphology, as well as cerebellar functions, but is not sufficient to induce a SCA7 phenotype. These data are consistent with the primary role of ATXN7 mutations in SCA7 disease and suggest that some other ATXN7-mediated interactions, beyond those mediated by GCN5, contribute to cerebellar pathology.

Reducing Gcn5 worsens retinal degeneration in SCA7 mice

Since the retina is another major site of neural degeneration in SCA7 patients (David et al., 1997; David et al., 1998), we next asked whether reducing Gcn5 levels affects the progression of retinal degeneration in the SCA7 mouse model. We examined the morphology of the retinas of control and *Atxn7*^{100Q/100Q} mice with or without *Gcn5* deletion allele at postnatal day 14 (P14), 1, 2, 4, or 8 months of age. At P14, when all cell types are formed in the retina, *Atxn7*^{100Q/100Q} and *Atxn7*^{100Q/100Q};*Gcn5*^{Δ/+} had retinal morphologies similar to those of control mice (Figure 21), indicating normal retinal development had occurred. However, by the age of 2 months, the retina of *Atxn7*^{100Q/100Q};*Gcn5*^{Δ/+} mice had a thinner

Figure 18. Purkinje cell-specific loss of *Gcn5* causes mild ataxia.

(A) Coordinated hind limb stretching during tail suspension of wild type, *Gcn5*^{Δ/+}, and *Gcn5*^{Δ/f};*Pcp2-cre*^{Tg} mice at 11 months of age. (B) Abnormal gait of *Gcn5* conditional null mice at 11 months of age. Walking gait was recorded by footprint analysis with red and blue footprints represent fore- and hind-paws, respectively. Quantified footprints show *Gcn5*^{Δ/f};*Pcp2-cre*^{Tg} mice have wider paired distance (wt, n= 3; *Gcn5*^{Δ/+}, n= 3; *Gcn5*^{Δ/f};*Pcp2-cre*^{Tg}, n= 3 ; *p<0.05 between wt and *Gcn5*^{Δ/f};*Pcp2-cre*^{Tg}, Kruskal-Wallis test). Data expressed as box plots (boxes, 25–75%; circles, <10 or >90%; lines, median).

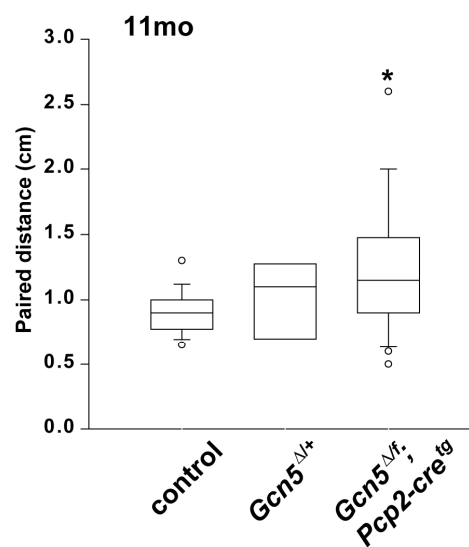
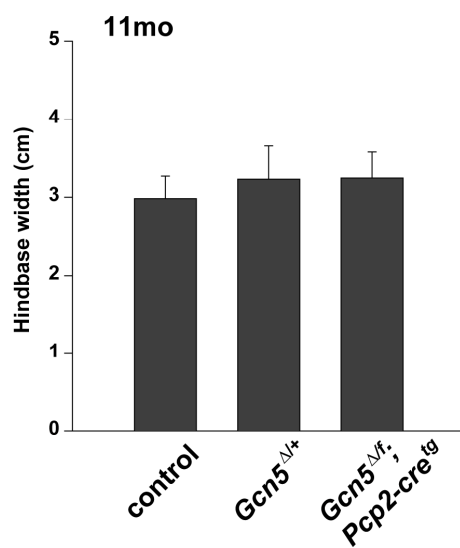
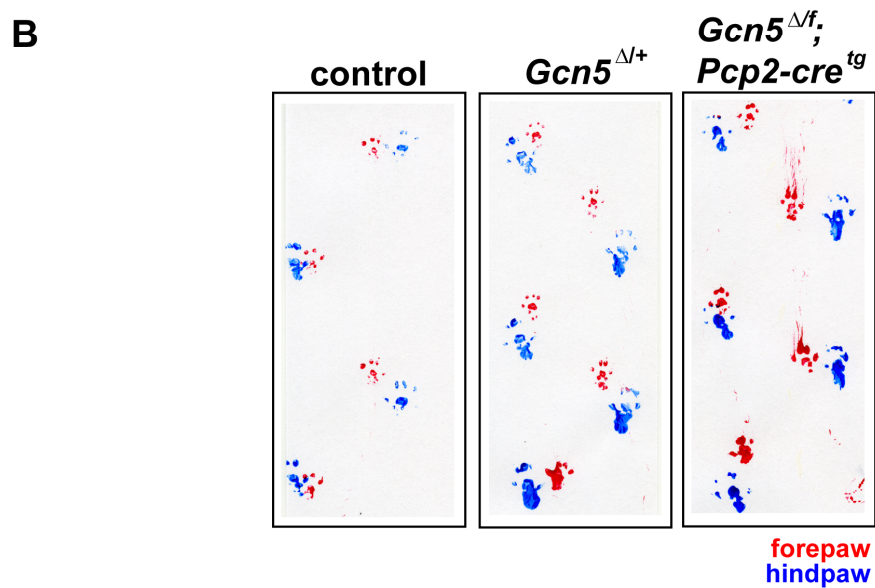
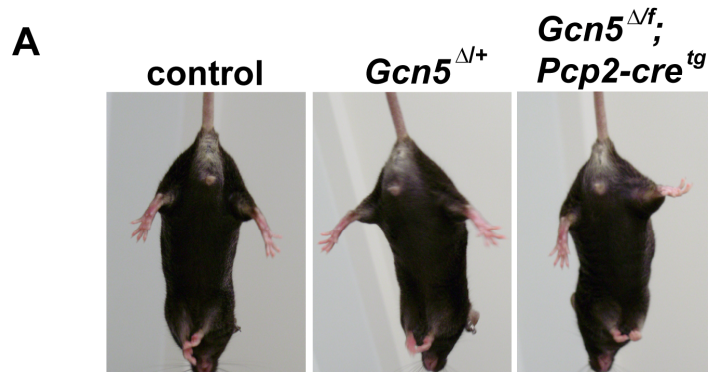


Figure 18

Figure 19. Purkinje cell-specific loss of *Gcn5* causes mild cerebellar atrophy.

Smaller cerebelli in *Gcn5*^{Δ/flox};*Pcp2-cre*^{Tg} compared to that of wt mice.

Representative pictures of mid-sagittal cerebelli of *Gcn5*^{Δ/+}, *Gcn5*^{+/-flox};*Pcp2-cre*^{Tg}, and *Gcn5*^{Δ/flox};*Pcp2-cre*^{Tg} mice at age of 2, 8 and 24 month.

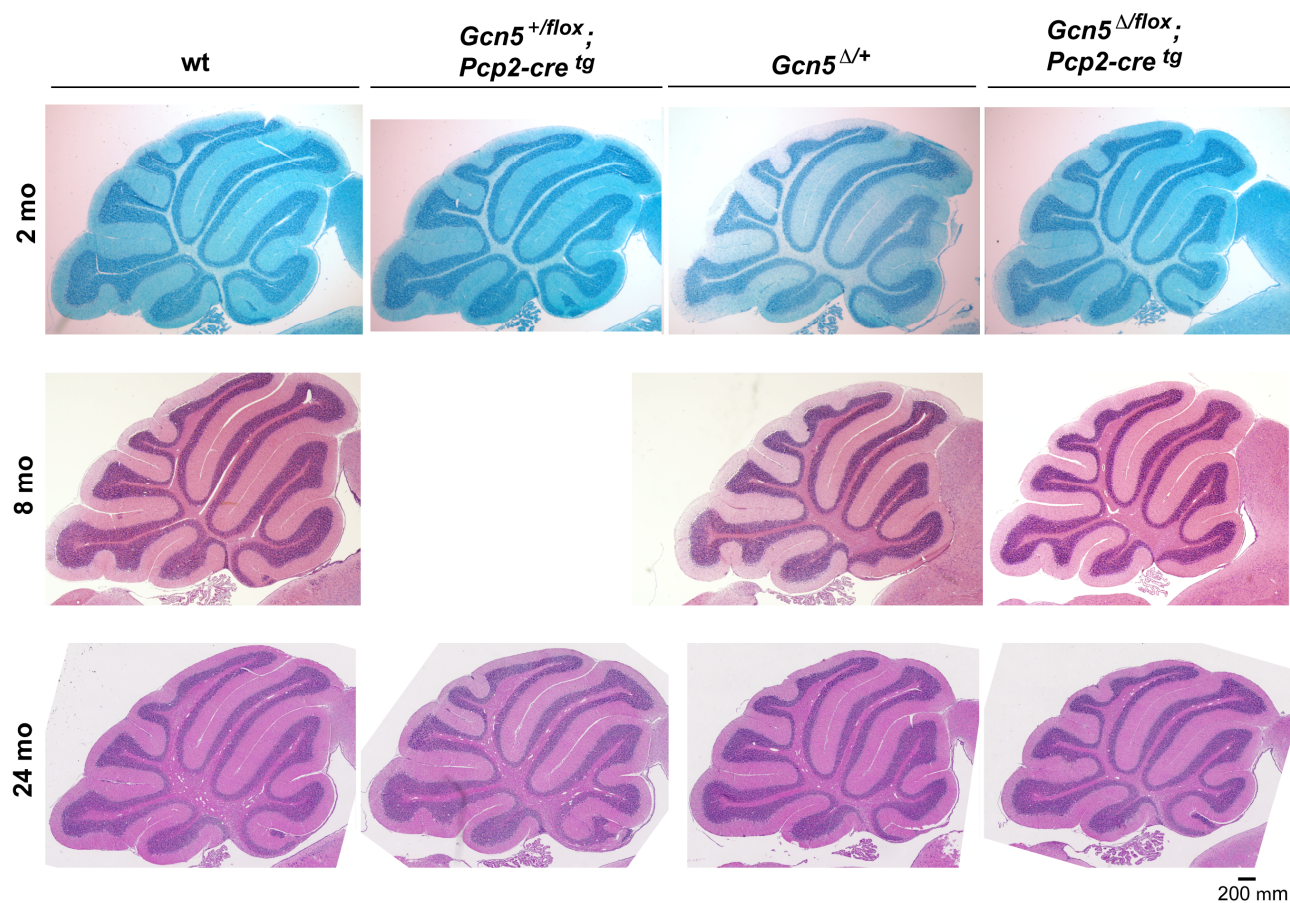


Figure 19

Figure 20. Level of Purkinje cell-specific transcripts in *Gcn5* conditional null mice.

Relative level of *Pcp2* and *Calbindin1* in the cerebellum of wt, *Gcn5*^{Δ/+}, and *Gcn5*^{Δ/flox};*Pcp2-cre*^{tg} mice at were determined by realtime RT PCR (n=3 mice, p<0.05, between wt *Gcn5*^{Δ/flox};*Pcp2-cre*^{tg} of 2 month old, Student's t test). Data are presented as mean± SD.

Purkinje cell protein 2

Calbindin-1

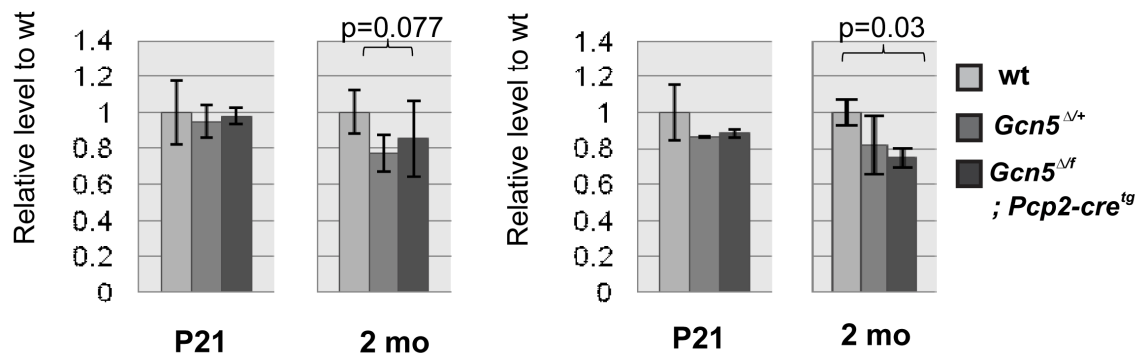


Figure 20

Figure 21. Reducing Gcn5 worsens retinal degeneration in *Atxn7*^{100Q/100Q} mice.

Representative images show progressively thinner retina in *Atxn7*^{100Q/100Q}; *Gcn5*^{Δ/+} mice at 2, 4, and 8 months of age, whereas mice of all genotypes have similar retinal structures at P14 using H&E staining. OS, outer segment; IS, inner segment; ONL, outer nuclear layer; INL, inner nuclear layer; GCL, ganglion cell layer.

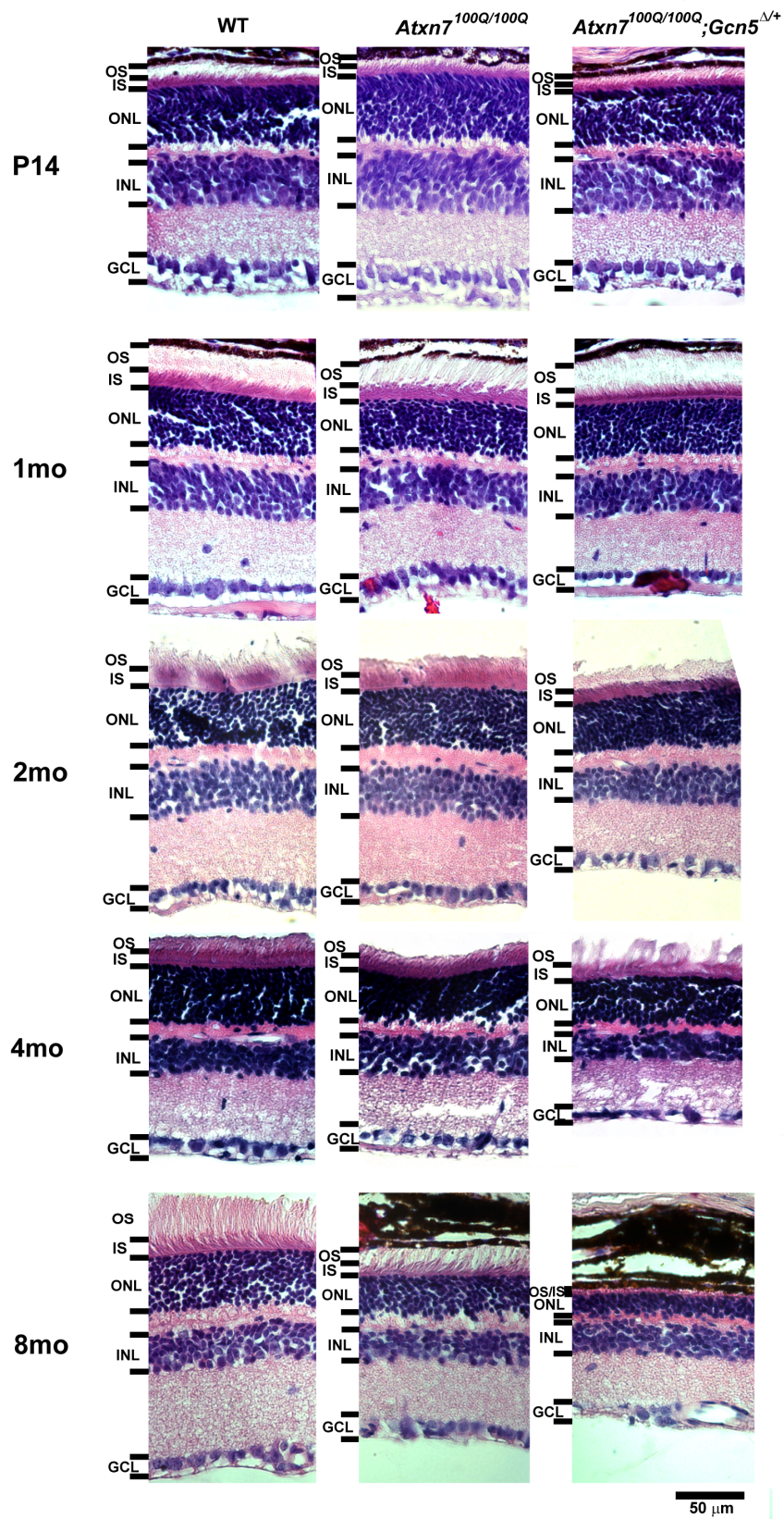


Figure 21

outer nuclear layer (ONL) when compared to those of control or *Atxn7*^{100Q/100Q} mice (Figure 21), indicating photoreceptor degeneration. Further thinning of the ONL was observed in *Atxn7*^{100Q/100Q};*Gcn5*^{Δ/+} retinas at 4 months of age, whereas only mild thinning of the ONL was observed in retinas of *Atxn7*^{100Q/100Q} mice (Figure 21). By the age of 8 months, retinal ONLs in both *Atxn7*^{100Q/100Q} and *Atxn7*^{100Q/100Q};*Gcn5*^{Δ/+} mice were dramatically thinner compared to those of the controls. The outer segment (OS) layer started to be thinner at age of 1.5 months in *Atxn7*^{100Q/100Q};*Gcn5*^{Δ/+} retinas and appeared to be completely gone in *Atxn7*^{100Q/100Q};*Gcn5*^{Δ/+} mice at this time (Figures 21 & 22). In summary, both *Atxn7*^{100Q/100Q} and *Atxn7*^{100Q/100Q};*Gcn5*^{Δ/+} mice developed retinal atrophy. However, this retinal atrophy occurred earlier in *Atxn7*^{100Q/100Q};*Gcn5*^{Δ/+} mice (first observed at 2 months in *Atxn7*^{100Q/100Q};*Gcn5*^{Δ/+} mice compared to 4 months in *Atxn7*^{100Q/100Q} mice), indicating that partial loss-of-function of Gcn5 enhances retinal degeneration.

Reducing Gcn5 does not affect retinal degeneration in SCA7 mice

Given that transcriptional deregulation is strongly associated with photoreceptor dysfunction and dystrophy in SCA7 mouse models (Helmlinger et al., 2006a; Palhan et al., 2005; Yoo et al., 2003), next I asked whether decreased Gcn5 expression induces transcriptional changes that accelerate retinal degeneration in SCA7 mice. I focused on eight transcripts (*Opn1sw*, *Opn1mw*, *Rho*, *Gnat1*, *Rom1*, *Grk*, *Rbp3*, and *Cnga3*) that were found previously to be decreased in early degenerating retinas of SCA7 mouse models, and one non-

Figure 22. *Atxn7*^{100Q/100Q};*Gcn5*^{Δ/+} mice have shorter outer segment at 1.5 month of age.

Electron microscopic pictures of the retina of wt, *Atxn7*^{100Q/100Q} and *Atxn7*^{100Q/100Q};*Gcn5*^{Δ/+} at 1.5 months of age. (A) 1000x magnification, and (B) 2000x magnification. PE, pigmented epithelium, OS, outer segment; IS, inner segment; ONL, outer nuclear layer; INL, inner nuclear layer; OPL, outer plexiform layer.

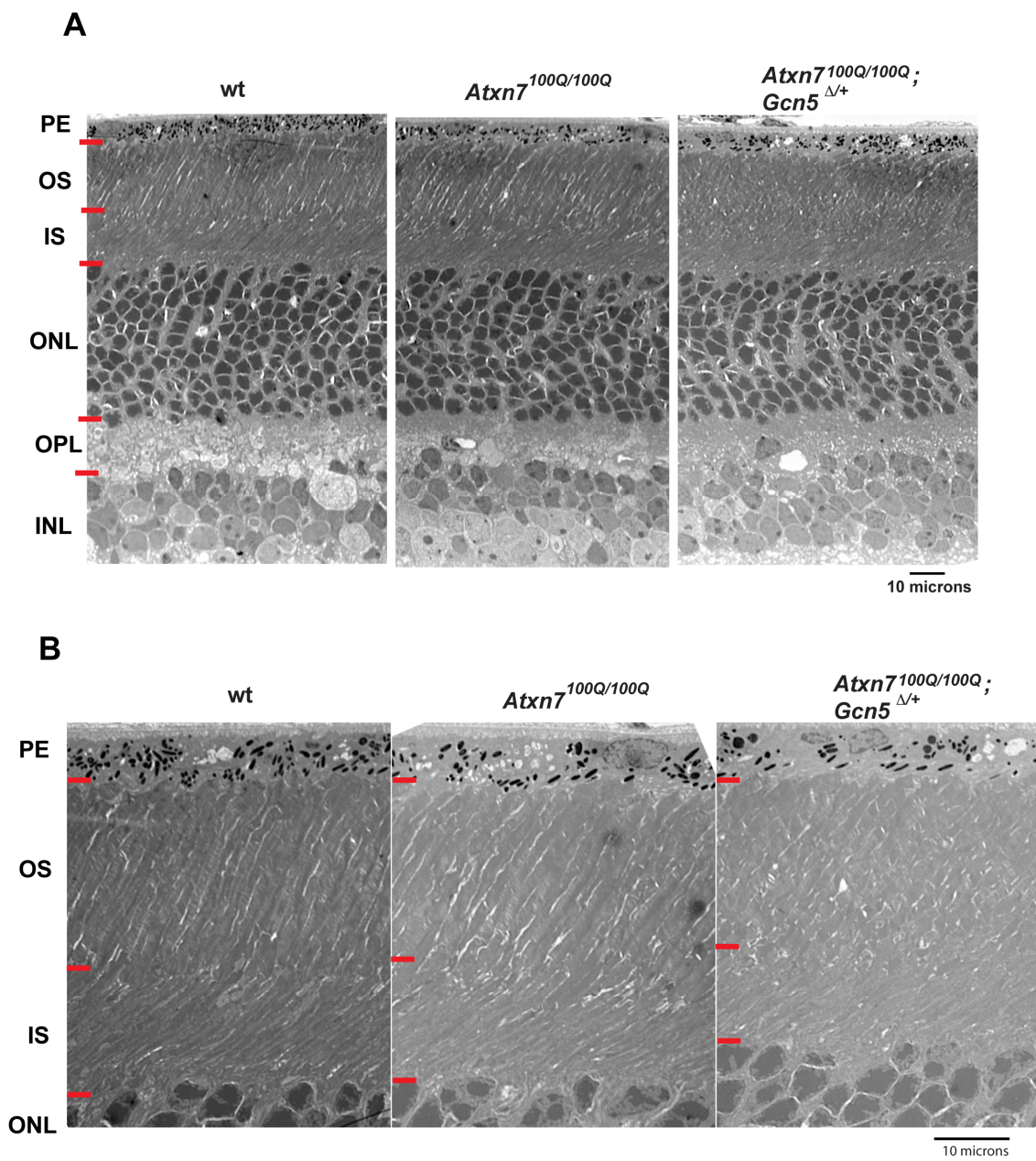


Figure 22

SCA7 target (*Crx*) as a control (Helmlinger et al., 2006a; Palhan et al., 2005; (Helmlinger et al., 2006a; Palhan et al., 2005; Yoo et al., 2003). RNAs were quantified after extracted from retinas of *Atxn7*^{100Q/100Q}, *Atxn7*^{100Q/100Q};*Gcn5*^{Δ/+}, and control mice at P14, 1 month, 1.5 months, and 4 month of age. Consistent with our histological results, expression of all of the SCA7 targets examined was similar in all genotypes at P14; however, expression of these genes progressively decreased from 1.5 to 4 months in the SCA7 mice (Figure 23). The pattern of transcriptional decrease was consistent with that previously reported for *Atxn7*^{266Q/5Q} mice (Yoo et al., 2003). While levels of *Crx* transcript remained steady, a gradual decrease of cone-specific transcripts (*Opn1sw*, *Opn1mw*), followed by rod-specific (*Rho*, *Gnat1*, *Rom1*) and cone-rod shared (*Grk*, *Rbp3*) transcripts was detected in both *Atxn7*^{100Q/100Q} and *Atxn7*^{100Q/100Q};*Gcn5*^{Δ/+} retinas. Transcript levels were decreased to a similar degree in both *Atxn7*^{100Q/100Q} and *Atxn7*^{100Q/100Q};*Gcn5*^{Δ/+} retinas from 1 to 1.5 months. This trend continued to 4 months of age, except that the level of *Gnat1* was lower in *Atxn7*^{100Q/100Q};*Gcn5*^{Δ/+} than in *Atxn7*^{100Q/100Q} mice (Figure 23). Although *Atxn7*^{100Q/100Q};*Gcn5*^{Δ/+} mice undergo accelerated retinal degeneration, the finding that transcript deregulation remains similar during early retinal degeneration in *Atxn7*^{100Q/100Q};*Gcn5*^{Δ/+} and *Atxn7*^{100Q/100Q} mice suggests that reducing *Gcn5* exacerbates retinal atrophy by mechanisms other than affecting expression of known SCA7 target genes.

Potential role of *Gcn5* in the late neural development

Figure 23. Gradual decrease of SCA7 target transcripts in both *Atxn7*^{100Q/100Q} and *Atxn7*^{100Q/100Q};*Gcn5*^{Δ/+} mice.

Relative transcript levels (normalized to β-actin) to wild type (dotted line) in the retinas of *Gcn5*^{Δ/+} (blue line), *Atxn7*^{100Q/100Q} (red line), and *Atxn7*^{100Q/100Q};*Gcn5*^{Δ/+} (purple line) mice at P14, 1 month, 1.5 months and 4 months of age (n=3 mice, *p<0.05 or ** p<0.01 between wt and *Atxn7*^{100Q/100Q}, or wt and *Atxn7*^{100Q/100Q};*Gcn5*^{Δ/+}, Student's t test). Data are presented as mean± SD.

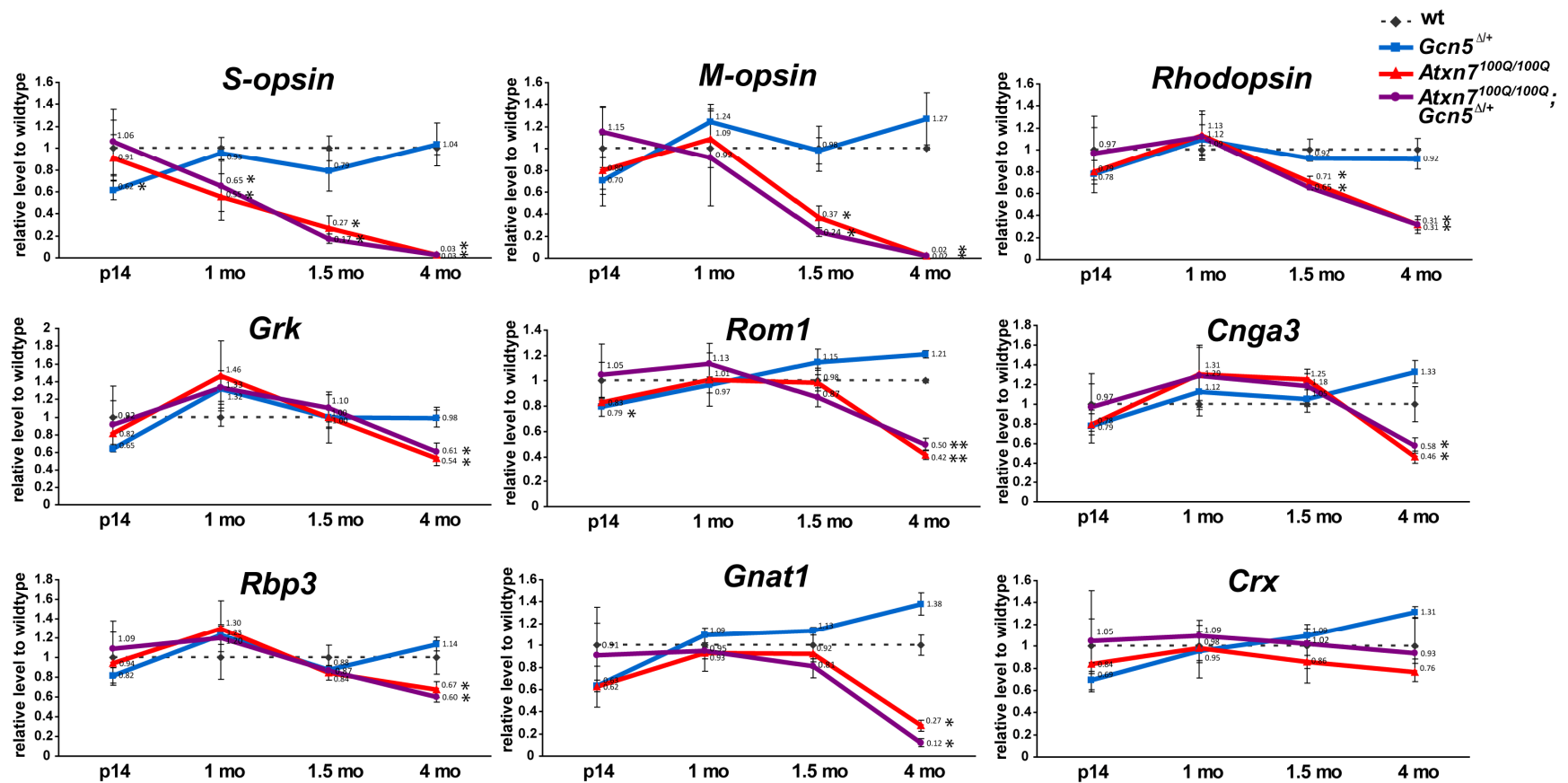


Figure 23

Knowing that Gcn5 plays an important role in maintaining normal functions of mature neurons, I then asked whether level of Gcn5 is also critical for functions or patterning of postmitotic neurons.

The hindbrain neurons undergo two different types of migration after being generated by the neural progenitors and therefore are potential cells to test the role of Gcn5 in neural migration. At E18.5, the Purkinje cells and the interneurons of the preBotzinger complex (preBotC) in the hindbrains are generated and migrate to their designated position in the newborn mice. Purkinje cells migrated to the cerebellum to stimulate and guide the generation and patterning of the granule cells. Interneurons in the preBotC connected the simulation from the brainstem and the motor neurons in the dorsal ganglia to start and maintain breathing pattern soon after birth. To test whether Gcn5 functions are important in these neurons, I obtained *Gcn5* hypomorphic mice, which express least amount of Gcn5 at E18.5 mice, and tested whether any defect occurred at these two sites.

Since Purkinje cells are still immature for functions coordinating motor behaviors at E18.5, first I tested whether cerebellar patterning is affected in *Gcn5* hypomorphic mice. By H&E staining, cerebellar morphology of wt, *Gcn5*^{fn/+} and *Gcn5*^{fn/fn} mice was examined. At E18.5, the cerebellum forms in all genotypes, however the size of the cerebellum is smaller in *Gcn5* hypomorphic mice. Furthermore, potentially lobule formation is also partly disrupted/delayed, since less gyri were formed in the cerebellum of *Gcn5* hypomorphic mice (Figure 24).

Figure 24. Cerebellar morphology of Gcn5 hypomorphic mice at E18.5.

Representative pictures of H&E stained sagittal section of hindbrain region of wt, *Gcn5^{fn/+}*, *Gcn5^{fn/fn}* mice at E18.5. The cerebellar gyri were marked with asterisks.

E18.5 cerebellum



Figure 24

I also preliminarily examined breathing functions in *Gcn5* hypomorphic mice, since disruption of preBotC development should abrogate its functions controlling respiratory pattern. After mucus clearing and stimulation of mild touching, wildtype and *Gcn5*^{fn/+} mice were able to start smooth breathing pattern following short period of gasping. After smooth breathing, the lung is full of air for every wildtype and *Gcn5*^{fn/+} mice. However, after the same clearing and stimulation procedures, although *Gcn5*^{fn/fn} mice had gasping, however % fail to transit into smooth breathing pattern and eventually stopped gasping. As a result, the lung contains small amount of air from gasping, however the deoxygenated blood under skin results in darker appearance when compared to wildtype or *Gcn5*^{fn/+} littermates (Figure 25). This preliminary result that *Gcn5* hypomorphic mice show appearance that likely caused by breathing defects suggests a potential link of *Gcn5* function to neuronal patterning of BotC during hindbrain development.

Figure 25. Differential appearance of $Gcn5^{fn/fn}$ mice at E18.5.

Picture of a representative litter from crossing of $Gcn5^{fn/+}$ female and male after cleaning and mild stimulation. Wildtype and $Gcn5^{fn/+}$ mice showed pink appearance and $Gcn5^{fn/fn}$ showed darker pink. Arrowheads point to the light-colored lung that was expanded due to successfully breathing. Asterisks indicate less expanded lung.

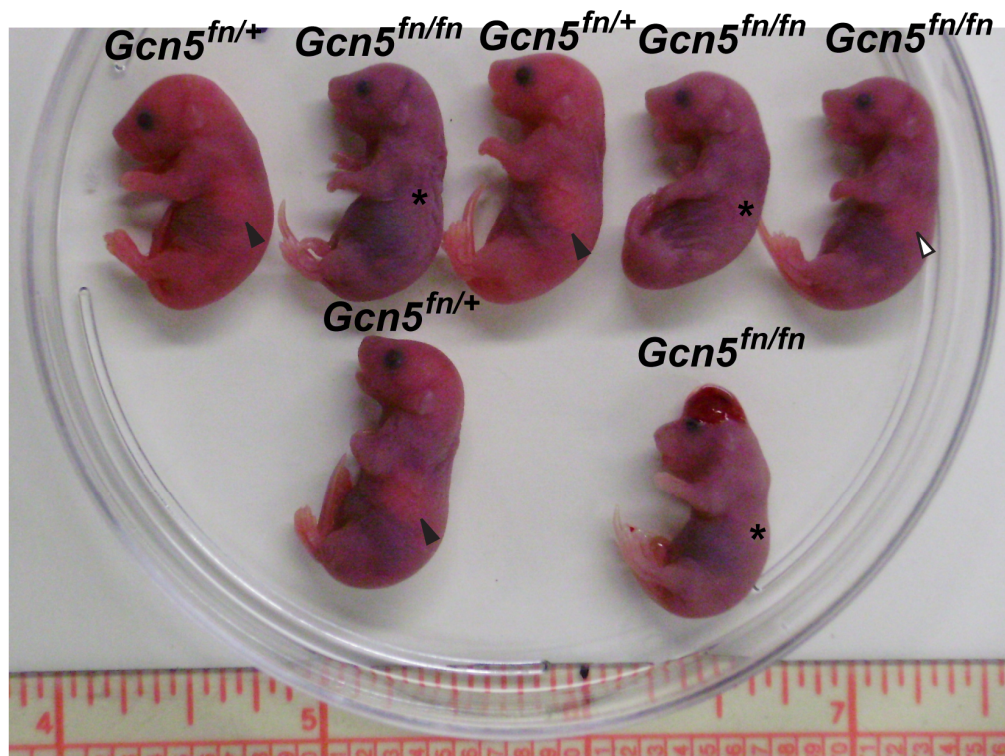


Figure 25

Chapter VI

Discussion & Future Directions

Among all 9 polyQ neurodegenerative diseases, neurotoxicity of both Spinocerebellar ataxia type 1 (SCA1), which is caused by polyQ-ATXN1, and Spinal Bulbar Muscular Atrophy (SBMA), which is caused by polyQ-AR, is known to be caused by disrupted or enhanced functions of several different interactors of the host protein (Chevalier-Larsen et al., 2004; Crespo-Barreto et al., 2010; Duvick et al., 2010; Gehrking et al., 2011; Goold et al., 2007; Katsuno et al., 2002; Lam et al., 2006b; Lim et al., 2008b; Mizutani et al., 2005; Tsuda et al., 2005). Most intriguingly, polyQ-Atxn1 leads to gain- or loss-of-function in two different interacting complexes, RMB17 and Capicua, respectively (Lam et al., 2006a; Lim et al., 2008a). Similarly, my findings that reduced function of Gcn5 accelerates neurodegeneration in SCA7 mice suggest that polyQ-Atxn7 causes neurotoxicity by hindering functions of the SAGA complex. My findings here with polyQ-Atxn7 support the idea that polyQ-proteins affect the functions of complexes interacting with the host protein, providing a shared cause of neurotoxicity in polyQ diseases.

Mice bearing 100Q-Atxn7 show short lifespan, ataxia and photoreceptor degeneration that resemble the major clinical signs in SCA7 patients. The adult onset of phenotypes in these mice strongly suggests that the 100Q-Atxn7 expressing mice are good models for adult onset SCA7.

Since Purkinje cell specific polyQ-Atxn7 expression or loss of Gcn5 specifically in the Purkinje cells (Garden et al., 2002; this work) both lack early neurodegeneration, which distinguish these lines from mice that express polyQ-Atxn7 in the whole body (Helmlinger et al., 2006c; Helmlinger et al., 2004a; Lee

et al., 2009; McMahon et al., 2005a), I propose that polyQ-Atxn7 in multiple cell types contributes to dysfunction and neuronal loss in SCA7 mouse. Likely, polyQ-Atxn7 leads to similar effect as loss of Gcn5 in the Purkinje cell to cause phenotypes of similar spectrums. Notably, Bergmann glia expressing polyQ-Atxn7 lead to a full spectrum of neurodegeneration and ataxia, as seen in mice expressing polyQ-Atxn7 in the full body, suggesting most of the neurotoxicity in the cerebellum comes from toxic effects in the glial cells. Based on this assumption, my finding that reducing Gcn5 accelerates both timing of onset and severity of neurodegeneration in Atxn7-100Q mice suggests that partial loss of Gcn5 function likely contributes to the toxicity caused by Bergmann glia in the SCA7 mice.

In the SCA7 retina, a non-cell autonomous neurotoxicity can also be a prevalent source of neurotoxicity, as several photoreceptor/retinal degenerative diseases develop non-cell autonomous neurotoxicity (reviewed by Wright, 2010; Bramall et al., 2010). However, no evidence yet supports this point for SCA7 retinal degeneration. Since reducing Gcn5 does not exacerbate transcriptional down regulation of the photoreceptor-specific genes, a Gcn5-independent mechanism must lead to this transcriptional defect in SCA7.

The evidence provided in this study supports that loss of Gcn5 functions specifically leads to neurotoxicity regardless of its ubiquitous expression pattern. I propose that this differential toxicity reflects differing Gcn5 functions in mitotic and postmitotic cells. Unique functions of Gcn5 in postmitotic neurons are likely essential to support normal neuronal functions but not survival.

Loss of Gcn5 function contributes to neurodegeneration in SCA7 mouse

PolyQ-Atxn7 generates neurotoxicity cell-autonomously and non-cell autonomously. Here I will discuss how altered Gcn5 functions might contribute to neurotoxicity in both of these cases.

In this study, although decreasing level of Gcn5 is critical in accelerating neurodegenerative phenotypes of SCA7, at this moment, it remains an interesting question of which functions of Gcn5 are altered to cause neurotoxicity. Currently, Gcn5 is known to have HAT and Usp22 enzymatic activity-facilitating (Atanasov et al., 2009) functions.

In this study, although no direct evidence supports that altered Gcn5 HAT activity is involved in neurotoxicity, my preliminary data using immunofluorescent staining showed that total levels of acetylated histone H3K9/K14, one substrate of Gcn5, is reduced in the Purkinje cells of both *Atxn7*^{100Q/100Q} and *Gcn5*^{f/Δ};*Pcp2-cre*^{tg} mice at 4 months of age (data not shown). Since Gcn5 is one of the HATs responsible for acetylation of H3K9/K14, its HAT activity could potentially be reduced in SCA7 affected neurons. Therefore potentially, identifying functions of substrates of Gcn5 in the neurons maybe a key to understanding neurotoxicity of SCA7. However interestingly, loss of Gcn5 in the Purkinje cells leads to only mild cerebellar dysfunction, which suggests that Gcn5 functions may be at least partly redundant in the Purkinje cells. Potentially, the highly similar paralog of Gcn5 in mammals, PCAF, could complement loss of Gcn5, since it has similar conserved HAT activity and is also expressed in the same cell populations. If this were the

case, depleting both Gcn5 and PCAF would cause a more severe neuronal defect in the Purkinje cells than Gcn5 depletion alone.

Since Gcn5 also functions to facilitate the DUB activity of Usp22 in SAGA, it is highly possible that this DUB activity is affected in SCA7 neurons. Atxn7 is part of the DUB module. Although no direct evidence yet shows that abnormal DUB activity is critical to neurotoxicity in SCA7, the abnormal accumulation of ubiquitin/ ubiquitinated proteins in polyQ diseases argues a lower rate of deubiquitination. Although this accumulation of ubiquitin occurs in both degenerating and non-degenerating cells, it is still possible that the abnormal aggregation of ubiquitin is associated with neuron-specific toxicity in SCA7. Next I will discuss this possibility in detail.

Potential role of ubiquitin and Usp22 DUB activity in SCA7

Intra- or interneuronal aggregation of ubiquitinated proteins, for example, Lewy bodies and neurofibrillary tangles, is widely observed and identified as serological features that associate with neurodegenerative diseases (reviewed by Alves-Rodrigues et al., 1998). Also, defects in the ubiquitin and unfolded protein turnover systems, such as chaperones and the ubiquitin-proteasome system, has been shown to lead to neurotoxicity (reviewed by Ciechanover and Brundin, 2003; Muchowski and Wacker, 2005). Defects in ubiquitin ligases, such as UBE3A, UBE1, Parkin, and deubiquitinases, such as ATXN3, Usp14, and UCHL1, have been linked to neurodegeneration (Imai et al., 2000; Kishino et al., 1997; Milla et al., 2002; Saigoh et al., 1999; Wilson et al., 2002; Wintermeyer et

al., 2000), suggesting imbalance in homeostasis of ubiquitin and ubiquitinated proteins could drive neurotoxicity.

In earlier studies, the accumulation of ubiquitin was hypothesized as an indicator of disrupted proteasomal functions in Alzheimer's disease and as an inducer of both formation of nuclear inclusions and cell death in polyQ neurodegenerative diseases (de Pril et al., 2004; Fischer et al., 2003). However one later study clearly showed that normal activity of the proteasome exists through out the neuropathology in affected photoreceptors of SCA7 mice (Bowman et al., 2005). This finding suggests that SCA7 neurons potentially have abnormal homeostasis of ubiquitin, rather than a problem in protein turnover per se, that may result from defects in deubiquitinase or ubiquitin ligase activities.

Although it is not clear how abnormal ubiquitin aggregation might be related to generation of polyQ neurotoxicity in the disease state, several reports suggested healthy mature neurons utilize ubiquitin differentially. Mature neurons that have exited the cell cycle require plasticity and the ability to reset synaptic functions and chromatin modifications potentially via utilizing ubiquitin modification. If these processes are critical for neuronal functions, it maybe a key to answer whether and how unbalanced ubiquitin leads to neurotoxicity. This difference in utilizing ubiquitin among various cell types could potentially determine the differential cell vulnerability in neurodegenerative diseases. One recent study showed that neurons maintain distinctively higher amount of free ubiquitin than other cell types (Kaiser et al., 2011). This evidence suggested that although ubiquitin is ubiquitously utilized in all cell types, postmitotic neurons likely utilize the ubiquitin

proteasome system distinctively from other cell types. One potential biological function of higher level of ubiquitin in mature neurons might be for maintaining the postmitotic status. Previously, the level of free ubiquitin was found associated with ubiquitin status of histone H2A in mammalian cells (Dantuma et al., 2006). More recently, the level of Ub-H2B, which is highly regulated by E3-Ub-DUB which involves in removing ubiquitin, is critical for normal chromatin packing (Fierz et al., 2011). These findings along with the evidence that upon deficiency of enzymes of the ubiquitin proteasome system, postmitotic neurons undergo apoptosis accompanied with aberrant *de novo* DNA synthesis (Staropoli and Abeliovich, 2005), suggests that postmitotic neurons likely utilize ubiquitin proteasome system to maintain unique Ub status on chromatin for preventing chromatin decondensation and reentry into the cell cycle. Further understanding of this under-explored area of protein ubiquitination imbalance in neurodegeneration will require greater definition of the enzymes catalyzing ubiquitination and deubiquitination in neurons.

Interestingly, a link between neurodegeneration and decondensed chromatin that might be associated with an unbalanced free Ub pool was observed SCA7 transgenic mice in that heterochromatic structures were opened in severely affected neurons (Helmlinger et al., 2006a). However this phenomenon might also be a late pathological event and not the cause of early cytotoxicity, as in our slow-progressing SCA7 mouse, no disrupted heterochromatin was observed in early degenerating neurons (Fig 22). Depleting GCN5 reduces the enzymatic activity of USP22 (Atanassov et al., 2009). My preliminary immunofluorescent

staining data showed mild accumulation of ubiquitinated proteins in *Gcn5*-null Purkinje cells, suggesting that loss of *Gcn5* also affects turnover of ubiquitinated proteins, potentially by obstructing activity of Usp22. Disrupted functions of Usp22 DUB, which regulates the Ub status of its specific targets, such as histone H2A and H2B as well as potentially the free Ub pool (reviewed by Shabek and Ciechanover, 2010), could be involved in SCA7 neuropathy, perhaps causing the late unpacking of heterochromatin.

Implication of non-transcriptional functions of Gcn5/SAGA involved in the early degenerating retina of SCA7.

SAGA complex is best known for its transcriptional coactivator functions through its HAT and DUB activities. Although previous studies based on yeast and cultured mammalian cells indicate that polyQ-Atxn7 disrupts transcriptional coactivator functions of SAGA (Helmlinger et al., 2006c; Helmlinger et al., 2004a; Lee et al., 2009; McMahon et al., 2005a), evidence provided in this study argues that such changes are only marginally due to loss of *Gcn5*.

The early defects in the degenerating neurons should be the primary cause of neurotoxicity in SCA7. Intriguingly, with accelerated retinal degeneration, the pattern of transcriptional down regulation of SCA7 targets was not further changed in the retina of *Atxn7*^{100Q/100Q} mice expressing less *Gcn5* (Figures 20-22). These data suggest that partial loss of *Gcn5* function might contribute to retinal pathogenesis through affecting other targets than those tested here, which were previously defined as down regulated in SCA7 retinas. Although other, yet

to be defined transcriptional targets of Gcn5 may be involved in SCA7, the possibility also remains that non-transcriptional targets of Gcn5/SAGA direct the accelerated retinal degeneration in SCA7 mice depleted of Gcn5. Therefore identifying transcriptional and non-transcriptional targets of Gcn5/SAGA will give insights to how polyQ-Atxn7 causes neurotoxicity. Secondly, since down-regulation of *Opn1sw*, *Opn1mw*, and *Rho* likely causes photoreceptor dysfunction in SCA7 (Yoo et al., 2003), the lack of additional effects on transcriptional down-regulation of these genes in *Atxn7*^{100Q/100Q};*Gcn5*^{Δ/+} mice suggests that altered function of Gcn5 is not the sole contributor of SCA7 neurotoxicity. Likely a Gcn5-independent mechanism underlies this transcriptional down regulation in SCA7. The independence of Gcn5 level in the transcriptional down regulation of SCA7 targets could also be the reason why two previous reports found divergent enrichment/function of Gcn5 during transcriptional down regulation in SCA7 retina (Helmlinger et al., 2006a; Palhan et al., 2005).

Since Atxn7 is part of DUB submodule of SAGA, possibilities are that functions of the DUB module are also altered by polyQ-Atxn7. Previous evidence provided by Atanasov et. al. suggests that the DUB function of USP22 also regulates protein stability (Atanasov et al., 2009). My data suggests the potential involvement of non-transcriptional functions of SAGA in SCA7 pathogenesis, hence Usp22 functions in regulating protein stability may well be involved in neurotoxicity of polyQ-Atxn7.

In sum, my data suggest examining transcriptional and non-transcriptional functions of SAGA/Gcn5 in neurons will point out the potential pathways affected by polyQ-Atxn7.

Future direction- determine the functions of Gcn5 in photoreceptors and Bergmann glia in SCA7 neuropathogenesis

Since loss of Gcn5 function leads to neurotoxicity in SCA7 mice, finding targets of Gcn5 will expedite discovering therapeutics for SCA7. Evidence that decreased functions of Gcn5 accelerate degeneration of the photoreceptors in SCA7 mice (Figures 20 & 21) suggests that Gcn5 loss of function contributes to polyQ-Atxn7 neurotoxicity in photoreceptors. Since depletion of Gcn5 in Purkinje cells leads to only mild neuropathy, reduced function of Gcn5 potentially also affects Bergmann glia and leads to non-cell autonomous toxicity of Purkinje cells in SCA7. Therefore, I propose to identify genomic and protein targets of Gcn5 in photoreceptors and Bergmann glia, two cell types that are likely affected by neurotoxicity from hindered functions of Gcn5.

To identify transcriptional targets of Gcn5 that are involved in neurotoxicity of photoreceptors, I will utilize Biotin-tagged Gcn5 to determine the genomic loci associated with Gcn5 in these cells. Biotin-tagged Gcn5 provides stronger and more specific chromatin immunoprecipitation (ChIP) signals than the commercial Gcn5 antibodies available (Hirsch & Dent, personal communication). I will cross a Biotin-Gcn5 transgene, *CAG-stop-Biotin-Gcn5^{tg}*, which conditionally expresses Biotin-Gcn5 under control of Cre recombinase, into *Crx-cre^{tg}*, or

Atxn7^{100Q/100Q}; *Crx-cre*^{tg} mice. Since *Crx* promoter only drives expression of Cre recombinase in the photoreceptors, this crossing will allow photoreceptor-specific expression of Biotin-tagged Gcn5. The altered Gcn5 enriched genomic loci in SCA7 photoreceptors can then be identified by ChIP-seq for biotin using whole retinas. The targets of Gcn5 obtained from ChIP-seq can be confirmed by testing whether their transcripts are altered transcripts in the photoreceptors of *Gcn5* conditional null and SCA7 mice. To determine the profiles of transcripts, RNA-seq using RNA from retinas of *Crx-cre*^{tg}, *Gcn5*^{flox/flox}; *Crx-cre*^{tg}, and *Atxn7*^{100Q/100Q}; *Crx-cre*^{tg} mice will be compared.

Next, the protein substrates of Gcn5 will be identified by enriching acetylated proteins from photoreceptors. To do this, photoreceptors will be marked by fluorescent protein, EGFP that is expressed by *Crx-EGFP*^{tg}, and sorted by FACS. The acetylated protein can then be enriched by immunoprecipitation (IP) using anti acetyl-lysine antibody from the protein lysates of these cells. The acetylated proteins will then be separated by 2-D gel for better resolution of individual proteins. To identify Gcn5 substrates, I will compare the 2-D gel patterns of acetylated protein enriched from *Gcn5*^{flox/flox}; *Crx-cre*^{tg}; *Crx-EGFP*^{tg} and *Gcn5*^{+/+}; *Crx-cre*^{tg}; *Crx-EGFP*^{tg}. I expect to see some of the acetylated proteins are less abundant in Gcn5 null photoreceptors. The acetylated proteins that are differentially abundant will further be isolated and identified by mass spectrometry (MS). To further confirm if the identified protein substrates of Gcn5 are differentially acetylated in polyQ-Atxn7 photoreceptors, I will compare the abundance of in enriched acetylated proteins in the photoreceptors of

Atxn7^{100Q/100Q} and wildtype mice using protein-specific antibody. The acetylated proteins that potentially associate with SCA7 neurotoxicity are likely identified in both *Gcn5*-tagged and SCA7 mice.

To test whether *Gcn5* leads to defect in Bergmann glia, which in turn leads to abnormal cerebellar function, I propose to use Bergmann glia-specific cre transgene (Custer et al., 2006) to drive conditional depletion of *Gcn5* in *Gcn5*^{Δflox};*Gfa2-cre*^{tg};*Gfap-EGFP*^{tg} mice. Motor coordination of these mice could be examined and compared to that of *Atxn7*^{100Q/100Q} mice. To identify *Gcn5* transcriptional targets that potentially associate with cerebellar functions, RNA-seq can be used to identify transcript profile of FACS sorted EGFP-positive Bergmann glia enriched from cerebellum of *Gcn5*^{Δflox};*Gfa2-cre*^{tg};*Gfap-EGFP*^{tg} mice. To further confirm which transcriptional targets of *Gcn5* are affected in the Bergmann glia of SCA7 mice, RNA-seq and ChIP-seq would be used to determine the profile of transcripts and *Gcn5* enrichment in the genome, respectively, in FACS-sorted Bergmann glia from mice with transgene expresses Biotin-tagged *Gcn5* in *Atxn7*^{100Q/100Q};*Gfap-EGFP*^{tg} background and *Biotin-Gcn5*^{tg};*Gfap-EGFP*^{tg} mice.

Acetylation of HAT substrates of *Gcn5* is likely lower in *Gcn5* null cells. Thus the acetylated substrates of *Gcn5* should be less abundant in *Gcn5* null cells compared to that of wildtype cells. A pull-down assay using anti-acetylated lysine antibody could be used to catch acetylated proteins in enriched Bergmann glia. Protein targets of *Gcn5* HAT in the Bergmann glia could then be identified by comparing the pattern of acetylated proteins separated by 2-D gel using lysates

from Bergmann glia of *Gcn5^{Δflox};Gfa2-cre^{tg};Gfap-EGFP^{tg}* and *Gcn5^{+/+};Gfa2-cre^{tg};Gfap-EGFP^{tg}* mice. The acetylated proteins that are differentially abundant will further be identified by mass spectrometry (MS).

The evidence provided by proposed experiments will determine the targets of Gcn5 in the photoreceptor and Bergmann glia that potentially involves in SCA7 neuropathy.

Future direction- Role of Usp22 in SCA7

The clear role of loss-of-Gcn5 function in pathogenesis of SCA7 mice demonstrated in this study pointed Gcn5 as the potential therapeutic target. Moreover, knocking down *Gcn5* does not disrupt overall SAGA integrity (Atanassov et al., 2009) but does cause depletion of the other enzymatic activity, DUB of Usp22, of SAGA. In addition, Atxn7 is in the DUB submodule that Usp22 resides in. Therefore, altered functions of Usp22 could also involve in neurotoxicity of polyQ-Atxn7. Testing the role of Usp22 involvement in the SCA7 pathogenesis using genetic strategy will address this question. Since knocking down *Gcn5* reduces USP22 activity (Atanassov et al., 2009), part of the enhanced phenotypes of SCA7 mice by reducing Gcn5 could be contributed by Usp22 loss-of-function. Therefore, at this point, it is fair to ask whether loss of functions of Usp22 also involves in neurotoxicity; and what are the proteins Usp22 affects.

Usp22 null mice likely die as embryos (preliminary data from Koutelou & Dent, personal communication), therefore to test the role of losing Usp22 function in

mature neuronal tissues in adult mice, I will utilize conditional alleles. Introducing conditional *Usp22* alleles that reduce level of Usp22 specifically in the Purkinje cells, Bergmann glia, or the photoreceptors would answer whether loss of Usp22 function involves in cerebellar or retinal degeneration. The Purkinje cell, Bergmann glial, or photoreceptor conditional *Usp22* depletion mice would carry *Usp22^{flox/flox};Pcp2-cre^{tg}*, *Usp22^{flox/flox};Gfa2-cre^{tg}*, *Usp22^{flox/flox};Crx-cre^{tg}*, or respectively. Cerebellar or retinal functions of these mice can then be determined by rotarod, footprint, dowel, and wire hang tests for motor coordination; and electroretinography for photoreceptor electrical responses.

To determine the potential substrates of Usp22 in the neurons and glia, I propose to identify the hyper-ubiquitinated proteins in *Usp22* null cells compared to wildtype cells. In order to purify ubiquitinated proteins, *Usp22* conditional null mice will be introduced with 6xHis-tag ubiquitin (Ub) reporter transgene that also conditionally expressing his-tagged Ub under control of the cre recombinase that is expressed in the cell type of interest. Since His-tagged Ub is only expressed in the cell types of interest, no further cell type enrichment is required prior to protein extraction. However, to prevent fast proteasome-mediated degradation of ubiquitinated proteins, injections of proteasome inhibitors into the vitreous cavity or brain ventricles may be necessary for the retina or cerebellum, respectively. Nuclear or cytosolic fraction of His-tagged ubiquitinated proteins can be purified using Ni²⁺-affinity chromatography-purified and then subject to mass spectrometry (MS) for peptide identification.

Identifying targets of Usp22 will further suggest potential role of this DUB in neuronal functions and provide insight in how Usp22 involves in neurotoxicity. Revealing whether and how Usp22 involves in neurodegeneration will not only provide targets for designing small molecule drugs for SCA7 patients, but also suggest potential mechanisms that might shared between neurodegenerative diseases with defects in ubiquitin turnover.

Potential role of Gcn5 in immature neurons

Since Gcn5 is highly expressed in the hindbrain (RNA *in situ* data from Allen Brain Institutes), Gcn5 likely also functions in the neurons of the hindbrain during late embryonic development. The preliminary evidence obtained with Gcn5 hypomorphic mice (Figures 23-24) here also suggested that Gcn5 likely has important role during hindbrain development.

Future direction- role of Gcn5 in immature neurons in the hindbrain

Previous evidence in *Drosophila* suggests that Usp22 (or Nonstop in *Drosophila*) SAGA complex is involved in neurite projection (Weake et al., 2008). This evidence strongly suggests that function of SAGA is involved in development of nervous system.

The preliminary results in my work suggest that proper level of Gcn5 potentially is essential for normal hindbrain development. Specifically, cerebellum and preBotC, the nucleus controls and starts breathing patterns, are likely being affected in *Gcn5^{fn/fn}* mice at E18.5 (Figures 23 & 24). To this end, I will ask which

processes during hindbrain development does Gcn5 involve in; and what are the substrates of Gcn5 in these neurons. Identifying Gcn5 targets in various cell types can give further understanding on how polyQ diseases leads to differential neurotoxicity and adult-onset neurodegeneration.

The development of hindbrain requires proper neurogenesis, migration, neurite projection and synapse connection. Therefore, to determine which steps Gcn5 is involved in, I propose to examine whether there is any defect in each processes occurred in *Gcn5^{fn/fn}* mice. To test if Gcn5 mutant has similar neurogenesis compared to wildtype mice, BrdU and anti-phospho-histone H3ser10 antibody labeling will mark proliferating cells in cerebellum and brainstem of E18.5 embryos. To determine whether there is a defect in migration of these neurons then leads to abnormal patterning, anti-neurokinin 1 receptor (NK1R) or Calbindin1 (Calb1) antibody labeling will mark interneurons of preBotC or cerebellum for its position. Since these markers are cytoplasmic or membranous, they can also determine the shapes of neurons and their neurites. To determine whether correct neurite connections were made in brainstem of *Gcn5^{fn/fn}* mice, single neuron electrophysiology examination will answer the question however it requires specialty equipments and personal.

Specific sets of genes are expressed for each cellular function during neuronal development. Therefore, the transcriptional coactivator function of Gcn5 is likely involved in turning on certain genes during hindbrain development. To identify Gcn5 targets in the neurons of hindbrains at E18.5, the Gcn5-bound DNA regions can be identified by ChIP-seq after enrichment by Straptavidin-

immunoprecipitation from hindbrain of the mice carrying the transgene that expresses Biotin-tagged Gcn5 (*Biotin-Gcn5^{tg}*). The targets of Gcn5 can be further confirmed by analyzing the profile of transcripts in E18.5 *Gcn5^{fn/fn}* mice using RNA-seq analysis. The gene ontology of Gcn5 targets will suggest the pathways and the processes that Gcn5 might regulate. The evidence provided by the proposed experiments will give the first glance of how Gcn5 is involved in neuronal development.

Bibliography

- Aleman, T.S., Cideciyan, A.V., Volpe, N.J., Stevanin, G., Brice, A., and Jacobson, S.G. (2002). Spinocerebellar ataxia type 7 (SCA7) shows a cone-rod dystrophy phenotype. *Experimental Eye Research* 74, 737-745.
- Atanassov, B.S., Evrard, Y.A., Multani, A.S., Zhang, Z., Tora, L., Devys, D., Chang, S., and Dent, S.Y. (2009). Gcn5 and SAGA regulate shelterin protein turnover and telomere maintenance. *Molecular Cell* 35, 352-364.
- Barski, J.J., Dethleffsen, K., and Meyer, M. (2000). Cre recombinase expression in cerebellar Purkinje cells. *genesis* 28, 93-98.
- Barski, J.J., Mörl, K., and Meyer, M. (2002). Conditional inactivation of the calbindin D-28k (Calb1) gene by Cre/loxP-mediated recombination. *genesis* 32, 165-168.
- Bonnet, J., Wang, Y.-H., Spedale, G., Atkinson, R.A., Romier, C., Hamiche, A., Pijnappel, W.W.M.P., Timmers, H.T.M., Tora, L., Devys, D., and Kieffer B. (2010). The structural plasticity of SCA7 domains defines their differential nucleosome-binding properties. *EMBO Rep* 11, 612-618.

Bowman, A.B., Yoo, S.Y., Dantuma, N.P., and Zoghbi, H.Y. (2005). Neuronal dysfunction in a polyglutamine disease model occurs in the absence of ubiquitin-proteasome system impairment and inversely correlates with the degree of nuclear inclusion formation. *Hum Mol Genet* 14, 679-691.

Bu, P., Evrard, Y.A., Lozano, G., and Dent, S.Y. (2007). Loss of Gcn5 acetyltransferase activity leads to neural tube closure defects and exencephaly in mouse embryos. *Molecular & Cellular Biology* 27, 3405-3416.

Carpenter, C.S., and Schmacher, G.A. (1966). Familial Infantile Cerebellar Atrophy Associated With Retinal Degeneration. *Archives of Neurology* 14, 82-94.

Carter, R.J., Lione, L.A., Humby, T., Mangiarini, L., Mahal, A., Bates, G.P., Dunnett, S.B., and Morton, A.J. (1999). Characterization of Progressive Motor Deficits in Mice Transgenic for the Human Huntington's Disease Mutation. *J Neurosci* 19, 3248-3257.

Chevalier-Larsen, E.S., O'Brien, C.J., Wang, H., Jenkins, S.C., Holder, L., Lieberman, A.P., and Merry, D.E. (2004). Castration restores function and

neurofilament alterations of aged symptomatic males in a transgenic mouse model of spinal and bulbar muscular atrophy. *J Neurosci* 24, 4778-4786.

Ciechanover, A., and Brundin, P. (2003). The ubiquitin proteasome system in neurodegenerative diseases: sometimes the chicken, sometimes the egg. *Neuron* 40, 427-446.

Conacci-Sorrell, M., Ngouenet, C., and Eisenman, R.N. Myc-Nick: A Cytoplasmic Cleavage Product of Myc that Promotes [alpha]-Tubulin Acetylation and Cell Differentiation. *Cell* 142, 480-493.

Crespo-Barreto, J., Fryer, J.D., Shaw, C.A., Orr, H.T., and Zoghbi, H.Y. (2010). Partial loss of ataxin-1 function contributes to transcriptional dysregulation in spinocerebellar ataxia type 1 pathogenesis. *PLoS Genet* 6, e1001021.

Custer, S.K., Garden, G.A., Gill, N., Rueb, U., Libby, R.T., Schultz, C., Guyenet, S.J., Deller, T., Westrum, L.E., Sopher, B.L., and La Spada, A.R. (2006).

Bergmann glia expression of polyglutamine-expanded ataxin-7 produces neurodegeneration by impairing glutamate transport. *Nat Neurosci* 9, 1302-1311.

Dantuma, N.P., Groothuis, T.A.M., Salomons, F.A., and Neefjes, J. (2006). A

dynamic ubiquitin equilibrium couples proteasomal activity to chromatin

remodeling. *The Journal of Cell Biology* 173, 19-26.

David, G., Abbas, N., Stevanin, G., Durr, A., Yvert, G., Cancel, G., Weber, C.,

Imbert, G., Saudou, F., Antoniou, E., Drabkin, H., Gemmill, R., Giunti, P.,

Benomar, A., Wood, N., Ruberg, M., Agid, Y., Mandel, J.L., and Brice, A. (1997).

Cloning of the SCA7 gene reveals a highly unstable CAG repeat expansion.

Nature Genetics 17, 65-70.

David, G., Durr, A., Stevanin, G., Cancel, G., Abbas, N., Benomar, A., Belal, S.,

Lebre, A.-S., Abada-Bendib, M., Grid, D., Holmberg, M., Yahyaoui, M., Hentati,

F., Chkili, T., Agid, Y., and Brice, A. (1998). Molecular and Clinical Correlations in

Autosomal Dominant Cerebellar Ataxia with Progressive Macular Dystrophy

(SCA7). *Hum Mol Genet* 7, 165-170.

de Pril, R., Fischer, D.F., Maat-Schieman, M.L.C., Hobo, B., de Vos, R.A.I.,

Brunt, E.R., Hol, E.M., Roos, R.A.C., and van Leeuwen, F.W. (2004).

Accumulation of aberrant ubiquitin induces aggregate formation and cell death in polyglutamine diseases. *Human Molecular Genetics* 13, 1803-1813.

Dhalluin, C., Carlson, J.E., Zeng, L., He, C., Aggarwal, A.K., and Zhou, M.-M. (1999). Structure and ligand of a histone acetyltransferase bromodomain. *Nature* 399, 491-496.

Duvick, L., Barnes, J., Ebner, B., Agrawal, S., Andresen, M., Lim, J., Giesler, G.J., Zoghbi, H.Y., and Orr, H.T. (2010). SCA1-like disease in mice expressing wild-type ataxin-1 with a serine to aspartic acid replacement at residue 776. *Neuron* 67, 929-935.

Enevoldson, T.P., Sanders, M.D., and Harding, A.E. (1994). Autosomal dominant cerebellar ataxia with pigmentary macular dystrophy. A clinical and genetic study of eight families. *Brain* 117 (Pt 3), 445-460.

Faiola, F., Liu, X., Lo, S., Pan, S., Zhang, K., Lyman, E., Farina, A., and Martinez, E. (2005). Dual Regulation of c-Myc by p300 via Acetylation-Dependent Control of Myc Protein Turnover and Coactivation of Myc-Induced Transcription. *Mol Cell Biol* 25, 10220-10234.

Fierz, B., Chatterjee, C., McGinty, R.K., Bar-Dagan, M., Raleigh, D.P., and Muir, T.W. (2011). Histone H2B ubiquitylation disrupts local and higher-order chromatin compaction. *Nat Chem Biol* 7, 113-119.

Fischer, D.F., De Vos, R.A.I., Van Dijk, R., De Vrij, F.M.S., Prorer, E.A., Sonnemans, M.A.F., Verhage, M.C., Sluijs, J.A., Hobo, B., Zouambia, M., Steur, E.N., Kamphorst, W., Hol, E.M., and Van Leeuwen, F.W. (2003). Disease-specific accumulation of mutant ubiquitin as a marker for proteasomal dysfunction in the brain. *The FASEB Journal* 17, 2014-2024.

Gamper, A.M., Kim, J., and Roeder, R.G. (2009). The STAGA Subunit ADA2b Is an Important Regulator of Human GCN5 Catalysis. *Mol Cell Biol* 29, 266-280.

Garden, G.A., Libby, R.T., Fu, Y.-H., Kinoshita, Y., Huang, J., Possin, D.E., Smith, A.C., Martinez, R.A., Fine, G.C., Grote, S.K., Ware, C.B., Einum, D.D., Morrison, R.S., Ptacek, L.J., Sopher, B.L., and La Spada, A.R. (2002).

Polyglutamine-Expanded Ataxin-7 Promotes Non-Cell-Autonomous Purkinje Cell Degeneration and Displays Proteolytic Cleavage in Ataxic Transgenic Mice. *The Journal of Neuroscience* 22, 4897-4905.

Gehrking, K.M., Andresen, J.M., Duvick, L., Lough, J., Zoghbi, H.Y., and Orr, H.T. (2011). Partial loss of Tip60 slows mid-stage neurodegeneration in a spinocerebellar ataxia type 1 (SCA1) mouse model. *Hum Mol Genet* 20, 2204-2212.

Giunti, P., Stevanin, G., Worth, P.F., David, G., Brice, A., and Wood, N.W. (1999). Molecular and Clinical Study of 18 Families with ADCA Type II: Evidence for Genetic Heterogeneity and De Novo Mutation. *The American Journal of Human Genetics* 64, 1594-1603.

Goold, R., Hubank, M., Hunt, A., Holton, J., Menon, R.P., Revesz, T., Pandolfo, M., and Matilla-Duenas, A. (2007). Down-regulation of the dopamine receptor D2 in mice lacking ataxin 1. *Hum Mol Genet* 16, 2122-2134.

Gouw, L.G., Digre, K.B., Harris, C.P., Haines, J.H., and Ptacek, L.J. (1994). Autosomal dominant cerebellar ataxia with retinal degeneration: clinical, neuropathologic, and genetic analysis of a large kindred. *Neurology* 44, 1441-1447.

Grant, P.A., Eberharter, A., John, S., Cook, R.G., Turner, B.M., and Workman, J.L. (1999). Expanded lysine acetylation specificity of Gcn5 in native complexes. *Journal of Biological Chemistry* 274, 5895-5900.

Grattan-Smith, P.J., Healey, S., Grigg, J.R., and Christodoulou, J. (2001). Spinocerebellar ataxia type 7: a distinctive form of autosomal dominant cerebellar ataxia with retinopathy and marked genetic anticipation. *Journal of Paediatrics & Child Health* 37, 81-84.

Guelman, S., Kozuka, K., Mao, Y., Pham, V., Solloway, M.J., Wang, J., Wu, J., Lill, J.R., and Zha, J. (2009). The Double-Histone-Acetyltransferase Complex ATAC Is Essential for Mammalian Development. *Mol Cell Biol* 29, 1176-1188.

Hayakawa, F., Towatari, M., Ozawa, Y., Tomita, A., Privalsky, M.L., and Saito, H. (2004). Functional regulation of GATA-2 by acetylation. *Journal of Leukocyte Biology* 75, 529-540.

Helmlinger, D., Hardy, S., Abou-Sleymane, G., Eberlin, A., Bowman, A.B., Gansmüller, A., Picaud, S., Zoghbi, H.Y., Trottier, Y., Tora, L., and Devys, D.

(2006a). Glutamine-Expanded Ataxin-7 Alters TFTC/STAGA Recruitment and Chromatin Structure Leading to Photoreceptor Dysfunction. *PLoS Biol* 4, e67.

Helmlinger, D., Hardy, S., Eberlin, A., Devys, D., and Tora, L. (2006b). Both normal and polyglutamine- expanded ataxin-7 are components of TFTC-type GCN5 histone acetyltransferase- containing complexes. *Biochemical Society Symposia*, 155-163.

Helmlinger, D., Hardy, S., Sasorith, S., Klein, F., Robert, F., Weber, C., Miguët, L., Potier, N., Van-Dorsselaer, A., Wurtz, J.M., Mandel, J.L., Tora, L., and Devys, D. (2004). Ataxin-7 is a subunit of GCN5 histone acetyltransferase-containing complexes. *Hum Mol Genet* 13, 1257-1265.

Hodawadekar, S.C., and Marmorstein, R. (2007). Chemistry of acetyl transfer by histone modifying enzymes: structure, mechanism and implications for effector design. *Oncogene* 26, 5528-5540.

Holmberg, M., Duyckaerts, C., Dürr, A., Cancel, G.r., Gourfinkel-An, I., Damier, P., Faucheux, B., Trottier, Y., Hirsch, E.C., Agid, Y., and Brice, A. (1998).

Spinocerebellar Ataxia Type 7 (SCA7): A Neurodegenerative Disorder With Neuronal Intranuclear Inclusions. *Human Molecular Genetics* 7, 913-918.

Imai, Y., Soda, M., and Takahashi, R. (2000). Parkin suppresses unfolded protein stress-induced cell death through its E3 ubiquitin-protein ligase activity. *J Biol Chem* 275, 35661-35664.

Jobsis, G.J., Weber, J.W., Barth, P.G., Keizers, H., Baas, F., van Schooneveld, M.J., van Hilten, J.J., Troost, D., Geesink, H.H., and Bolhuis, P.A. (1997).

Autosomal dominant cerebellar ataxia with retinal degeneration (ADCA II): clinical and neuropathological findings in two pedigrees and genetic linkage to 3p12-p21.1. *Journal of Neurology, Neurosurgery & Psychiatry* 62, 367-371.

Jonasson, J., Ström, A.-L., Hart, P., Brännström, T., Forsgren, L., and Holmberg, M. (2002). Expression of ataxin-7 in CNS and non-CNS tissue of normal and SCA7 individuals. *Acta Neuropathologica* 104, 29-37.

Kaiser, S.E., Riley, B.E., Shaler, T.A., Trevino, R.S., Becker, C.H., Schulman, H., and Kopito, R.R. (2011). Protein standard absolute quantification (PSAQ) method for the measurement of cellular ubiquitin pools. *Nat Methods* 8, 691-696.

Kanno, Y., Tokuda, H., Nakajima, K., Ishisaki, A., Shibata, T., Numata, O., and Kozawa, O. (2004). Involvement of SAPK/JNK in prostaglandin E1-induced VEGF synthesis in osteoblast-like cells. *Molecular and Cellular Endocrinology* 220, 89-95.

Katsuno, M., Adachi, H., Kume, A., Li, M., Nakagomi, Y., Niwa, H., Sang, C., Kobayashi, Y., Doyu, M., and Sobue, G. (2002). Testosterone reduction prevents phenotypic expression in a transgenic mouse model of spinal and bulbar muscular atrophy. *Neuron* 35, 843-854.

Kelly, T.J., Lerin, C., Haas, W., Gygi, S.P., and Puigserver, P. (2009). GCN5-mediated transcriptional control of the metabolic coactivator PGC-1beta through lysine acetylation. *Journal of Biological Chemistry* 284, 19945-19952.

Kishino, T., Lalande, M., and Wagstaff, J. (1997). UBE3A/E6-AP mutations cause Angelman syndrome. *Nat Genet* 15, 70-73.

Kouzarides, T. (2007). Chromatin Modifications and Their Function. *Cell* 128, 693-705.

Kuo, M.-H., Brownell, J.E., Sobel, R.E., Ranalli, T.A., Cook, R.G., Edmondson, D.G., Roth, S.Y., and Allis, C.D. (1996). Transcription-linked acetylation by Gcn5p of histones H3 and H4 at specific lysines. *Nature* **383**, 269-272.

La Spada, A.R., Fu, Y.-H., Sopher, B.L., Libby, R.T., Wang, X., Li, L.Y., Einum, D.D., Huang, J., Possin, D.E., Smith, A.C., Martinez, R.A., Koszdin, K.L., Treuting, P.M., Ware, C.B., Hurley, J.B., Ptáček, L.J., and Chen, S. (2001). Polyglutamine-Expanded Ataxin-7 Antagonizes CRX Function and Induces Cone-Rod Dystrophy in a Mouse Model of SCA7. *Neuron* **31**, 913-927.

Lam, Y.C., Bowman, A.B., Jafar-Nejad, P., Lim, J., Richman, R., Fryer, J.D., Hyun, E.D., Duvick, L.A., Orr, H.T., Botas, J., and Zoghbi, H.Y. (2006). ATAXIN-1 Interacts with the Repressor Capicua in Its Native Complex to Cause SCA1 Neuropathology. *Cell* **127**, 1335-1347.

Latouche, M., Fragner, P., Martin, E., El Hachimi, K.H., Zander, C., Sittler, A., Ruberg, M., Brice, A., and Stevanin, G. (2006). Polyglutamine and polyalanine expansions in ataxin7 result in different types of aggregation and levels of toxicity. *Mol Cell Neurosci* **31**, 438-445.

Lee, K.K., Swanson, S.K., Florens, L., Washburn, M.P., and Workman, J.L.

(2009). Yeast Sgf73/Ataxin-7 serves to anchor the deubiquitination module into both SAGA and Slik (SALSA) HAT complexes. *Epigenetics Chromatin* 2, 2.

Lerin, C., Rodgers, J.T., Kalume, D.E., Kim, S.-h., Pandey, A., and Puigserver, P.

(2006). GCN5 acetyltransferase complex controls glucose metabolism through transcriptional repression of PGC-1[alpha]. *Cell Metabolism* 3, 429-438.

Li, S., and Shogren-Knaak, M.A. (2009). The Gcn5 bromodomain of the SAGA complex facilitates cooperative and cross-tail acetylation of nucleosomes.

Journal of Biological Chemistry 284, 9411-9417.

Lim, J., Crespo-Barreto, J., Jafar-Nejad, P., Bowman, A.B., Richman, R., Hill,

D.E., Orr, H.T., and Zoghbi, H.Y. (2008). Opposing effects of polyglutamine expansion on native protein complexes contribute to SCA1. *Nature* 452, 713-718.

Lin, W., Srajer, G., Evrard, Y.A., Phan, H.M., Furuta, Y., and Dent, S.Y. (2007).

Developmental potential of Gcn5(-/-) embryonic stem cells in vivo and in vitro.

Developmental Dynamics 236, 1547-1557.

Lin, W., Zhang, Z., Chen, C.H., Behringer, R.R., and Dent, S.Y. (2008). Proper Gcn5 histone acetyltransferase expression is required for normal anteroposterior patterning of the mouse skeleton. *Development Growth & Differentiation* 50, 321-330.

Mao, X., Gluck, N., Li, D., Maine, G.N., Li, H., Zaidi, I.W., Repaka, A., Mayo, M.W., and Burstein, E. (2009). GCN5 is a required cofactor for a ubiquitin ligase that targets NF-kappaB/RelA. *Genes & Development* 23, 849-861.

Martin, J., Krols, L., Ceuterick, C., Van Broeckhoven, C., Van Regemorter, N., Hayer-Delatte, F., Brucher, J., de Barsy, T., Szliwowski, H., Evrard, P., Tassignon, M.J., Smet-Dieleman, H., and Willems, P.J. (1994). On an autosomal dominant form of retinal-cerebellar degeneration: an autopsy study of five patients in one family. *Acta Neuropathologica* 88, 277-286.

McMahon, S.J., Pray-Grant, M.G., Schieltz, D., Yates, J.R., 3rd, and Grant, P.A. (2005). Polyglutamine-expanded spinocerebellar ataxia-7 protein disrupts normal SAGA and SLIK histone acetyltransferase activity. *Proc Natl Acad Sci U S A* 102, 8478-8482.

Michalik, A., Martin, J.J., and Van Broeckhoven, C. (2004). Spinocerebellar ataxia type 7 associated with pigmentary retinal dystrophy. *European Journal of Human Genetics* 12, 2-15.

Milla, M.A., Butler, E., Huete, A.R., Wilson, C.F., Anderson, O., and Gustafson, J.P. (2002). Expressed sequence tag-based gene expression analysis under aluminum stress in rye. *Plant Physiol* 130, 1706-1716.

Mizutani, A., Wang, L., Rajan, H., Vig, P.J., Alaynick, W.A., Thaler, J.P., and Tsai, C.C. (2005). Boat, an AXH domain protein, suppresses the cytotoxicity of mutant ataxin-1. *EMBO J* 24, 3339-3351.

Muchowski, P.J., and Wacker, J.L. (2005). Modulation of neurodegeneration by molecular chaperones. *Nat Rev Neurosci* 6, 11-22.

Neetens, A., Martin, J.J., Libert, J., and Den Ende, P.V. (1990). Autosomal dominant cone dystrophy-cerebellar atrophy (ADCoCA) (modified ADCA Harding II). *Neuro-Ophthalmology* 10, 261-275.

Orpinell, M., Fournier, M., Riss, A., Nagy, Z., Krebs, A.R., Frontini, M., and Tora, L. (2010). The ATAC acetyl transferase complex controls mitotic progression by targeting non-histone substrates. *EMBO Journal* 29, 2381-2394.

Palhan, V.B., Chen, S., Peng, G.-H., Tjernberg, A., Gamper, A.M., Fan, Y., Chait, B.T., La Spada, A.R., and Roeder, R.G. (2005). Polyglutamine-expanded ataxin-7 inhibits STAGA histone acetyltransferase activity to produce retinal degeneration. *Proceedings of the National Academy of Sciences of the United States of America* 102, 8472-8477.

Paolinelli, R., Mendoza-Maldonado, R., Cereseto, A., and Giacca, M. (2009). Acetylation by GCN5 regulates CDC6 phosphorylation in the S phase of the cell cycle. *Nature Structural & Molecular Biology* 16, 412-420.

Patel, J.H., Du, Y., Ard, P.G., Phillips, C., Carella, B., Chen, C.-J., Rakowski, C., Chatterjee, C., Lieberman, P.M., Lane, W.S., Blobel, G.A., and McMahon, S.B. (2004). The c-MYC Oncoprotein Is a Substrate of the Acetyltransferases hGCN5/PCAF and TIP60. *Mol Cell Biol* 24, 10826-10834.

Roth, S.Y., Denu, J.M., and Allis, C.D. (2001). HISTONE

ACETYLTRANSFERASES. *Annual Review of Biochemistry* 70, 81-120.

Rub, U., Brunt, E.R., Gierga, K., Seidel, K., Schultz, C., Schols, L., Auburger, G.,

Heinsen, H., Ippel, P.F., Glimmerveen, W.F., Wittebol-Post, D., Arai, K., Deller,

T., and de Vos, R.A. (2005). Spinocerebellar ataxia type 7 (SCA7): first report of

a systematic neuropathological study of the brain of a patient with a very short

expanded CAG-repeat. *Brain Pathology* 15, 287-295.

Sabo, A., Lusic, M., Cereseto, A., and Giacca, M. (2008). Acetylation of

Conserved Lysines in the Catalytic Core of Cyclin-Dependent Kinase 9 Inhibits

Kinase Activity and Regulates Transcription. *Mol Cell Biol* 28, 2201-2212.

Saigoh, K., Wang, Y.L., Suh, J.G., Yamanishi, T., Sakai, Y., Kiyosawa, H.,

Harada, T., Ichihara, N., Wakana, S., Kikuchi, T., and Wada, K. (1999).

Intragenic deletion in the gene encoding ubiquitin carboxy-terminal hydrolase in

gad mice. *Nat Genet* 23, 47-51.

Shabek, N., and Ciechanover, A. (2010). Degradation of ubiquitin: the fate of the

cellular reaper. *Cell Cycle* 9, 523-530.

Staropoli, J.F., and Abeliovich, A. (2005). The ubiquitin-proteasome pathway is necessary for maintenance of the postmitotic status of neurons. *J Mol Neurosci* 27, 175-183.

Tsivgoulis, G., Vassilopoulou, S., Rallis, K., Markomichelakis, N., and Spengos, K. (2008). Spinocerebellar ataxia type 7 presenting as Stargardt's disease. *Journal of Neurology* 255, 456-458.

Tsuda, H., Jafar-Nejad, H., Patel, A.J., Sun, Y., Chen, H.K., Rose, M.F., Venken, K.J., Botas, J., Orr, H.T., Bellen, H.J., Zoghbi, H.Y. (2005). The AXH domain of Ataxin-1 mediates neurodegeneration through its interaction with Gfi-1/Senseless proteins. *Cell* 122, 633-644.

van de Warrenburg, B.P., Frenken, C.W., Ausems, M.G., Kleefstra, T., Sinke, R.J., Knoers, N.V., and Kremer, H.P. (2001). Striking anticipation in spinocerebellar ataxia type 7: the infantile phenotype. *Journal of Neurology* 248, 911-914.

Weake, V.M., Lee, K.K., Guelman, S., Lin, C.H., Seidel, C., Abmayr, S.M., and Workman, J.L. (2008). SAGA-mediated H2B deubiquitination controls the

development of neuronal connectivity in the *Drosophila* visual system. *EMBO J* 27, 394-405.

Wilson, S.M., Bhattacharyya, B., Rachel, R.A., Coppola, V., Tessarollo, L., Householder, D.B., Fletcher, C.F., Miller, R.J., Copeland, N.G., and Jenkins, N.A. (2002). Synaptic defects in ataxia mice result from a mutation in *Usp14*, encoding a ubiquitin-specific protease. *Nat Genet* 32, 420-425.

Wintermeyer, P., Kruger, R., Kuhn, W., Muller, T., Voitalla, D., Berg, D., Becker, G., Leroy, E., Polymeropoulos, M., Berger, K., Przuntek, H., Schöls, L., Epplen, J.T., and Riess, O. (2000). Mutation analysis and association studies of the *UCHL1* gene in German Parkinson's disease patients. *Neuroreport* 11, 2079-2082.

Wiper-Bergeron, N., Salem, H.A., Tomlinson, J.J., Wu, D., and HachÃ, R.J.G. (2007). Glucocorticoid-stimulated preadipocyte differentiation is mediated through acetylation of C/EBP by GCN5. *Proceedings of the National Academy of Sciences* 104, 2703-2708.

Xu, W., Edmondson, D.G., Evrard, Y.A., Wakamiya, M., Behringer, R.R., and Roth, S.Y. (2000). Loss of Gcn5l2 leads to increased apoptosis and mesodermal defects during mouse development. *Nature Genetics* 26, 229-232.

Xu, W., Edmondson, D.G., and Roth, S.Y. (1998). Mammalian GCN5 and P/CAF acetyltransferases have homologous amino-terminal domains important for recognition of nucleosomal substrates. *Molecular & Cellular Biology* 18, 5659-5669.

Yoo, S.-Y., Pennesi, M.E., Weeber, E.J., Xu, B., Atkinson, R., Chen, S., Armstrong, D.L., Wu, S.M., Sweatt, J.D., and Zoghbi, H.Y. (2003). SCA7 Knockin Mice Model Human SCA7 and Reveal Gradual Accumulation of Mutant Ataxin-7 in Neurons and Abnormalities in Short-Term Plasticity. *Neuron* 37, 383-401.

Yvert, G., Lindenberg, K.S., Picaud, S., Landwehrmeyer, G.B., Sahel, J.-A., and Mandel, J.-L. (2000). Expanded polyglutamines induce neurodegeneration and trans-neuronal alterations in cerebellum and retina of SCA7 transgenic mice. *Hum Mol Genet* 9, 2491-2506.

Yvert, G.I., Lindenberg, K.S., Devys, D., Helmlinger, D., Landwehrmeyer, G.B., and Mandel, J.-L. (2001). SCA7 mouse models show selective stabilization of mutant ataxin-7 and similar cellular responses in different neuronal cell types. *Human Molecular Genetics* 10, 1679-1692.

Zhang, X.-Y., Varthi, M., Sykes, S.M., Phillips, C., Warzecha, C., Zhu, W., Wyce, A., Thorne, A.W., Berger, S.L., and McMahon, S.B. (2008). The Putative Cancer Stem Cell Marker USP22 Is a Subunit of the Human SAGA Complex Required for Activated Transcription and Cell-Cycle Progression. *Molecular Cell* 29, 102-111.

Zhao, Y., Lang, G., Ito, S., Bonnet, J., Metzger, E., Sawatsubashi, S., Suzuki, E., Le Guezennec, X., Stunnenberg, H.G., Krasnov, A., Georgieva, S.G., Schüle, R., Takeyama, K., Kato, S., Tora, L., and Devys, D. (2008). A TFTC/STAGA Module Mediates Histone H2A and H2B Deubiquitination, Coactivates Nuclear Receptors, and Counteracts Heterochromatin Silencing. *Molecular Cell* 29, 92-101.

Vita

Yi Chun (EJ) Chen was born in Taipei City, Taiwan on May 13, 1977. Yi Chun is the daughter of Su-Ching Liu and Feng-Hsiung Chen. In 1991, she attended Affiliated Senior High School of National Taiwan Normal University. After completing high school in 1995, she attended Kaohsiung Medical University in Kaohsiung, Taiwan majoring in Biology. During college, she performed research on gene expression of Epstein-Barr Virus in Dr. Soo-Ray Wang's laboratory at the Department of Microbiology and Immunology of National Yang Ming University. Yi Chun graduated from Kaohsiung Medical University in June 1999 with a degree of Bachelor of Arts in Biology. In August of 1999, she entered the Master degree program in National Cheng Kung University, Tainan, Taiwan where she joined the laboratory of Dr. Huan-Yao Lei and developed a murine model for enterovirus 71 infection. After obtained her degree of Master of Science in 2002, she studies the interactom of enterovirus 71 in Dr. Hsiu-Ming Shih's lab at National Health Research Institutes, Taiwan. In 2004, she entered Graduate School of Biomedical Science of University of Texas M.D. Anderson Cancer Center, where she joined Dr. Sharon Y.R. Dent's lab for her dissertation research.

Publications:

Chen, Y.C., Grant, P.A., Dent, S.Y. SCA7: Is the rub in the DUB? *Manuscript in preparation*

Chen, Y.C., Gatchel, J.R., Lewis, R.W., Mao, C.A., Grant, P.A., Zoghbi, H.Y., Dent, S.Y. Gcn5 loss-of-function accelerates cerebellar and retinal degeneration in a SCA7 mouse model. *Hum Mol Genet.* 2011 Oct 27. [Epub ahead of print]

Chen, S.C., Chang, L.Y., Wang, Y.W., Chen, Y.C., Weng, K.F., Shih, S.R., Shih, H.M. Sumoylation-promoted enterovirus 71 3C degradation correlates with a reduction in viral replication and cell apoptosis. *J Biol Chem.* 2011 Sep 9;286(36):31373-84.

Lin, W., Zhang, Z., Srajer, G., Chen, Y.C., Huang, M., Phan, H.M., Dent, S.Y. Proper expression of the Gcn5 histone acetyltransferase is required for neural tube closure in mouse embryos. *Dev Dyn.* 2008 Apr;237(4):928-40.

Chen, Y.C., Yu, C.K., Wang, Y.F., Liu, C.C., Su, I.J., Lei, H.Y. A murine oral enterovirus 71 infection model with central nervous system involvement. *J Gen Virol.* 2004 Jan;85(Pt 1):69-77.

Permanent address:

7447 Cambridge St. #67

Houston, TX 77054